

**Ministry of Higher Education and Scientific Research
University of Baghdad
Institute of Laser for Postgraduate Studies**



The Effect of Laser Densification on Prepared Nanostructured SiO₂ by Sol-Gel Technique

**A Thesis Submitted to the Institute of Laser for
Postgraduate Studies, University of Baghdad in Partial
Fulfillment of the Requirements for the Degree of Master
of Science in Laser / Physics**

By

Noor Mohammed Abdulmalek

B.Sc. Physics Science – 2014

Supervisor

Asst. Prof. Dr. Mohamed K. Dhahir

2018 A.D.

1439 A.H.

Certification

I certify that this thesis was prepared under my supervision at the Institute of Laser for Postgraduate Studies, University of Baghdad, as a partial fulfillment of requirements for the Degree of "Master of Science in Laser/ Physics".

Signature:

Name: **Dr. Mohamed K. Dhahir**

Title: **Asst. Professor**

Address: Institute of Laser for Postgraduate studies,
University of Baghdad.

Date: / / 2018

(Supervisor)

In view of the available recommendation, I forward this thesis for debate by the examining committee.

Signature:

Name: **Asst. Prof. Dr. Shelan Khasro Tawfeeq**

Title: Head of the Scientific Committee.

Address: Institute of Laser for Postgraduate studies,
University of Baghdad.

Date : / / 2018

Examination Committee Certification

We certify that we have read this thesis "**The Effect of Laser Densification on Prepared Nanostructured SiO₂ by Sol-Gel Technique**" and as examining committee examined the student in its content and in our opinion it is adequate with standers as a thesis for the degree of **Master in Science in Laser / Physics**.

Signature:

Name: **Dr. Zainab Fadhil Mahdi**

Title: **Assist Professor**

Address: **Institute of Laser for**

Postgraduate Studies /

University of Baghdad

Date: / / **2018**

(Chairman)

Signature:

Name: **Dr. Mohammed K. Khalaf**

Title: **Professor**

Address: **Head of Plasma Department**

/Applied Physics Center/

Ministry of Science and Technology

Date: / / **2018**

(Member)

Signature:

Name: **Dr. Hanaa M. Yaseen**

Title: **Lecturer**

Address: **Physics Department/College of Science
for Women**

/University of Baghdad

Date: / / **2018**

(Member)

Signature:

Name: **Dr. Mohamed K. Dhahir**

Title: **Assist Professor**

Address: **Institute of Laser for**

Postgraduate Studies /

University of Baghdad

Date: / / **2018**

(Supervisor)

Approval by the deanship of Institute of Laser for Postgraduate Studies / University of Baghdad.

Signature:

Name: **Dr. Abdul-Hady M. Al-Janabi**

Title: **Professor**

Address: **Dean of the Institute of Laser**

for Postgraduate Studies /

University of Baghdad

Date: / / **2018**

بِسْمِ اللَّهِ الرَّحْمَنِ الرَّحِيمِ

مَرِيئًا وَسِعَتْ كُلَّ شَيْءٍ رَحْمَتُهُ وَعِلْمُهُ

صدق الله العظيم

سورة غافر

الآية 7

Dedicated to my Parents ;

*For their encouragement and support that enabled me to achieve
my goals.*

Acknowledgments

I would like to express my deep gratitude and respect to my supervisor **Asst. Prof. Dr. Mohamed K. Dhahir** for suggested this work and his guidance throughout this research.

I acknowledge **Dr. Hanaa M. Yaseen**, from Physics Department College of Science for women for helping me to understand the Sol-Gel preparation method. I'd like to thank **Dr. Mohammed Alwan**, from Physics Department College of Science for his great help in provision of the chemical material.

Thanks are extended to **Prof. Dr. Abdul-Hadi M. Al-Janabi**, for his continuous support and grateful care during the period of research.

It is a pleasure to thank **Dr. Hussein A. Jawad**, for his continuous support, encouragement, and help during the period of research.

I would like to express my gratitude and thanks for **Dr. Zainab F. Mahdi** for allowing me to use the chemical Lab for my chemical experiment. Deep gratitude to **Dr. Layla M. Hassan**, (Head of the Medical and Biological Applications department) for giving me the chance to use the Diode laser and the oven.

Thanks go to **Dr. Ziad A. Taha** (Head of the Engineering and Industrial Applications department), **Dr. Shelan Kh. Tawfeeq** (Head of the Scientific Committee), **Dr. Mazin M. Elias**, **Dr. Mahmoud Sh. Mahmoud**, **Dr. Fadhil A. Umran**, and **Dr. Hanan J. Taher** for their help and care.

Special thanks to **Mr. Maher A. Gatea**, for his great help and **Mr. Atheer**, for his help in design the dip coating technique.

Finally, I introduce my thanks to **Mrs. Hiba Kadhim**, **Mr. Saif Akeel**, and all my friends in the Master's study.

Abstract

The current work aim is to prepare nanostructure Silicon Dioxide by Sol-Gel method including densification with conventional and Laser techniques.

Nanostructure thin films of Silicon Dioxide were prepared by mixing Tetraethylorthosilicate, Ethanol, deionized water, and HCL or NaOH as a catalyst, with different pH values (4,7, and 9). All films were synthesized in the same conditions involving (Molar ratio, Stirrer time, Aging time, and Drying temperature). The films were heat treated using the oven at 200°C for 2 hours or by lasers for 15 minutes. Three types of laser were used in the densification process ; a He-Ne laser (632 nm, 0.056 mW/cm²), a diode laser (410 nm, 56.8 mW/cm²), and diode laser (532 nm, 284.09 to 1079.5 mW/cm²). Films were analyzed by X-ray diffraction (XRD), the UV–VIS absorption spectroscopy, Fourier Transformation Infrared Spectrometer (FTIR), Atomic Force Microscopy (AFM), Field Emission Scanning electron microscopy (FESEM), and Zeta potential.

XRD patterns showed that the structure of SiO₂ thin films were amorphous in both oven and Diode laser (532 nm). On the other hand a shift in the Bragg's diffraction angle was appeared when using Diode laser (410 nm) and the structure was converted to cristobalite structure. UV–VIS spectra revealed that the maximum absorption at 196.8 nm confirm the formation of silica nanoparticles. In addition, the FTIR results verified a successful preparation of SiO₂ nanoparticles. The AFM analysis and FESEM images showed that the structure of thin films is composed of spherical nanometric SiO₂ Particles. A good stability of Zeta potential had been detected for SiO₂ colloidal with pH=9.

From the obtained results, it was concluded that modified structure of SiO₂ nanostructure thin films could be prepared by laser densification. Laser densification of synthesized SiO₂ nanoparticles by Sol-Gel technique exceeded rather than oven densification at 200°C.

List of contents

Chapter One: Introduction & Basic concepts

Section	Subject	Page
1.1	Introduction	1
1.2	Nanomaterials	3
1.3	Silicon Dioxide Nanoparticles	5
1.4	Synthesis of Silicon Dioxide Nanoparticles	5
1.4.1	Sol-Gel method	7
1.5	Steps of Sol-Gel method	8
1.5.1	Hydrolysis & Condensation Reactions	8
1.5.2	Aging & Drying	9
1.5.3	Densification	10
1.6	Influence of Technological Parameters in sol-gel process	11
1.6.1	The Precursor	11
1.6.2	pH/Catalysts	11
1.6.3	The Water: TEOS Molar Ratio	11
1.6.4	The Temperature, Aging and Drying	12
1.7	Coating Techniques of Thin Film	12
1.7.1	Dip Coating Technique	12
1.8	Applications of Silica Nanoparticles	14
1.9	Laser Densification	15
1.10	Literature Survey	17
1.11	Aim of the work	20

Chapter Two : Experimental part

Section	Subject	Page
2.1	Introduction	21
2.2	Procedure	21
2.2.1	Chemical Materials	21
2.2.2	Samples Preparation	22
2.2.3	Thin Films preparation	23
2.2.4	Densification Process	24
2.3	Identification Techniques	28
2.3.1	X-Ray Diffraction (XRD)	28
2.3.2	UV-VIS Spectrophotometer	29
2.3.3	Fourier Transformation Infrared Spectrometer (FTIR)	30
2.3.4	Atomic force microscopy (AFM)	31
2.3.5	Thickness measurement	31
2.3.6	Field Emission Scanning Electron Microscope (FESEM)	32
2.3.7	Zeta Potential analysis	33

Chapter Three : Results & Discussion

Section	Subject	Page
3.1	Introduction	34
3.2	Structure properties of SiO ₂ Nanostructure	34
3.2.1	X-Ray Diffraction Analysis (XRD)	34

Section	Subject	Page
3.3	Optical properties of SiO ₂ Nanostructure	36
3.3.1	UV-VIS spectroscopy	36
3.3.2	Fourier Transformation Infrared Spectrometer (FTIR)	37
3.4	Morphological Properties of SiO ₂ Nanostructure	45
3.4.1	Atomic Force Microscope (AFM)	45
3.4.2	Field Emission Scanning Electron Microscope (FESEM) characteristics	58
3.4.3	Thickness Measurement	65
3.4.4	Zeta-Potential analysis of SiO ₂ nano-solution	66
3.5	Conclusions	71
3.6	Future Work	72

List of Figures

Chapter One: Introduction and Basic concepts

Figure	Title	page
1.1	The Top-Down and Bottom-Up approaches to produce nanomaterials	4
1.2	The methods of synthesize SiO ₂ NPs	6
1.3	Steps of Sol-Gel Synthesis Method	10
1.4	Dip coating process	13
1.5	Gelation process during dip coating process	13
1.6	Schematic of laser processing	16

Chapter Two: Experimental Part

Figure	Title	Page
2.1	SiO ₂ samples with different pH values	22
2.2	Magnetic Stirrer.	23
2.3	Dip Coating Technique.	24
2.4	Schematic diagram of the experimental set up	25
2.5	The Experimental Setup.	26
2.6	The Preparation Steps of SiO ₂ Nanostructure Thin Films by Sol-Gel Technique	26
2.7	Block diagram of the Characterization of SiO ₂ Thin Films.	28
2.8	X-Ray Diffractometer (XRD)	29

Figure	Title	Page
2.9	UV-VIS Spectrophotometer.	30
2.10	Fourier Transformation Infrared Spectrometer.	30
2.11	Atomic Force Microscope (AFM)	31
2.12	Thin Film Measurement System	32
2.13	Field Emission Scanning Electron Microscope (FESEM)	32
2.14	Zeta Potential Analyzer	33

Chapter Three: Results and Discussion

Figure	Title	Pages
3.1	The XRD pattern of SiO ₂ Nanostructure densified by Oven (200 °C), DPSS Laser (532 nm), and Diode Laser (410 nm)	36
3.2	Absorbance spectra of SiO ₂ nano-sol with different pH values	37
3.3	The FTIR spectra of SiO ₂ samples with different pH values densified by Oven	39
3.4	The FTIR spectra of SiO ₂ samples with different pH values densified by He-Ne laser	39
3.5	The FTIR spectra of SiO ₂ samples with different pH values densified by Diode laser	40
3.6	The FTIR spectra of SiO ₂ samples with different pH values densified by DPSS laser (1079.5 mW/cm ²).	40
3.7	The FTIR spectra of SiO ₂ samples with different pH values densified by DPSS laser (284.09 mW/cm ²).	42
3.8	The FTIR spectra of SiO ₂ samples with different pH values densified by DPSS laser (568.1 mW/cm ²).	42

Figure	Title	Page
3.9	The FTIR spectra of SiO ₂ samples with different pH values densified by DPSS laser (852.2 mW/cm ²).	43
3.10	AFM images for SiO ₂ nanostructure thin film with pH=4 densified by Oven.	46
3.11	AFM images for SiO ₂ nanostructure thin film with pH=4 densified by He-Ne Laser (632nm).	47
3.12	AFM images for SiO ₂ nanostructure thin film with pH=4 densified by Diode Laser (410nm).	48
3.13	AFM images for SiO ₂ nanostructure thin film with pH=4 densified by DPSS Laser (532nm).	49
3.14	AFM images for SiO ₂ nanostructure thin film with pH=7 densified by Oven.	50
3.15	AFM images for SiO ₂ nanostructure thin film with pH=7 densified by He-Ne Laser (632nm).	51
3.16	AFM images for SiO ₂ nanostructure thin film with pH=7 densified by Diode Laser (410nm).	52
3.17	AFM images for SiO ₂ nanostructure thin film with pH=7 densified by DPSS Laser (532nm).	53
3.18	AFM images for SiO ₂ nanostructure thin film with pH=9 densified by Oven.	54
3.19	AFM images for SiO ₂ nanostructure thin film with pH=9 densified by He-Ne Laser (632nm).	55
3.20	AFM images for SiO ₂ nanostructure thin film with pH=9 densified by Diode Laser (410nm).	56
3.21	AFM images for SiO ₂ nanostructure thin film with pH=9 densified by DPSS Laser (532nm).	57
3.22	FESEM images for SiO ₂ nanostructure thin film with pH=4 densified by DPSS Laser (532 nm).	59
3.23	FESEM images for SiO ₂ nanostructure thin film with pH=4 densified by He-Ne Laser (632 nm).	59
3.24	FESEM images for SiO ₂ nanostructure thin film with pH=4 densified by Diode Laser (410 nm).	60
3.25	FESEM images for SiO ₂ nanostructure thin film with pH=7 densified by Oven.	61
3.26	FESEM images for SiO ₂ nanostructure thin film with pH=7 densified by DPSS Laser (532 nm).	61

Figure	Title	Page
3.27	FESEM images for SiO ₂ nanostructure thin film with pH=7 densified by He-Ne Laser (632 nm).	62
3.28	FESEM images for SiO ₂ nanostructure thin film with pH=9 densified by Oven.	63
3.29	FESEM images for SiO ₂ nanostructure thin film with pH=9 densified by Diode Laser (410 nm).	64
3.30	FESEM images for SiO ₂ nanostructure thin film with pH=9 densified by He-Ne Laser (632 nm).	64
3.31	The SiO ₂ sample with pH=4 a: zeta potential, b: the mobility	68
3.32	The SiO ₂ Sol. sample with pH=7 a: zeta potential, b: the mobility	69
3.33	The SiO ₂ Sol. sample with pH=9 a: zeta potential, b: the mobility	70

List of Tables

Chapter Two: Experimental Part

Table	Title	Page
2.1	Specifications of the chemical materials used.	21
2.2	Lasers Used for Densification Process.	25

Chapter Three: Results and Discussion

Table	Title	Page
3.1	XRD data for SiO ₂ sample densified by Diode laser (410 nm).	35
3.2	FTIR Bonds and Wavenumbers for SiO ₂ samples.	41
3.3	FTIR Bonds and Wavenumbers for SiO ₂ samples.	44
3.4	AFM parameters of SiO ₂ nanostructure thin films with pH=4 .	45
3.5	AFM parameters of SiO ₂ nanostructure thin films with pH=7 .	45
3.6	AFM parameters of SiO ₂ nanostructure thin films with pH=9 .	45
3.7	Thickness (nm) of SiO ₂ nanostructure thin films with pH=4.	65
3.8	Thickness (nm) of SiO ₂ nanostructure thin films with pH=7.	65
3.9	Thickness (nm) of SiO ₂ nanostructure thin films with pH=9.	66
3.10	Zeta Potential and the Mobility of SiO ₂ samples.	67

List of Symbols and abbreviations

Symbol	Meaning	Unit
SiO ₂ NPs	Silicon Dioxide nanoparticles	---
CVD	Chemical Vapor Deposition	---
CW	Continuous wave	---
DPSS	Diode Pumped Solid State Laser	---
nm	Nanometer	---
μm	Micrometer	---
R	Molar ratio	---
LED	Light Emitting Diode	---
UV	Ultraviolet	---
Å	Angstrom	---
°C	Silesian Degree	---
λ	Wavelength	nm
k	crystallite shape factor	---
θ	Bragg's diffraction angle	Degree
XRD	X-Ray Diffraction	---
FTIR	Fourier Transformation Infrared	---
UV-VIS	Ultraviolet- Visible	---
AFM	Atomic force microscopy	---
TEOS	Tetraethylorthosilicate	---
EtOH	Ethanol	---
FESEM	Field Emission Scanning Electron Microscopy	---

Symbol	Meaning	Page
t	Crystallite size	nm
β_{FWHM}	Full Width at Half Maximum	Degree
He-Ne	Helium Neon laser	---
HCL	Hydrochloric Acid	---
NaOH	Sodium hydroxide	---
min	Minute	---
mm	Millie meter	---
mA	Millie ampere	---
mW	Millie watt	---
W	Watt	---
DI	De-Ionized	---
I	Power Density	mWatt/cm ²
mV	Millie Volt	---

Chapter One

Introduction and Basic Concepts

1.1 Introduction

The "Nano" is a term that originated from the Greek nanos which means dwarf. It is one billionth of a meter. It's related to nanoscience and nanotechnology. This branch of science and technology deals with materials having at least one dimension in the size range of 1 to 100 nm [1].

Because of the promising electrical, optical, magnetic, and other properties, nanomaterials are of interest. These important properties have the potential for major influence in medicine, electronics, and other fields. The materials at the nanoscale can have distinct properties which can lead to greater chemical reactivity and affect their strength this related to increases in the surface area to volume ratio [2].

Out of all necessary fields of science and technology such as defense, aerospace, and dentistry, nanotechnology is rapidly sweeping and this includes in synthesis, characterization, design, and application of material and devices on the nanometer scale. The nanoscale provided an opportunity to improve novel classes of advanced materials which meet the request from high-tech applications for chemical, physical, and biological properties which differ from the individual molecules and atoms properties of bulk material [3]. In materials science, chemistry, and physics metal oxides play a very substantial function and using in fabrication of microelectronic circuits, coatings for the passivation of surfaces against corrosion, sensors, and as catalysts in technological applications [4]. Silicon Dioxide (SiO_2) has been a topic of intense research due to its stellar chemical and physical features.

Silicon dioxide exists in two forms : the amorphous form continues as the focus of much fundamental research to understand its electronic structure, bonding characterization, defects, and optical properties because it is the best form known. The second form is crystalline such as quartz [5].

The silicon dioxide had been synthesized by varied techniques. For applications in optical, microelectronics, electrical and such different fields there is an important interest in the synthesis of crystalline and uniform material. Sol-Gel method had been vastly shown a very adaptable manner wet chemical techniques for production of a large set of photonic materials in different configurations, including fibers and films for optical device applications, monoliths, and coatings [6]. The process was used in the 1930 by the Schott glass company in Germany to obtain metal alkoxides. A modern interest appears in the early of 1970 when monolithic inorganic gels formed at low temperatures and then converted to glasses without high temperature melting processes [6].

Due to its ability to control the particle size, size distribution and morphology through systematic monitoring of reaction parameters the Sol-Gel process is significantly used to produce pure silica particles [3]. A low temperature method, Sol-Gel is used for the fabrication of inorganic or composite organic materials such as glasses, thin films, ceramics or powders of high homogeneity and purity [6]. It is based on the mix-up liquid reactants on a molecular scale and solidification of solution into a porous amorphous oxide gel. It has attracted increasing scientific and technological attention [7].

Laser processing had been used to sample Sol-Gel films for different applications in slab waveguides, channels and optics. In addition, laser processing awards the possibility to densify selected layers within a multi-layer stack, by matching laser energy with selected absorbers in materials within the stack [8].

Sol-Gel process used to produce sensor materials for optical chemical sensors and biosensors [9]. This due to a number of advantages, including ease of fabrication and the design flexibility of the process. Furthermore, the versatility of the Sol-Gel process enables optimization of sensor by controlling Sol-Gel film properties such as thickness, coating length, and porosity [10].

1.2 Nanomaterials

The cornerstones of nanoscience and nanotechnology are nanoscale materials which defined as a collection of materials where at least one dimension is less than 100 nanometers [2]. Nanotechnology deals with small-sized materials or tiny structures. The standard dimension extends from sub nanometer to several hundred nanometers. A nanometer (nm) is one billionth of a meter, or 10^{-9} m [11]. The nanomaterials structure can be categorized by their dimensions. The nanoparticles are zero-dimensional nanostructures. Fibers, nanowires, and nanorods are the one-dimensional nanostructures. Thin films are the two-dimensional nanostructures. The applications in different scopes of nanomaterials based on their physical properties, large surface area and small volume and predictable to have a wide range in multiple fields such as optical communications, electronics, and biological systems [1].

At the nano scale the physical properties change while when the same material at bulk scale, its physical properties are fixed ignored of its size. The percentage of surface atoms increase in smaller particles and this increase, leading to change in chemical and physical behavior of the materials [12].

Due to their substantial applications in materials technologies including optics of nanodevices, electronics, and analytical technologies [13, 14]. SiO₂ Nanoparticles had a novel properties result from their specific structure, which differs from bulk such as photoluminescence [15, 16], and catalysis [17].

There were many methods had been used for obtaining silica particles which could be classified into two main approaches: top-down and bottom-up as shown in Fig.(1.1). Top-down or 'physical approach' characterized by decrease the dimensions of original size via utilizing special size decreasing techniques. Bottom-up or 'chemical approach' is a common way used for producing silica nanoparticles from molecular or atomic scale. Some of the vastly used methods for synthesizing silica nanoparticles are Sol-Gel method [18].

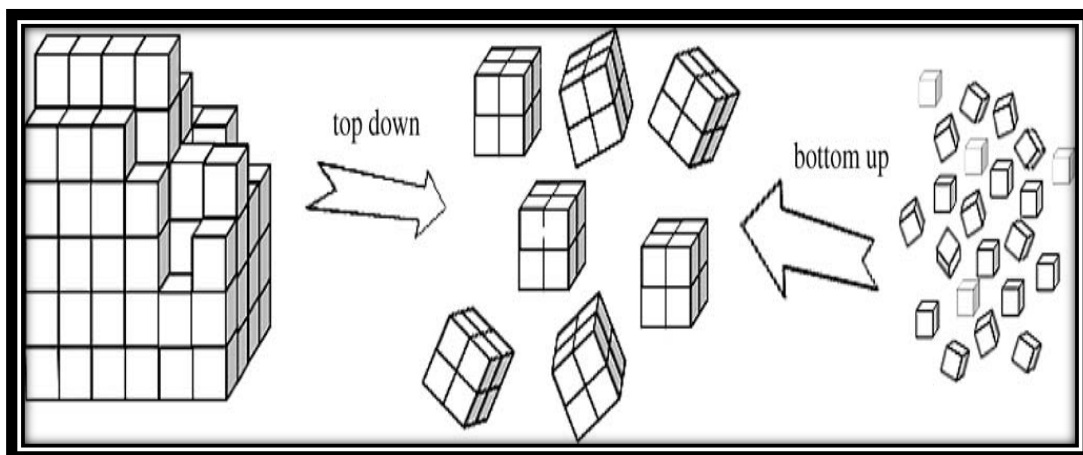


Fig.(1.1): represent the Top-Down and Bottom-Up approaches to produce nanomaterials [19].

1.3 Silicon Dioxide Nanoparticles (SiO₂ NPs)

Silicon Dioxide Nanoparticles are one of the most common minerals on earth and a basic component of sand, soil, and rocks, including quartzite and granite.

It could be found in both amorphous and crystalline forms [20]. The amorphous form is frequently found in a three-dimensional polytetrahydral structure where the two oxygen atoms of one SiO₂ molecule are associated with a silicon atom of another SiO₂ molecules, while crystalline silicon has the same structure as diamond [21]. Silica nanoparticles are inexpensive to produce, easy to prepare, and are used as additives or modifier in the formulation of plastics, paints, and rubber [20].

Furthermore, because of their easy preparation and wide uses in different industrial applications such as pigments, catalysis, thin film substrates, electronic and thermal insulators, they occupy a prominent position in scientific research [22]. They also used in variety products ranging from cosmetic to construction materials [23]. SiO₂ is an important kind of semiconductive material which used as the filler of plastic, rubber, coating and gooey because of its good properties of heat-resistance, weatherability and chemical stability [24]. Silicon has an indirect band gap material, unlike other semiconductors, and exhibits notable changes in electronic and optical properties [25].

1.4 Synthesis of Silicon Dioxide Nanoparticles

Generally, the methods for synthesis SiO₂ NPs could be classified into three broad categories: Physical, Biological, and Chemical synthesis, which illustrated in Fig.(1.2) [26].

The physical approach is characterized by reducing the dimension of the original size by utilizing special size reduction techniques. While, the chemical approach is a common way used to obtain silica nanoparticles from molecular or atomic scale [3].

Sol–Gel method seems to be one of the most attractive approach, offering the advantage of thin film preparation over a large area at a comparatively low cost amongst the multiple techniques available for preparation [6]. The structure of nano-oxides formed by Sol-Gel method depend on the nature of the precursors, the preparation condition, and the ion source [5].

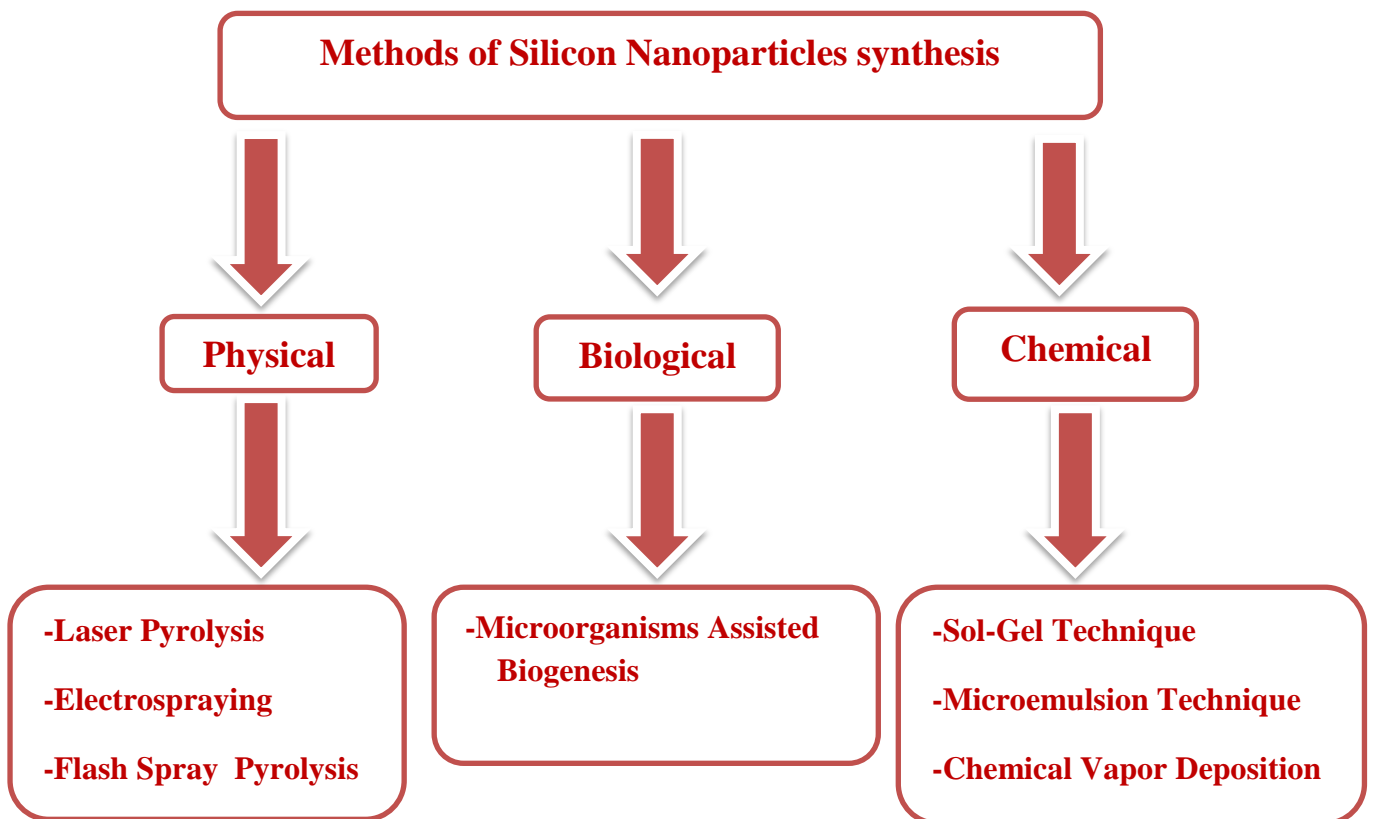


Fig. (1.2): Illustrates the methods of synthesizing SiO₂ NPs [26].

The Sol-Gel method is particularly useful. Its advantages are effective stoichiometric control and the production of ultrafine particles with a narrow size distribution in relatively short processing time at low temperatures [27].

1.4.1 Sol-Gel Method

A chemical technique that uses metal alkoxides as precursors for production and synthesis of glasses, composites and ceramics through a set of chemical-physical processes, including hydrolysis, condensation, and thermal treatment. Silicon alkoxide is one of the metal alkoxides used for the preparation of Sol-Gel materials [6,28]. It involves inorganic networks evolution through colloidal suspension (Sol) formation, and a network forming in a continuous liquid phase (gel) due to gelation of the sol, and finally the solvent removal.

There are some processing parameters affect the nature of the resultant siloxan particles as well as their aggregation state and, accordingly, govern the characteristics of a particular Sol-Gel inorganic network. The most important parameters are: catalyst, pH value of the solution, H_2O/Si molar ratio R , reaction temperature, and addition of drying control chemical additive. Thus, by controlling these factors, it is possible to vary the structure and properties of the Sol-Gel-derived inorganic network over wide ranges [28 - 30].

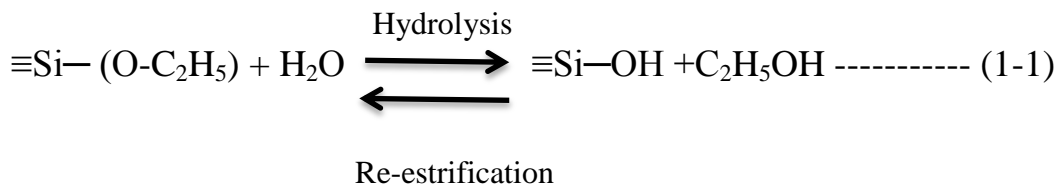
Using of Sol-Gel methods due to several advantages: ease of composition control, good homogeneity, low equipment cost, low processing temperature, and the ability to fabricate large area coatings.

Sol-Gel process enables better control of composition and optical properties of the materials with good control of thickness and refractive index, this is important to obtain suitable materials for optical applications [31]. The disadvantages, on the other side, as the high cost of the raw materials that makes it suitable only for high quality products, the large shrinkage in the final product, and long processing time [6, 29].

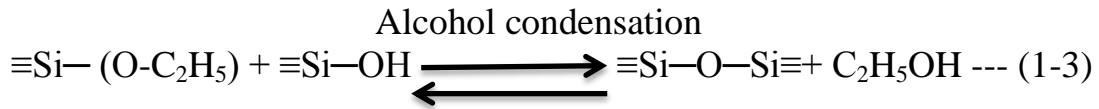
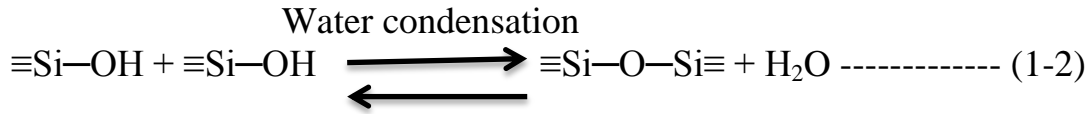
1.5 Steps of Sol-Gel Synthesis Method

1.5.1 Hydrolysis & Condensation Reactions

Hydrolysis of precursors is the first stage of Sol-Gel process that could be defined as the reaction of silicon alkoxide (TEOS) with water, forming a silicon hydroxide Si(OH) which is known as a silanol groups. Through this reaction a hydroxyl (OH) group attaches itself to silicon atom by replacing alkoxide group (O-C₂H₅), according to the following reaction [32]:



As soon as some hydrolyzed molecules are present in the solution, the condensation reaction starts taking place at the same time and with the same reaction path as the hydrolysis, depending on the R- molar ratio and catalyst present in solution. The condensation reaction can follow two different schemes as in equations (1-2) and (1-3), involving the silanol group Si(OH) produces siloxan bond (Si—O—Si) by-product of water or alcohol [32,33].



The two reaction path of condensation can occur instantaneously and at any pH value, but still one of them dominated depending on *R*-molar ratio.

1.5.2 Aging & Drying

Gel aging is an extension of the gelation process that involves a continuous change in properties and structure of the completely immersed gel in a liquid after the gel point. The gel has a high ratio of liquid and three dimensional interconnected pores inside the structure, so that drying process is the main step of removing the liquid from the tiny pores [34, 35].

Drying by evaporation leading to pressure gradients in the liquid within the pores, so the network is compressed more at the surface than in the bulk, causing further shrinkage of the gel network. In addition, the evaporation process increases the vapor-solid interface, which makes the liquid flows from the bulk of the gel to cover a small size of the surface, because the evaporation of the liquid cannot cover the whole surface without the creation of a meniscus on the pore surface [36,37].

As a gel dries, the stiffness of the solid phase increases, so the liquid pressure also increases, and when reaches its maximum value, the volumetric contraction rate of the gel will be slower than the rate of evaporation, and the solid phase becomes stiffer.

Beyond that point, further evaporation causes the liquid-vapor interface to move into the gel towards the bulk of the solid phase leaving a dry solid. This is a critical time because in it cracks of the gel typically occur. To avoid this phenomenon, a slow evaporation of the liquid is required [28, 38].

1.5.3 Densification

Densification is the last treatment process of Gel. Heat treatment at high temperature of the porous Gel is necessary to produce dense glass or ceramic from the Gel. After the high temperature treatment, the pores eliminated, and the densification temperature depends extremely on the degree of connection of the pores, dimension of the pores, and the surface area in the stature [39]. The Steps of Sol-Gel Synthesis Method are shown in Fig.(1.3) [40].

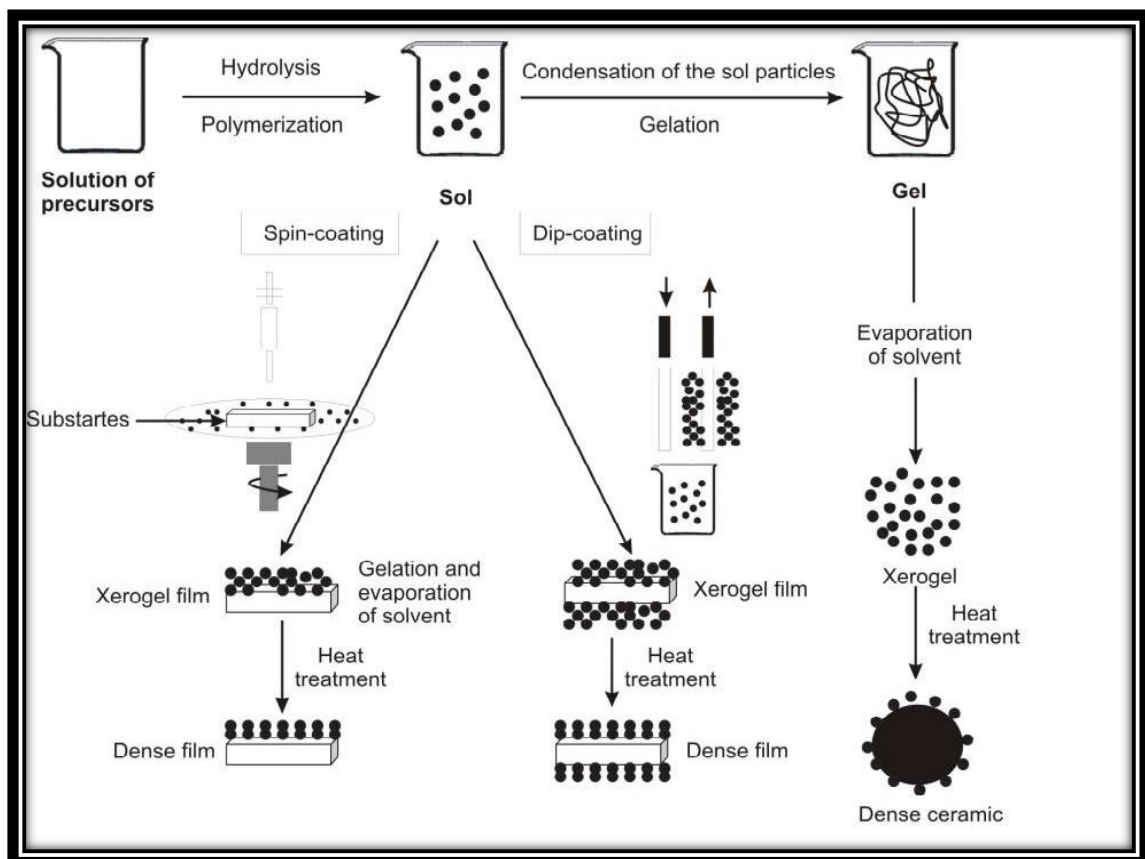


Fig. (1.3): Steps of Sol-Gel Synthesis Method [40].

1.6 The Effect of Technological Parameters in Sol-Gel Method

The Sol-Gel method could be explained as the transition from a liquid (colloidal or solution) into a solid (or multiphase gel). The structural and textural properties of the synthesized materials are affected by different parameters involved in the Sol-Gel technique. The initial reaction conditions such as :Precursor material, molar ratio (R) of reactants, pH, solvent composition, temperature, aging, and drying conditions are essentially influenced the sol-gel method [41].

1.6.1 Precursor

Sol-Gel precursors have to be reactive enough to participate in the gel formation and soluble in the reaction media. Alkoxisilanes and water reaction is very gentle to avoid phase separation and leading to good homogeneity [42].

1.6.2 pH/Catalysts

Silica dissolution and reprecipitation are affected by pH [43]. When the particulates have a high solubility in the sol, at high pH values, porous structures were obtained. Smooth pore networks and dense structure were obtained at low pH values due to low dissolution-reprecipitation rate [44].

Films thickness, porosity, shrinkage, and optical quality depend on the type of catalyst used for precursor solution preparation [45].

1.6.3 The Water: Precursor Molar Ratio

Hydrolysis and condensation rate increases with increasing the water content at fixed concentration of precursor. Molar ratio of reactants affect the gelation time and the pore size. Low water: precursor molar ratio means less gelation time [42].

1.6.4 The Temperature, Aging and Drying

Water, alcohol, and other volatile components losses due to drying under atmospheric conditions leads to gel shrinkage [43], and high stresses in the structure consequently [46]. Aging is a rather slow process at room temperature [47]. The increment in the porosity is due to increasing thermal treatment temperature.

1.7 Coating Techniques of Thin Film

The coating steps had to be done in a clean room and the substrate had to be cleaned totally in order to obtain wet chemical coatings with high optical qualities on transparent glass slides. Sol-Gel method for manufacturing thin films offers potential advantages over classical techniques such as : easy coating for large area, low thickness, and high purity. There are three common techniques which are used to make a thin film : Dip coating, Spin coating and Spray coating technique [48].

1.7.1 Dip Coating Technique

Dip coating technique is a process in which the substrate to be coated was immersed in a solution and then withdrawing with a specific withdrawal speed.

Where the substrate to be coated is immersed in a liquid and then withdrawn with a well-defined withdrawal speed with controlled atmosphere and temperature conditions. The schematic of the dip coating technique is shown in Fig.(1.4) [48].

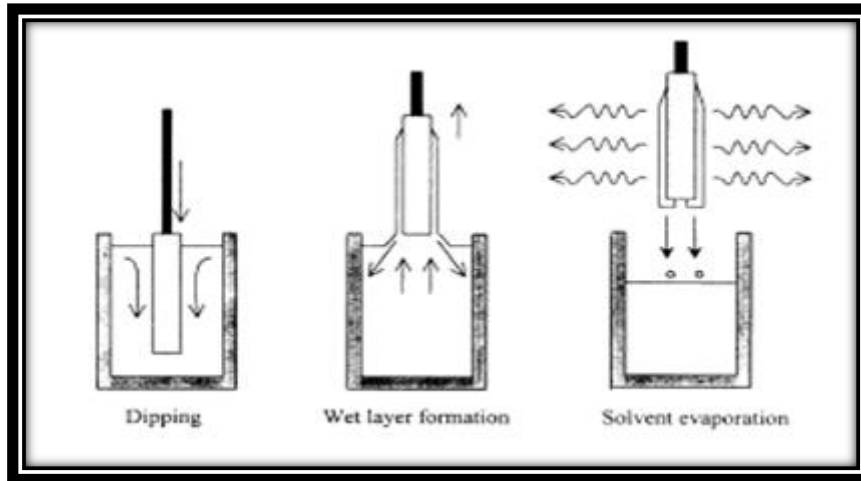


Fig.(1.4): Dip coating process: the substrate dipping in the solution, wet layer formation, and solvent evaporation [48].

In this technique, the atmosphere controls the evaporation of the solution and the following destabilization of the sols due to solvent evaporation leading to gelation and formation of transparent film because of small particles size (nanometer range) in the sol. The gelation process during dip coating process is shown in Fig.(1.5) [48].

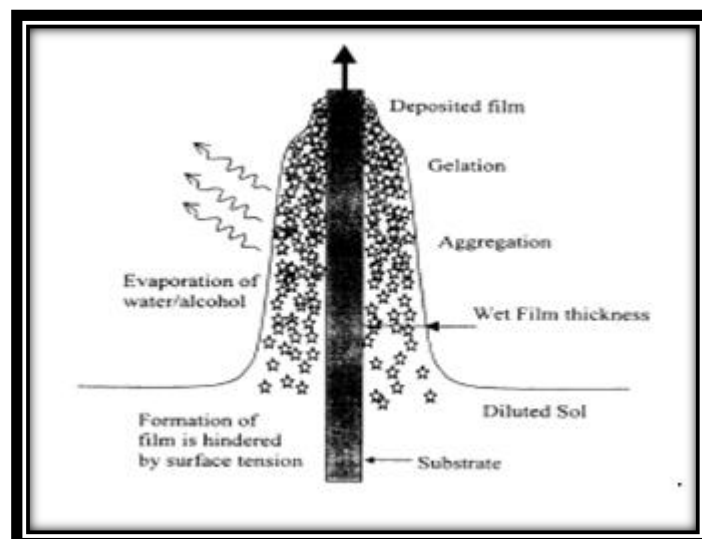


Fig.(1.5): Gelation process during dip coating process [48].

The obtained film had to be densified by heat treatment and the densification temperature depending on the composition. The withdrawal speed, liquid viscosity, and the solid content are mainly defined the coating thicknesses [48]. There were numerous forces acting on the coating at withdrawing which are : moving the substrates causing viscous drag upward, surface tension force, inertial force, surface tension gradient, and conjoining or disjoining pressure [49].

The important part of the dip-coating process is choosing a suitable viscosity of the thicknesses of the coating can be differed with high accuracy from 20 nm up to 50nm while maintaining optical quality [48].

1.8 Applications of Silica Nanoparticles

The importance of Silica Nanoparticle is in increasing due to their applications in optical devices, drug delivery, bioimaging, cosmetics, catalysis, polymeric fillers, and other biomedical fields. Researchers have already found that cell type, size, dose, surface area, time, and structural discrimination are closely linked to cytotoxicity of silica NPs [50]. In photomedicine the amorphous silica is used because of the high toxicity of crystalline silica (amorphous silica can be converted into crystalline silica by heating at high temperatures). The specific surface of the Silica NPs increasing by the porosity which allows the permeability of entrapped drugs and small molecules, e.g. oxygen, between the core and surface of the nanoparticles [51]. Silica NPs also used in Biomedical imaging, which help to diagnose fatal diseases in early stages and lead to more efficient treatments [50].

The applications of nanotechnology had expanded to several areas, such as electronics, medicine, and in cosmetic industries due to enhanced features included transparency, color, and solubility of particles at nanoscale. Silica NPs had been vastly used in cosmetics because of the nanoscaled size, which enables them to pass through human skin [50].

Silica nanoparticles are employing in electronic field for light emission applications.[52,53]. They are offer fascinating optical and electronic properties comparing with bulk silicon and have been investigated for photovoltaic applications [54-56]. Silicon nanostructures, such as nanowires, porous silicon nanowires and silicon nanoparticles are used as Photocatalysts [57-59].

1.9 Laser Densification

Laser Densification technique was used to heat the coating layer sufficiently to be densified without melting or warping the substrate. There are many differences between densifying a Sol-Gel coating in a furnace versus with a laser. The heating with a laser making organic burnout occur in a short time due to the effective heating of the laser beam. While when the heating is done with a furnace the organics can burnout on the order of several minutes. The Sol-Gel films successfully densified by laser radiation in a much faster time scale comparing with conventional oven process [60].

The optical losses in the laser-densified coating were higher than in the traditional densification using furnace firing for coating of the same composition [61].

During Laser firing, the heating and cooling occurs very rapidly depending on laser beam parameters [62,63] and affords the possibility of forming films with chemistries, structures, and, hence properties which are difficult or impossible to obtain in conventional furnace fired sol-gel films [8]. The properties of films densified by Laser are different than those fired by furnace. Laser firing allows the heat used to densify films to be concentrated near the surface, so high refractive index films may be densified on softer substrates under proper conditions. The most beneficial and exciting aspect of laser processing of sol-gel films is the potential for producing materials and systems with novel properties [8].

The most common techniques used for densifying sol-gel films with lasers are : direct and indirect Heating, as shown in Fig.(1.6) [8].

In the direct heating technique the sample is exposed to laser energy which was absorbed directly by the coating, by the substrate, or by both. The direct writing mode had been used in investigations of laser densification because of its simplicity. It could be more efficient than furnace technique [8].

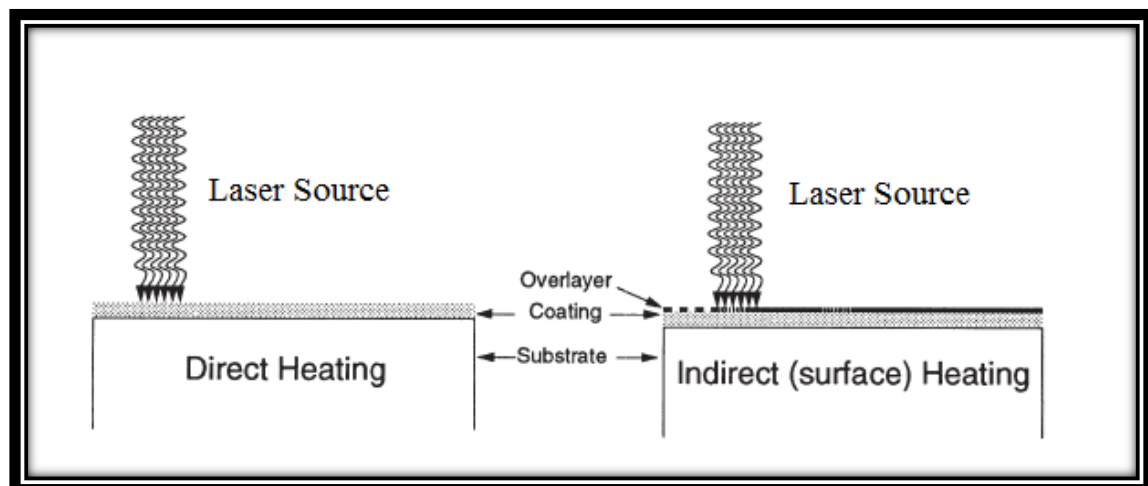


Fig.(1.6): Schematic of laser processing using (a) direct heating, and (b) indirect (surface) heating [8].

In "surface heating," or indirect writing technique a coating which is transparent to the laser radiation is covered with an absorbing over layer. The over layer (usually metallic) absorbs the laser energy, causing localized heating at the surface of the sol-gel film. This approach is more complicated than the direct heating process. The indirect heating had a few restrictions on the composition of the coating, the heating comes from the interaction of laser with the over layer, rather than with the sol-gel coating [8].

Laser densification was used to produce lenses and arrays of densified gel silica matrices at a critical processing conditions such as initial density of the matrix, laser parameters, and ambient atmosphere. It is used to achieve complete densification of gel-silica glass and produce a higher index region than that of the un-irradiated matrix. Lasers are used to modify surface properties, such as hardness or refractive index of materials [8].

Laser processing is more effective for treatment of thin surface layers [64] and improves the optical properties of the porous gel-silica substrate [8]. Laser densification could be used in wide applications in different fields such as impact on the silicalite optical characteristics, fuel cells, and glass ceramic tapes[65-67].

1.10 Literature Survey

Sol-Gel method is an easy and simple way for preparing a three-dimensional metal oxide and it did not require complicated equipment [68, 69]. The shape and formats of oxides could be controlled by Sol-gel processing [70].

Krchnavek R. R. et al. in 1984 [71] used an Ar⁺ ion laser (514.5 nm) to partially densify SiO₂ films on silicon substrates. The laser energy was transparent to the film, but absorbed by the substrate, which heated the coating from underneath.

Shaw J.D. et al. in 1990 [72] reported that laser densification of Sol-Gel silica is possible. There was an interaction between Sol-Gel prepared silica and 10.6 μm wavelength laser radiation. Hardening of the silica had been measured up to the value for fused silica.

Taylor J.D. et al. in 1990 [60] reported that coupling the Nd:YAG laser power to the sol-gel derived coatings produced localized surface heating on the samples. Laser firing is substantially different from furnace firing.

Zaugg T.C. et al. in 1991 [73] had densified SiO₂-TiO₂ films by scanning a CO₂ laser beam across the surface. He found that the refractive index of coatings densified by laser is higher than that of furnace fired coatings, even after annealing coatings to 700 °C.

Fabes B.D. et al. in 1992 [74] had used CO₂ laser to densify Sol-gel derived SiO₂-TiO₂ and WO₃ films. A competition between forming an appropriate morphology (smooth, uncracked films) and avoiding crystallization arises in the SiO₂-TiO₂ system when waveguides are formed by laser densification.

Taylor J.D. et al. in 1992 [61] reported that 10.6 μm CO₂ Laser irradiation had used to densify sol-gel derived silica coatings on SiO₂ and Si substrate. The evolution of the composition and properties of the laser-fired samples were different than for furnace-fired samples.

Birnie P.D. et al. in 1993 [75] reported that Laser processing was used to modify the spectral properties of local regions of sol-gel SiO_2 and SiO_2 - TiO_2 multilayer stacks coatings.

Fardad M. A. in 2000 [45] had found that the film thickness, shrinkage, porosity, and optical quality depend on the type of catalyst used in the preparation of the solution precursor.

Zhai J. et al. in 2001 [31] had prepared thin films of two binary titania-silica compositions by the Sol-Gel method and studied their crystallization as a function of heat treatment conditions using both conventional and CO_2 laser heating.

Rao K.S. et al. in 2005 [76] reported that using sol-gel process to prepare monodisperse and uniform-size silica nanoparticles. The silica particles were obtained by hydrolysis of tetraethylorthosilicate (TEOS) in ethanol medium. Various-sized particles in the range 20–460 nm were synthesized.

Kesmez O. et al. in 2010 [77] reported that antireflective nanometric SiO_2 films were formed on glass substrates by dip coating from a colloidal SiO_2 sol having an average particle size of 9 nm, obtained SiO_2 films were in 80–200 nm thickness range.

Krumov E. et al. in 2013 [78] reported that as a result of excimer laser irradiation, the film microstructure is strongly modified and a higher specific surface area is obtained. It is observed that amorphous to crystalline phase transition occurs in the exposed sol-gel ZrO_2 film areas.

Hawelka D. et al. in 2014 [79] reported that drying, gelation, and transformation of ZrO_2 printed sol-gel coatings was done by laser treatments.

CW Diode Laser was used to dry the wet thin film and remove the organic ingredients. A second Diode laser in pulsed operation was used for the functionalization of the films. The formation of a tetragonal ZrO_2 phase was achieved by laser treatment.

Khyoon A. H. et al. in 2016 [80] study the effect of pH variation on the particle size of SiO_2 thin films. He found that all films have nano scale and the particle size around (19-62) nm, the size of silica particles increases with increasing pH value of the solution.

1.11 Aim of the work

The specific aims of this project are:

1. Prepare SiO_2 nanostructured thin films with different pH values by Sol-Gel synthesis method using dip coating technique.
2. Study the effect of laser densification on prepared nanostructured SiO_2 thin films by sol-gel technique, and make a comparison between samples treated with an oven (conventional method) and others treated with laser (Laser Densification) and study their structure, optical properties, surface morphology, and the effect of the laser densification on the samples.

Chapter Two

Experimental Part

2.1 Introduction

This chapter includes all the experimental activities which have been done involving the chemical materials utilized, synthesis of SiO₂ nanostructure thin films, procedures, parameters effect, characterization devices (identification techniques) and other equipment.

2.2 Procedure

2.2.1 Chemical Materials

The precursor (TEOS), the solvent Ethanol (EtOH), and other chemical materials which were used in this study and their specifications are all listed in Table (2.1).

Table (2.1): Specifications of the chemical materials used.

Chemical material	Chemical formula	Molecular Weight (g/mol)	Purity %	Physical form	Density (g/cm ³)	Supplier
Tetraethylorthosilicate (TEOS)	Si(OC ₂ H ₅) ₄	208.33	98	Transparent liquid	0.933	Sigma-Aldrich (Germany)
Ethanol absolute (EtOH)	C ₂ H ₅ OH	46.07	99.9	Transparent liquid	0.785	—
Deionized Water	H ₂ O	18	high degree of purity - empty of additional ions	—	1	—
Hydrochloric Acid	HCl	36.46	35.4	Transparent liquid	1.19	General Drug House-India
Sodium hydroxide	NaOH	40.00		White	—	General Drug House-India

2.2.2 Samples Preparation

SiO₂ samples prepared in three groups with different pH values (acidic, neutral, and alkaline) shown in Fig.(2.1), as the following procedure :

The samples prepared by mixing tetraethoxysilicate (TEOS) as a precursor material (2 ml), Ethanol as a solvent (4 ml) (Solution A) with deionized water (4 ml), Ethanol (2 ml), and (50 μ l) of HCL or NaOH as a catalyst (Solution B). The samples prepared with a molar ratio (R=2). The mixture puts on the magnetic stirrer for 2 hours at room temperature, Fig. (2.2), then left in closed flasks for several days for aging.

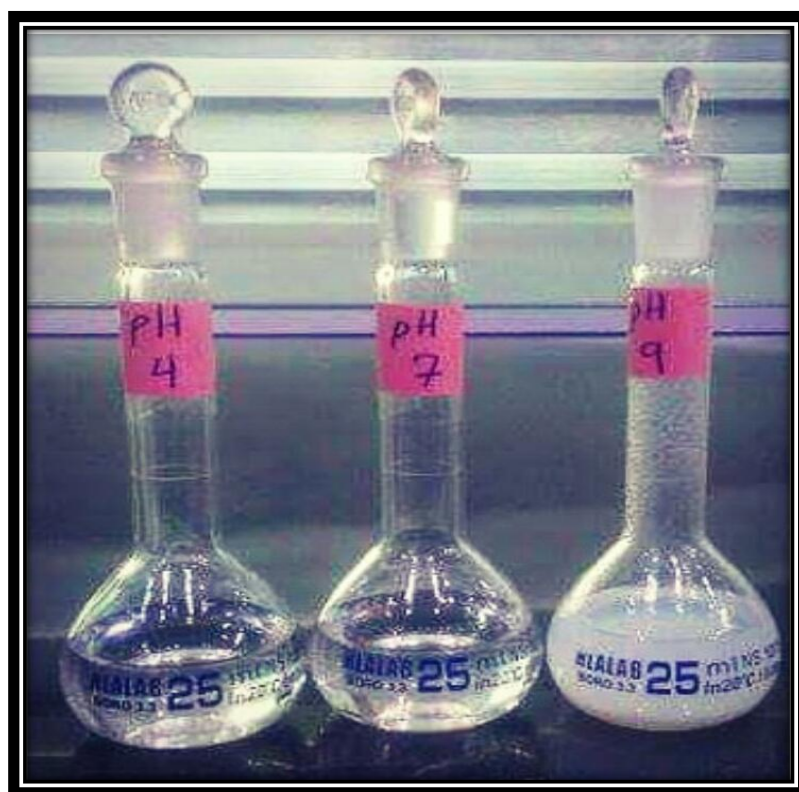


Fig.(2.1) : SiO₂ Samples with Different pH Values.

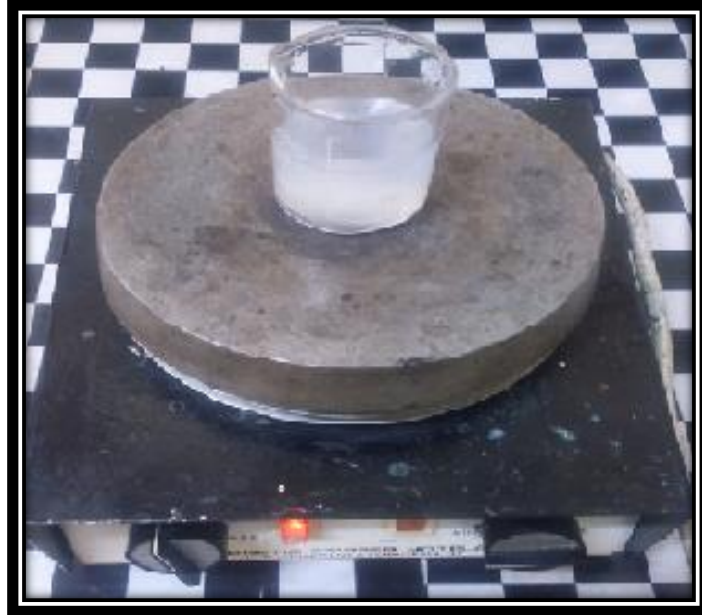


Fig.(2.2) : Magnetic Stirrer.

2.2.3 Thin Films preparation

Dip coating technique was used to fabricate SiO_2 nanostructure thin films at room temperature as shown in Fig.(2.3). SiO_2 thin films were made on glass microscope slides with dimension 25.4×76.2 mm and 1.2 mm thick, which had cleaned before using for deposition process. Ultrasonic cleaner was used for washing the slides with ethanol for 10 minutes. The steps of coating are: immerse the substrate into the sample, wet layer was formed by extracting the substrate, and the gelation of the layer by solvent evaporation. The cleaned glass slides were dipping in the mixture by a controlled withdrawal speed of 10 mm/min; the glass slides were carried out in the air at room temperature with similar speed. The dipping processes were repeated twice to get a thin layer of SiO_2 films. The resulting film then dried on a Hot Plate at 100°C for an hour.

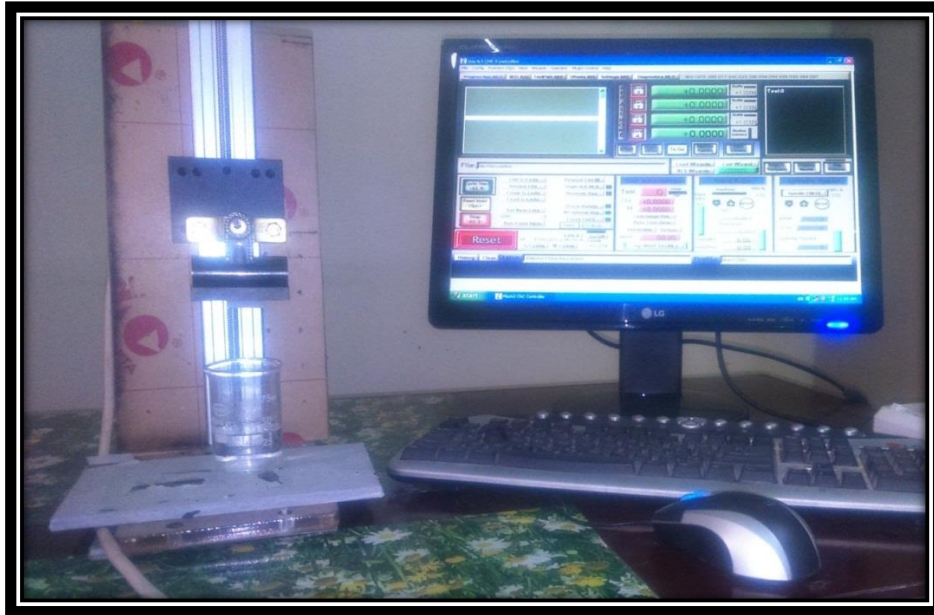


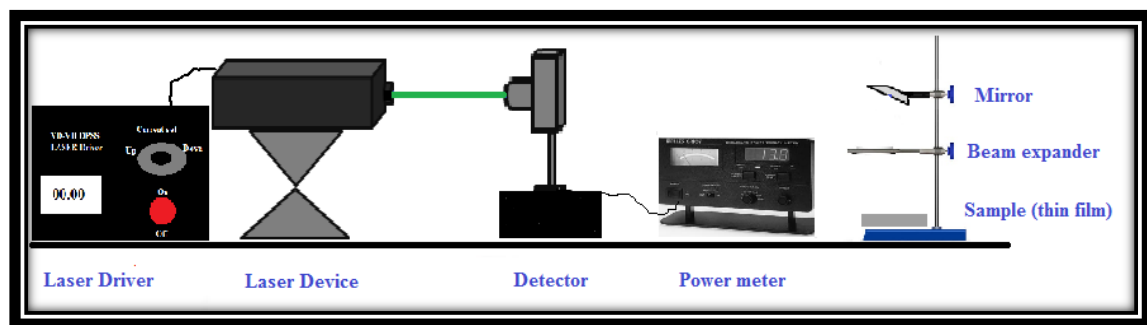
Fig.(2.3) : Dip Coating Technique.

2.2.4 Densification Process

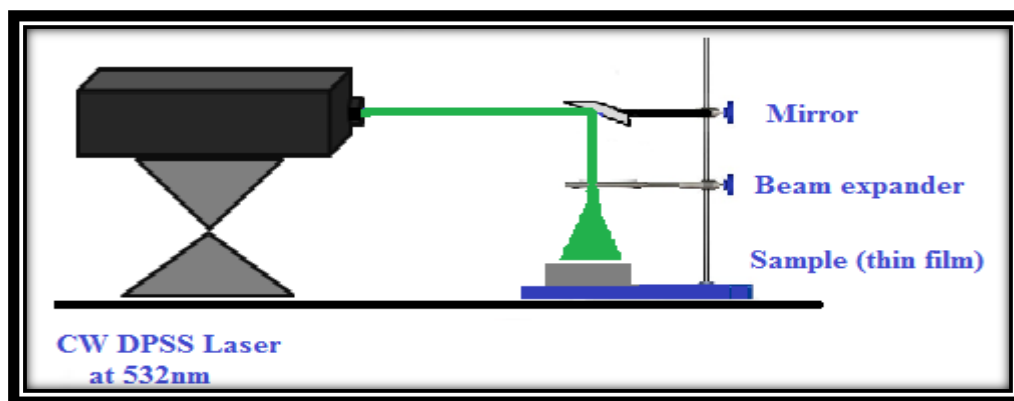
The final step for synthesis SiO_2 nanoparticles is densification process which done after drying process using oven and laser (heat treatment conditions of thin films using both conventional densification and laser densification). SiO_2 thin film densified by Oven at 200°C for 2 hours and others by lasers with different wavelengths and power densities for 15 minutes as shown in table (2.2). The lasers used are He-Ne laser (632 nm), CW Green Diode Pumped Solid State (DPSS) laser (532 nm), and Diode laser (410nm). The experimental setup is shown in Fig. (2.4), (2.5) that was used for the three types of laser which consist from; laser source, a mirror used to obtain a vertical alignment on the sample, and beam expander used to expand the laser beam and to extend it to the whole sample. The laser Power-meter supplied by (Melles Griot-America) was used for measuring the laser power.

Table (2.2): Lasers Used for Densification Process.

Laser Source	Wavelength λ (nm)	Power Density I (mW/cm ²)
He-Ne Laser	632	0.056
Diode Laser	410	56.8
DPSS Laser	532	284.09
		568.1
		852.2
		1079.5



(a)



(b)

Fig. (2.4): Schematic diagram of the Experimental Setup (a) Measuring the power, (b) The beam expanded on the sample.

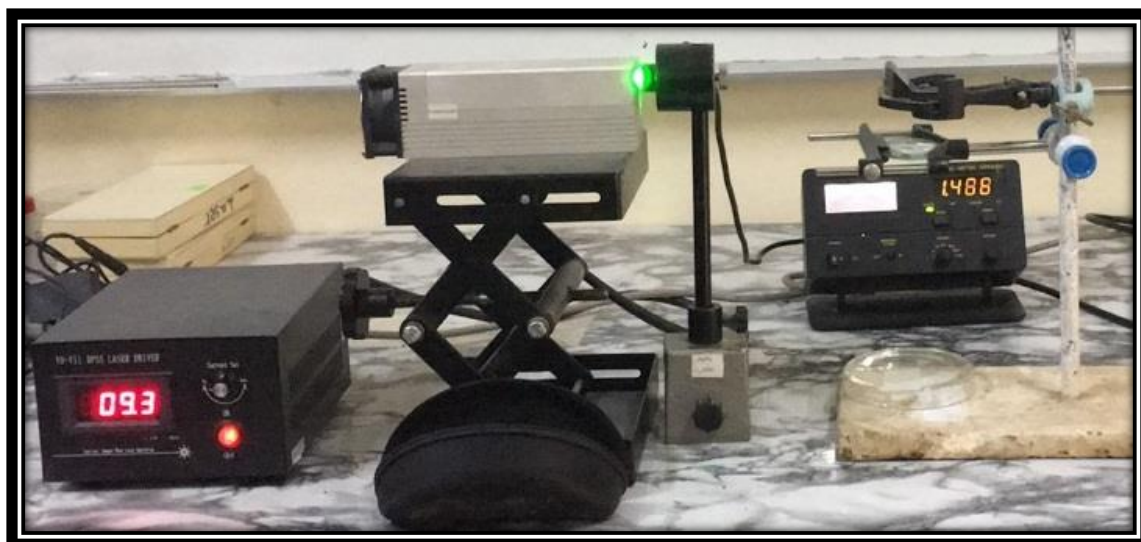
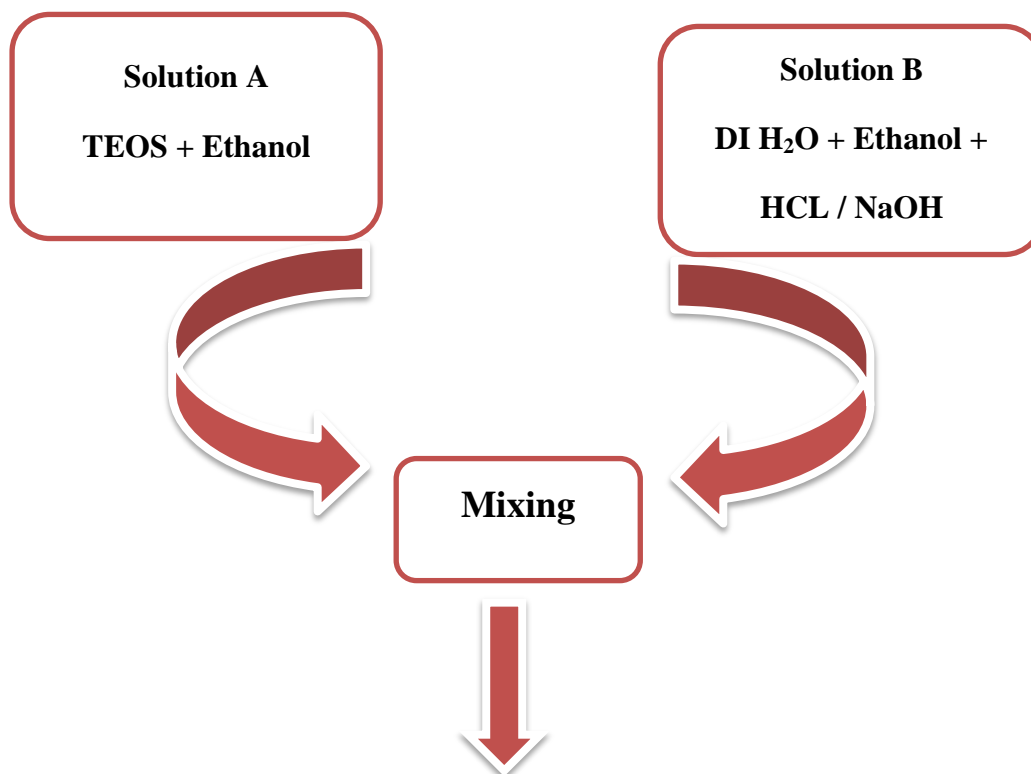


Fig.(2.5): The Experimental Setup.

The preparation steps of SiO₂ nanostructured thin films are shown in Fig. (2.6):



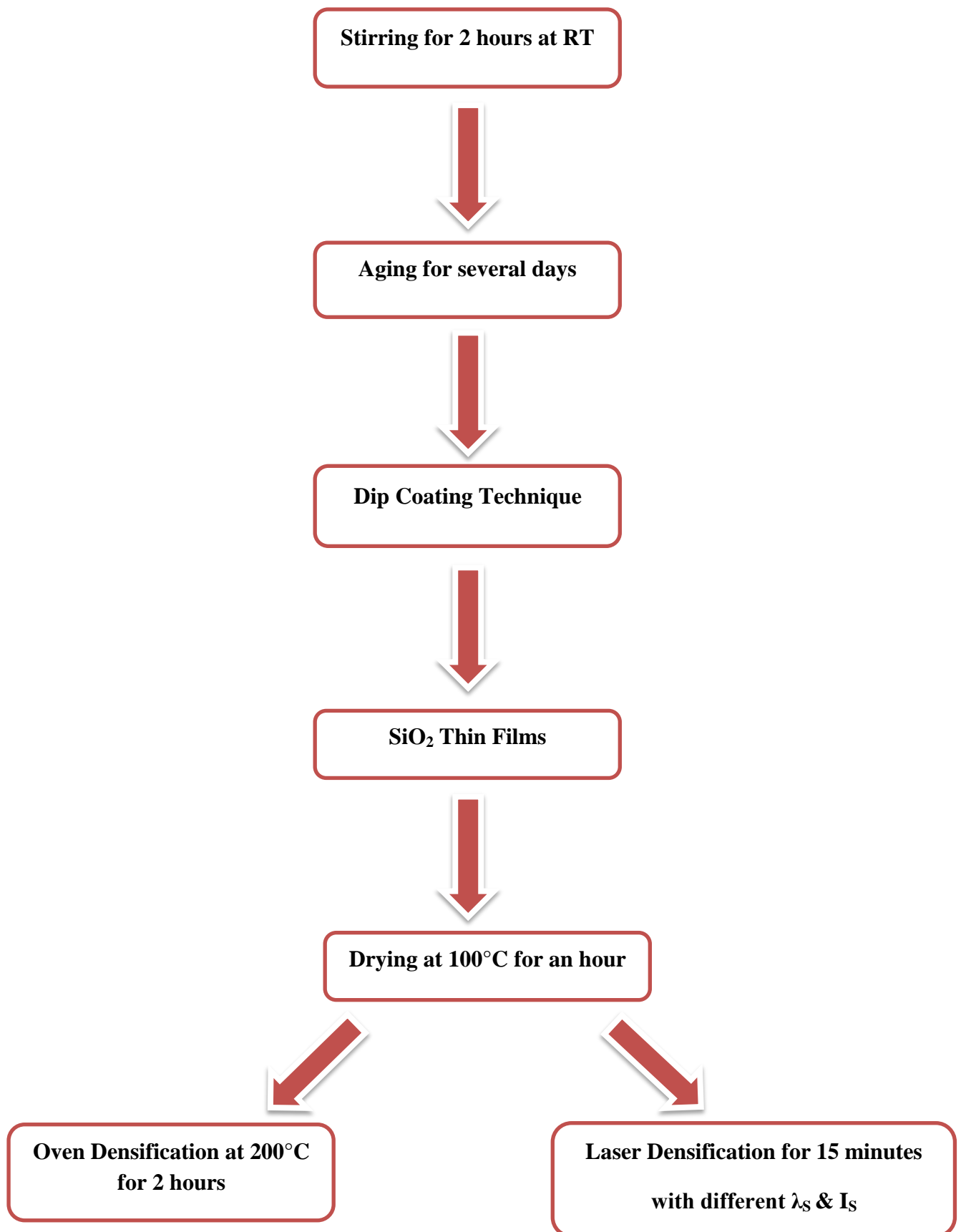


Fig.(2.6): Block Diagram shows the Preparation Steps of SiO₂ Nanostructured Thin Films by Sol-Gel Technique.

2.3 Identification Techniques

Structure measurements and Characterization of nanoparticles are important to realize and control the nanoparticles synthesis and their applications. It is performed using a variety of different techniques as shown in Fig.(2.7) :

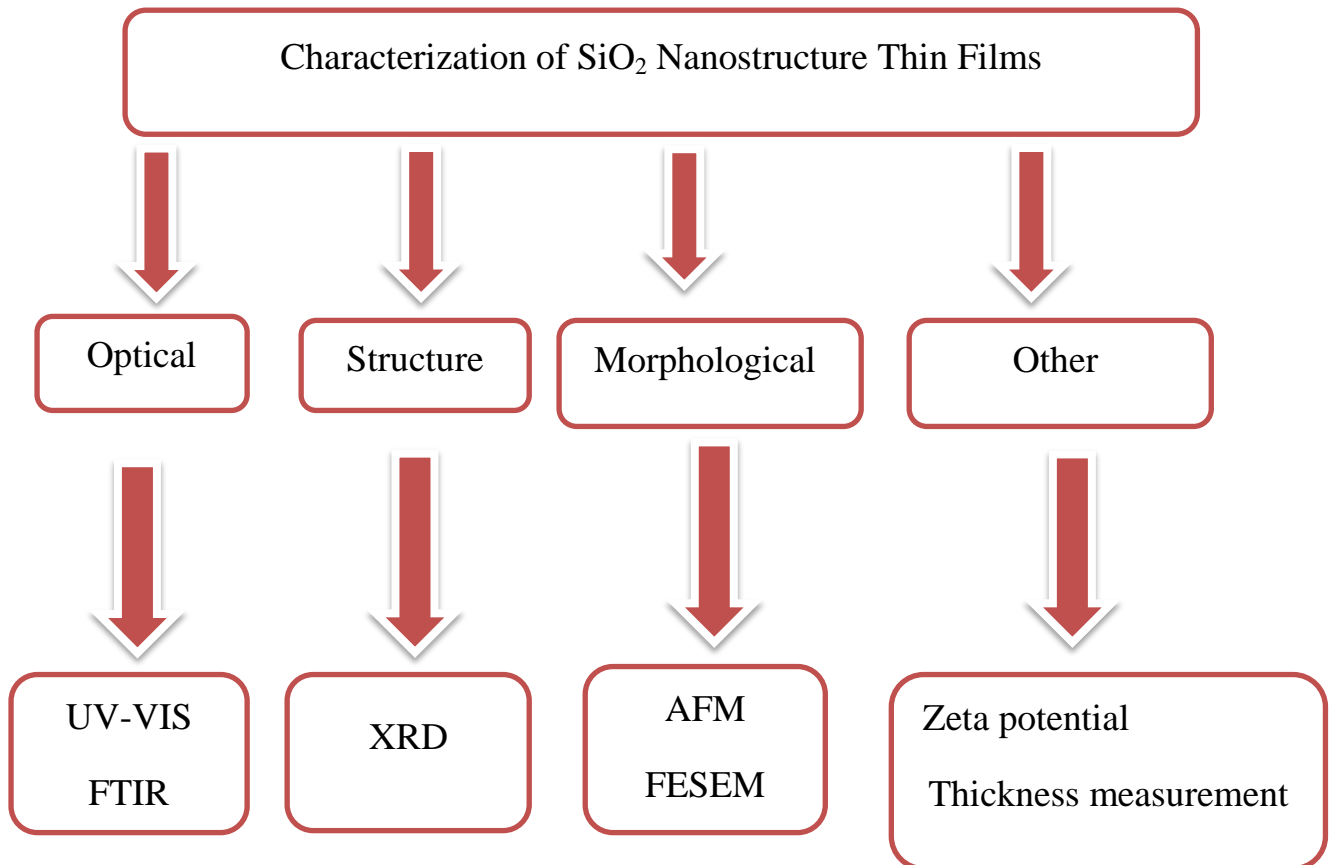


Fig. (2.7) Block diagram of the Characterization of SiO₂ Thin Films.

2.3.1 X-Ray Diffraction (XRD)

The X-ray diffraction (XRD) patterns were obtained (Philips X-pert 3040/60), Fig.(2.8), to determine the crystalline size. The XRD patterns were at the scanning range 2θ from 20° to 60° . (Baghdad University, college of science, geology department).

The X-ray diffraction is a useful method to study the structure of compounds and investigate the effect of thermal treatment on the improving of crystalline of prepared sample. It is a useful method to measure the average spacing between layers or rows of atoms. The average size of the crystallite was calculated from XRD peak broadening according to Debye–Scherer equation (2-1) as shown below [81] :

$$D = (K \lambda) / (\beta_{FWHM} \cos\theta) \dots\dots(2-1)$$

where, D: the crystallite size,

K: crystallite shape factor of a good approximation of (0.9),

λ : the wavelength of the incident X-ray ($\lambda = 0.154056$ nm),

β_{FWHM} : the Full-Width at Half-Maximum (FWHM) of the XRD,

θ : the Bragg angle.

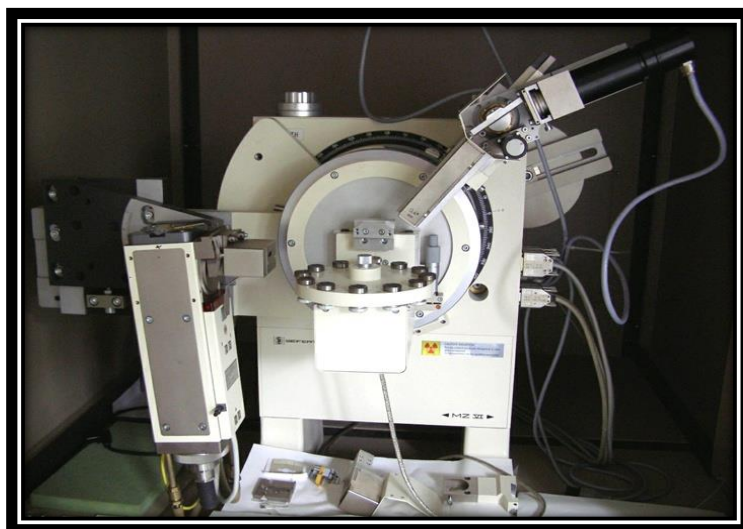


Fig.(2.8): X-Ray Diffractometer.

2.3.2 UV-VIS Spectrophotometer

UV–Vis spectroscopy was used to verify nano silica formation. The UV-VIS absorption spectrum of all prepared SiO₂ Solution samples measured using Shimadzu UV-VIS 1800 spectrophotometer, covering an average from (190 – 1100) nm, as shown in Fig.(2.9).

This instrument was computerized with a CRT screen and keyboard for operating the input value. (Baghdad University, college of science, chemistry department).

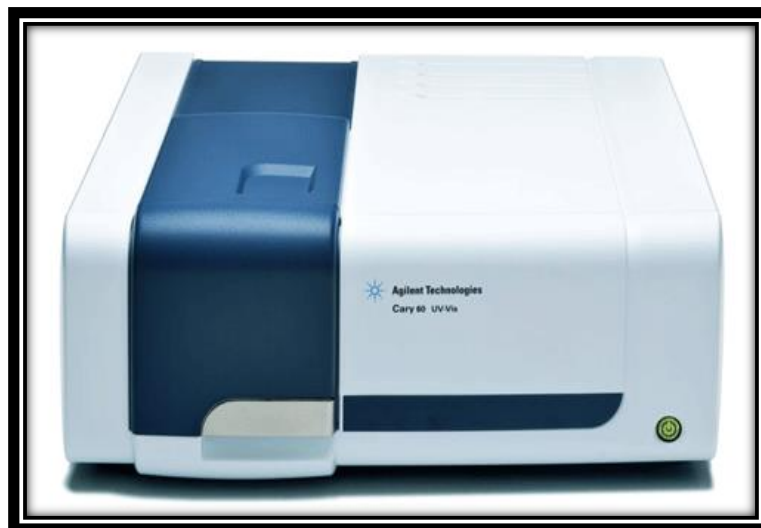


Fig. (2.9) The UV-VIS Spectrophotometer.

2.3.3 Fourier Transformation Infrared Spectrometer (FTIR)

The Fourier-transform infrared spectra was obtained using Shimadzu 8400S corporation FT-IR spectrophotometer (Baghdad University, college of science, chemistry department) as shown in Fig.(2.10). This technique was used to investigate the molecular structure of the densified SiO₂ nanoparticles.



Fig. (2.10): Fourier transformation infrared Spectrometer.

2.3.4 Atomic Force Microscopy (AFM)

The morphology and particle size could be determined by AFM. The topography measurements of the prepared samples were carried out using AA3000 Scanning Probe Microscope (Angstrom Advanced Inc. USA), of resolution 0.26 nm laterals and 0.1 nm vertical as shown in Fig.(2.11) (Baghdad University, college of science, chemistry department).



Fig.(2.11): Atomic Force Microscope.

2.3.5 Thickness measurement

The thickness of SiO_2 films was measured using Thin film measurement system model Epp 2000 as shown in Fig.(2.12). This system includes BLK-CXR-SR-25 spectrometer, rang 220-1100 nm, resolution < 2.5 nm, deuterium light sources R600-8-uv-vis reflectance probe, sample fixture with probe holder (Ministry of Science and Technology).



Fig. (2.12): Thin Film Measurement System Model Epp 2000.

2.3.6 Field Emission Scanning Electron Microscope (SEM)

The topography of the prepared films and particle size measurements were studied using Field Emission Scanning Electron Microscopes (FESEM) as shown in Fig.(2.13).



Fig.(2.13): Scanning Electron Microscope.

2.3.7 Zeta Potential analysis

Zeta potential analysis (Zeta plus Brookhaven- 90Bundle Instruments Corporation - USA) .(Ministry of Science and Technology), Fig.(2.14), was used to measure the potential difference between the dispersion medium and the stationary layer of fluid attached to the nanoparticle.



Fig.(2.14): Zeta Potential Analyzer.

Chapter Three

Results and Discussion

3.1 Introduction

In this chapter, the effect of conventional densification and laser densification of SiO₂ nanostructure thin films which prepared by sol-gel technique and a comparison between them will be investigated. The comparison between samples densified by oven and others by laser allows us to select a suitable method for densification process. Three different wavelengths in the visible region have been used to investigate the effect of wavelength due to these spectral regions are closed to the absorption peak of SiO₂. The lasers used are He-Ne laser (632 nm), DPSS laser (532 nm), and Diode laser (410 nm). The result of structure, morphological and optical properties of SiO₂ samples will be discussed in details. These results were obtained from measuring devices such as : X-ray diffraction (XRD), UV-VIS Spectrophotometer, Fourier Transformation Infrared Spectrometer (FTIR), Atomic Force Microscope (AFM), Field Emission Scanning Electron Microscope (FESEM), Zeta Potential Analysis, and Thickness measurement.

3.2 Structure properties of SiO₂ Nanoparticles

3.2.1 X-Ray Diffraction Analysis

Fig.(3.1) illustrated the X-Ray diffraction patterns of SiO₂ nanostructure thin films with (pH=7) prepared by Sol-Gel synthesis method characterized by X-Ray Diffractometer (XRD) using CuK_α ($\lambda = 1.54 \text{ \AA}$) as a radiation source. These samples were densified using oven (200°C), DPSS laser (532 nm), and Diode laser (410 nm) respectively. The pattern of SiO₂ sample densified by oven shows a broad band at the position $2\theta=24.5^\circ$ at the left side of the pattern.

When the DPSS laser used for the densification process the band have a little shift to the lower value of the diffraction angle ($2\theta=24.2^\circ$) and the diffraction peak intensity become higher. These results mean that the structure of SiO_2 is amorphous in nature which are in a good agreement with [82-84, 23].

The using of Diode laser (410 nm) making the band shifted to the left side of the pattern more than DPSS laser and Oven, producing the main diffraction peak of cristobalite structure at $2\theta= 21.7^\circ$, this result is in a good agreement with [85], and an increasing in the diffraction peak intensity indicating an improvement in the crystallinity of the material and show two broad bands in the range from ($2\theta=9.8^\circ$ to 30°). X-ray diffraction data for SiO_2 sample densified by Diode laser (410 nm) are summarized in table (3.1).

The obtained results proved that the power of different lasers did not affect on the structure of the material, while the wavelength was an effective parameter on laser densification, where the cristobalite structure was appeared only with Diode laser (410 nm) because it was closer to the absorption of SiO_2 .

Table (3.1): XRD data for SiO_2 sample densified by Diode laser (410 nm).

Diode laser (410 nm)	FWHM (rad.)	2θ (deg.)	t (nm)
Peak 1	0.21269	9.8	4.93
Peak 2	0.21269	21.7	4.46

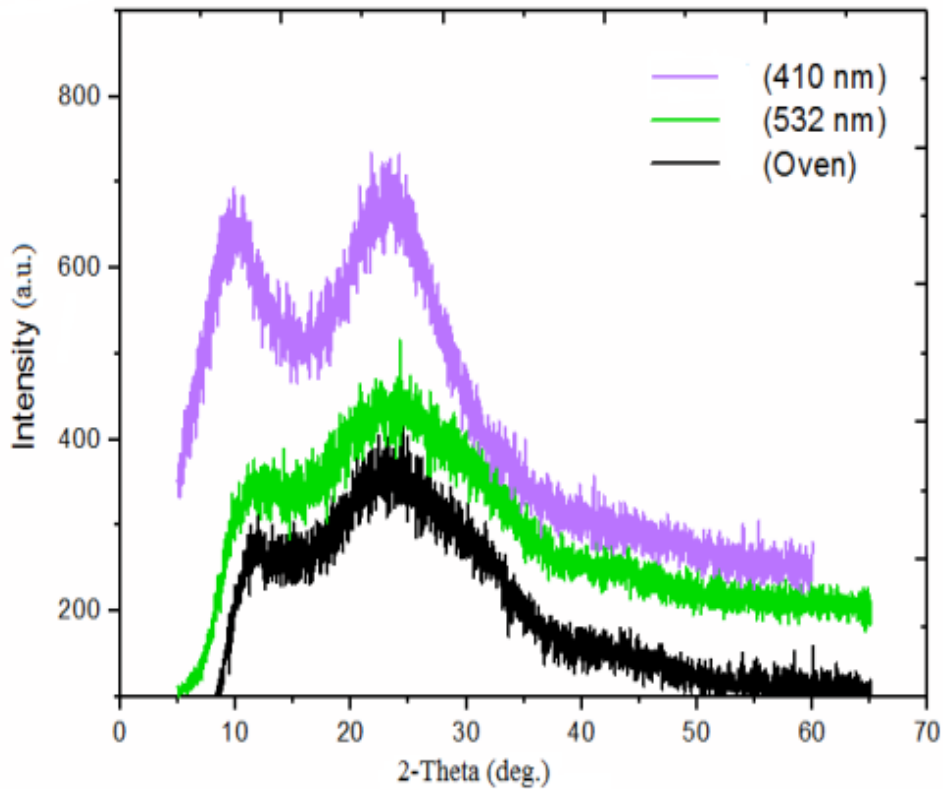


Fig. (3.1): The XRD pattern of SiO₂ samples densified by Oven (200 °C), DPSS laser (532 nm), and Diode laser (410 nm).

3.3 Optical properties of SiO₂ nanoparticles

3.3.1 UV-VIS spectroscopy

Optical properties of SiO₂ samples prepared by Sol-Gel method were measured by UV/Vis Spectrophotometer. The UV-Vis. Optical properties were in the range from (190 to 1100) nm at different pH values. The absorbance spectra of SiO₂ solution before the densification process prepared by Sol-Gel synthesis method with different pH values is shown in Fig.(3.2) which reveals the formation of silica by showing the absorption maxima at (200 nm) for SiO₂ sol. with pH=4, (198 nm) for SiO₂ sol. with pH=7, and (197 nm) for SiO₂ sol. with pH=9.

UV-visible spectroscopy results showing synthesized materials absorbance in the UV region and very low absorbance shows in the visible region. These results are in a good agreement with [5].

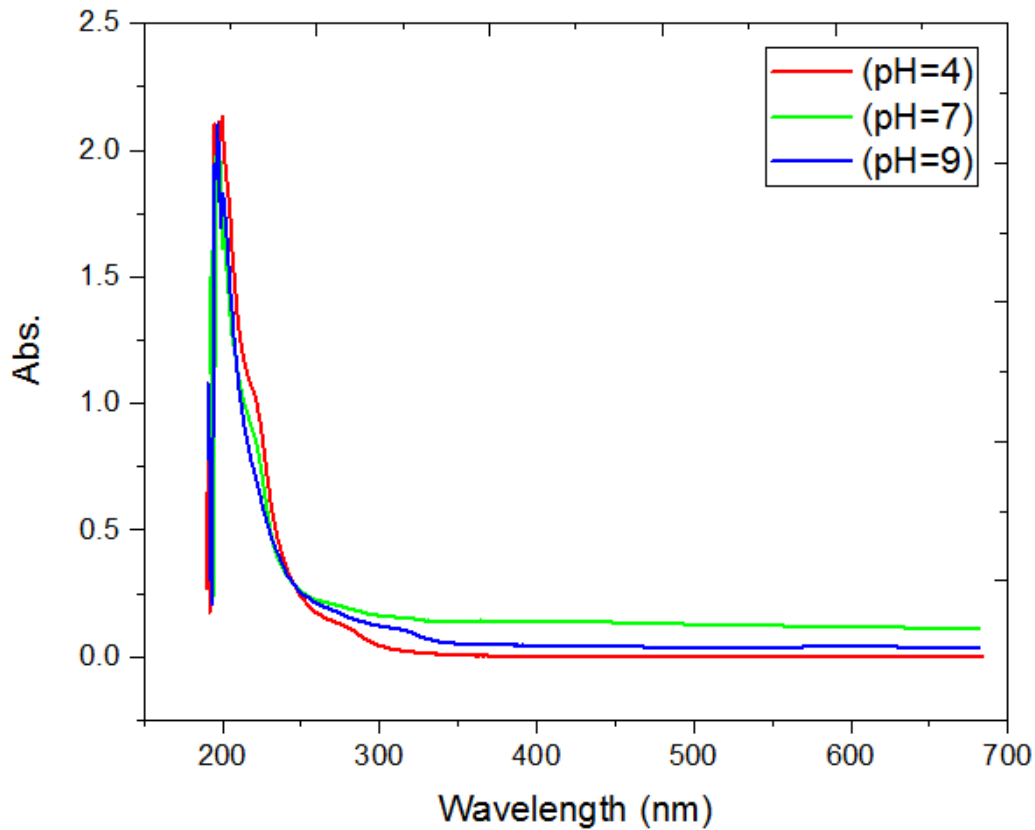


Fig.(3.2): Absorbance Spectra of SiO₂ Sol. with different pH values.

3.3.2 Fourier Transformation Infrared Spectrometer

FTIR spectra yield important information on the compactness of the silica network, molecular structure and composition of the sample. The FTIR spectra for SiO₂ samples after densification process in the range of 4000 cm⁻¹ to 400 cm⁻¹ at different pH values.

As shown in Fig.(3.3) to (3.9) IR spectra of SiO₂ samples vary according to their composition and may be able to show the occurrence of the complication and interaction between various constituents. Such interaction could induce changes in vibrational modes of the atoms or molecules in the material, which in turn changes the physical and chemical properties of the constituents of the complex.

Figures of FTIR spectra of SiO₂ samples with different pH values (4,7, & 9) densified by oven (200°C), DPSS laser (532 nm, with different power densities), Diode laser (410 nm), and He-Ne Laser (632 nm), showed three bands of Si–O–Si bond vibration. The bands of H–O–H bending vibration of H₂O and the O–H vibrations from different species. These results are in a good agreement with [86-88]. It is important to note the Si–OH band vibration which is in a good agreement with [89]. The Si-Si bond due to oxygen vacancies which is in a good agreement with [90, 91].

FTIR bonds and wavenumbers (1/cm) for SiO₂ samples with different pH values densified by oven and different laser wavelengths are summarized in table (3.2).

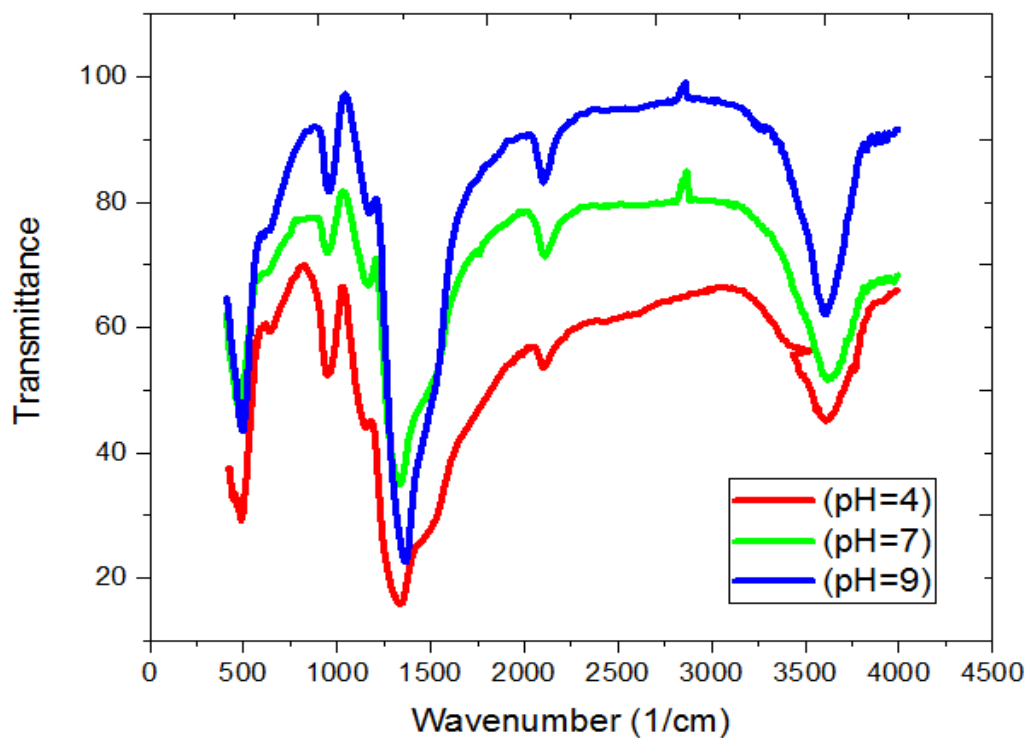


Fig.(3.3): FTIR spectra of SiO₂ samples with different pH values densified by Oven.

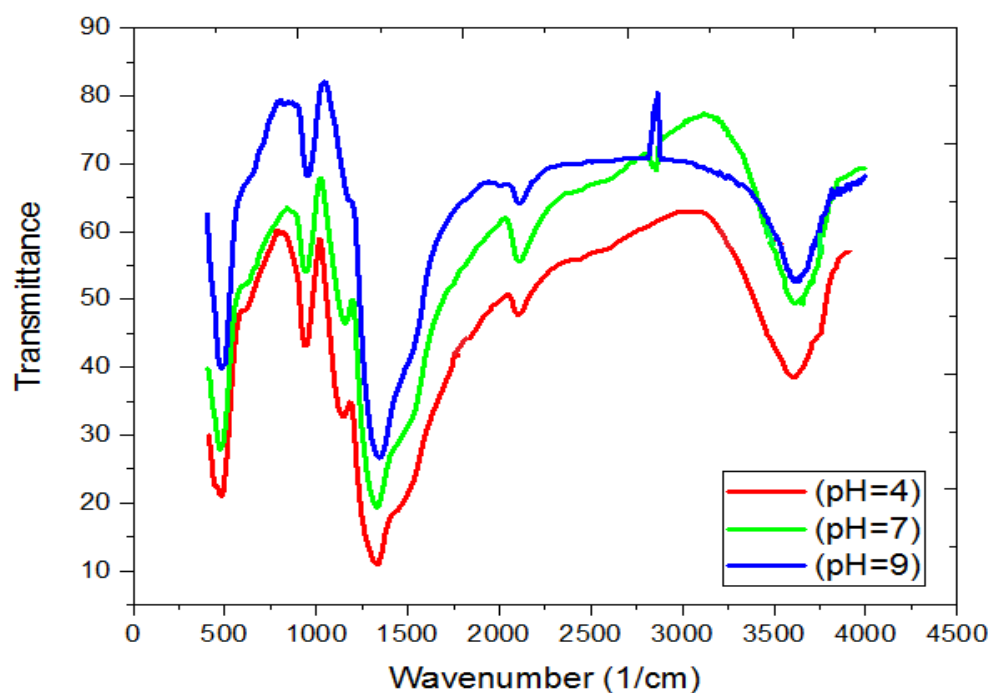


Fig.(3.4): FTIR spectra of SiO₂ samples with different pH values densified by He-Ne laser (632 nm).

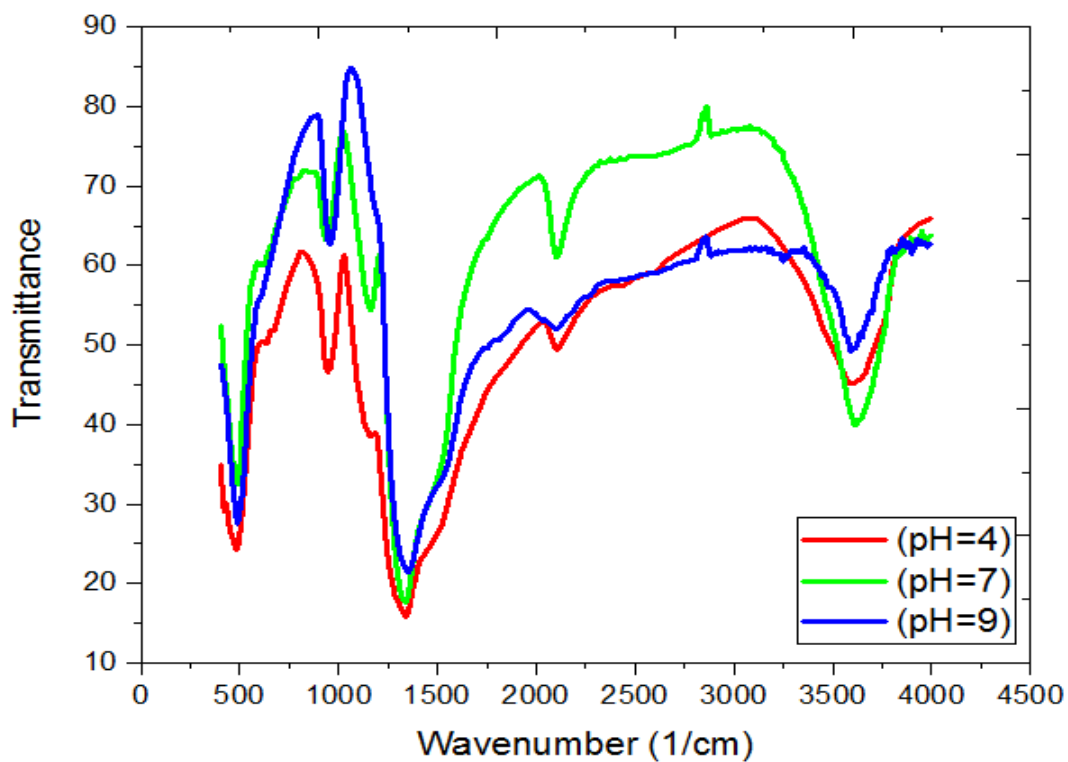


Fig.(3.5): FTIR spectra of SiO₂ samples with different pH values densified by Diode laser (410 nm).

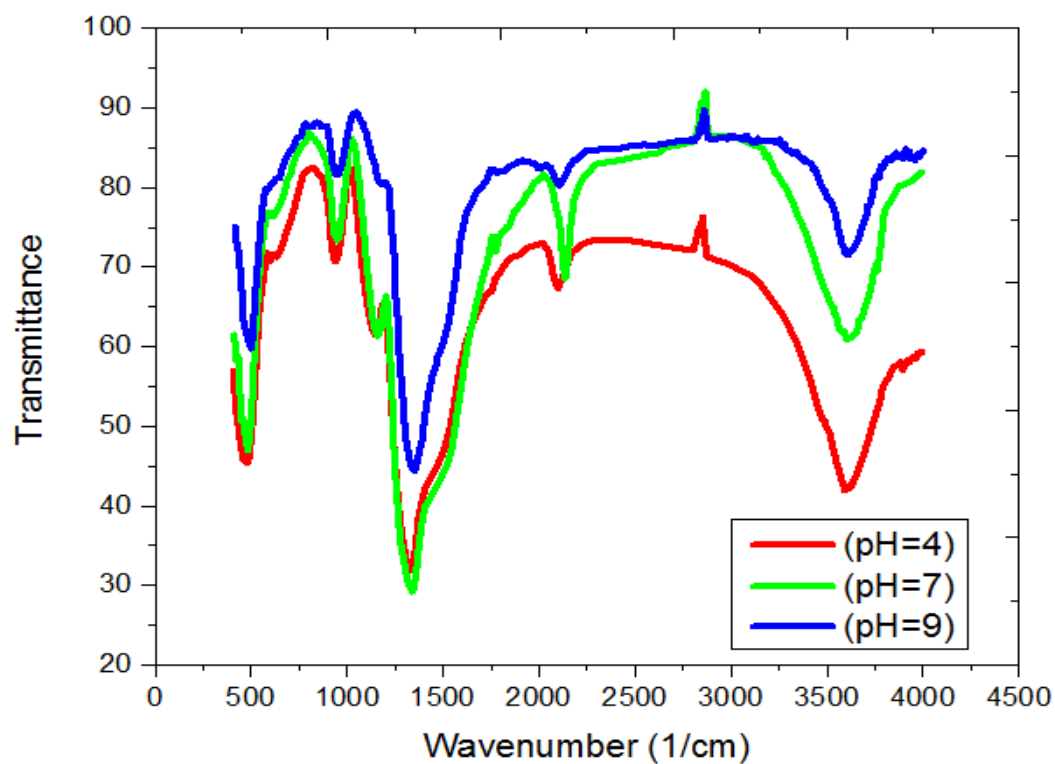


Fig.(3.6): FTIR spectra of SiO₂ samples with different pH values densified by DPSS laser (532 nm) (1079.5 mW/cm²).

Table (3.2): FTIR bonds and Wavenumbers (1/cm) for SiO₂ samples with different pH values densified by Oven, DPSS laser (532 nm) (1079.5 mW/cm²), Diode laser (410 nm), and He-Ne laser (632 nm).

Bond Type	Wavenumber (1/cm) for Oven	Wavenumber (1/cm) for DPSS Laser	Wavenumber (1/cm) for Diode Laser	Wavenumber (1/cm) for He-Ne Laser	pH value
Si-O-Si	478	478	487	487	4
Si-O-Si	832	797	806	815	
Si-O-Si	1034	1024	1015	1015	
Si-O-Si	478	468	487	496	7
Si-O-Si	860	860	870	888	
Si-O-Si	1024	1034	1024	1015	
Si-O-Si	468	496	496	478	9
Si-O-Si	851	806	870	870	
Si-O-Si	1050	1043	1060	1052	
H-O-H	1343	1334	1353	1353	4
H-O-H	1344	1325	1344	1344	7
H-O-H	1344	1362	1344	1334	9
O-H	3604	3595	3595	3604	4
O-H	3622	3604	3613	3622	7
O-H	3604	3604	3595	3613	9
Si-OH	942	952	942	942	4
Si-OH	942	933	942	942	7
Si-OH	942	942	952	961	9
Si-Si	605	633	605	605	4
Si-Si	633	586	605	614	7
Si-Si	596	586	586	586	9

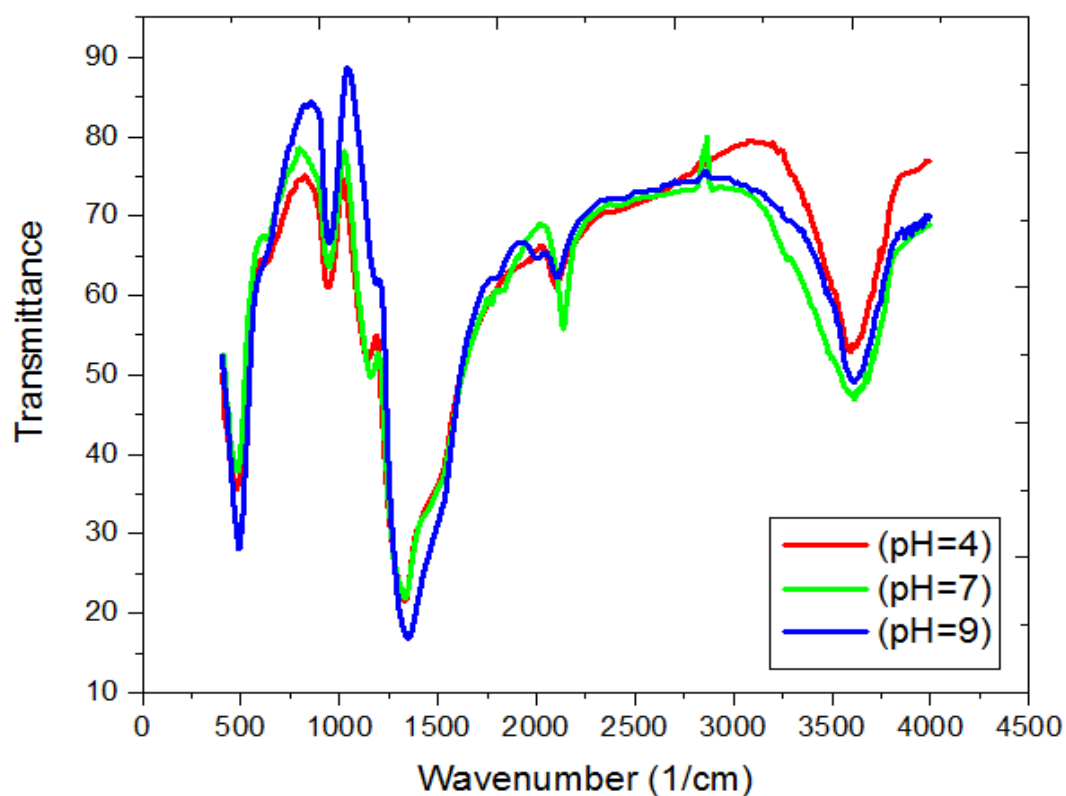


Fig.(3.7): FTIR spectra of SiO₂ samples with different pH values densified by DPSS laser (532 nm) (284.09 mW/cm²).

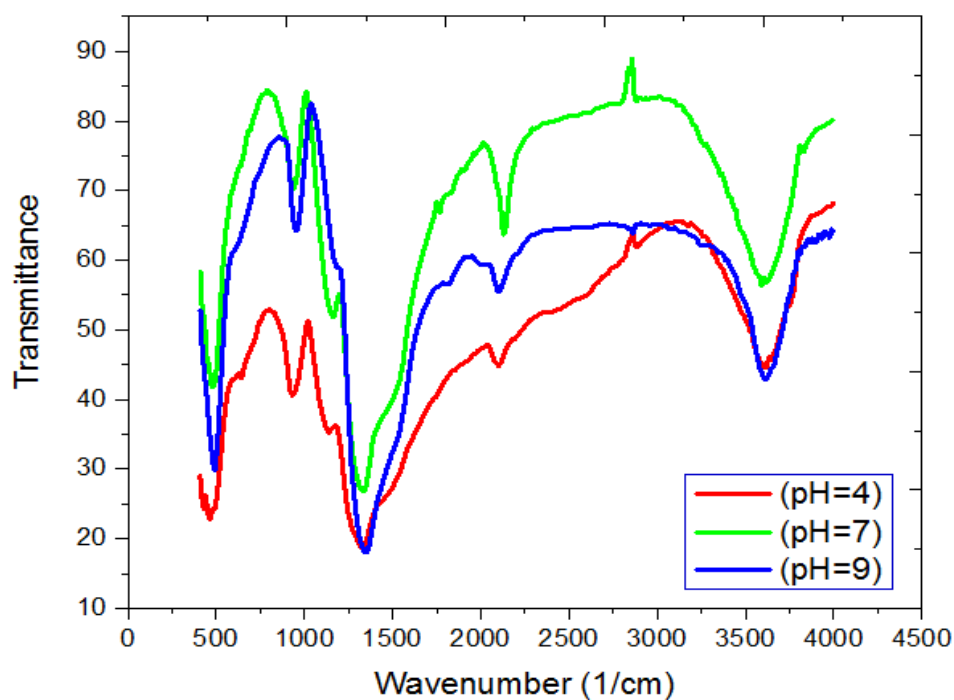


Fig.(3.8): FTIR spectra of SiO₂ samples with different pH values densified by DPSS laser (532 nm) (568.1 mW/cm²).

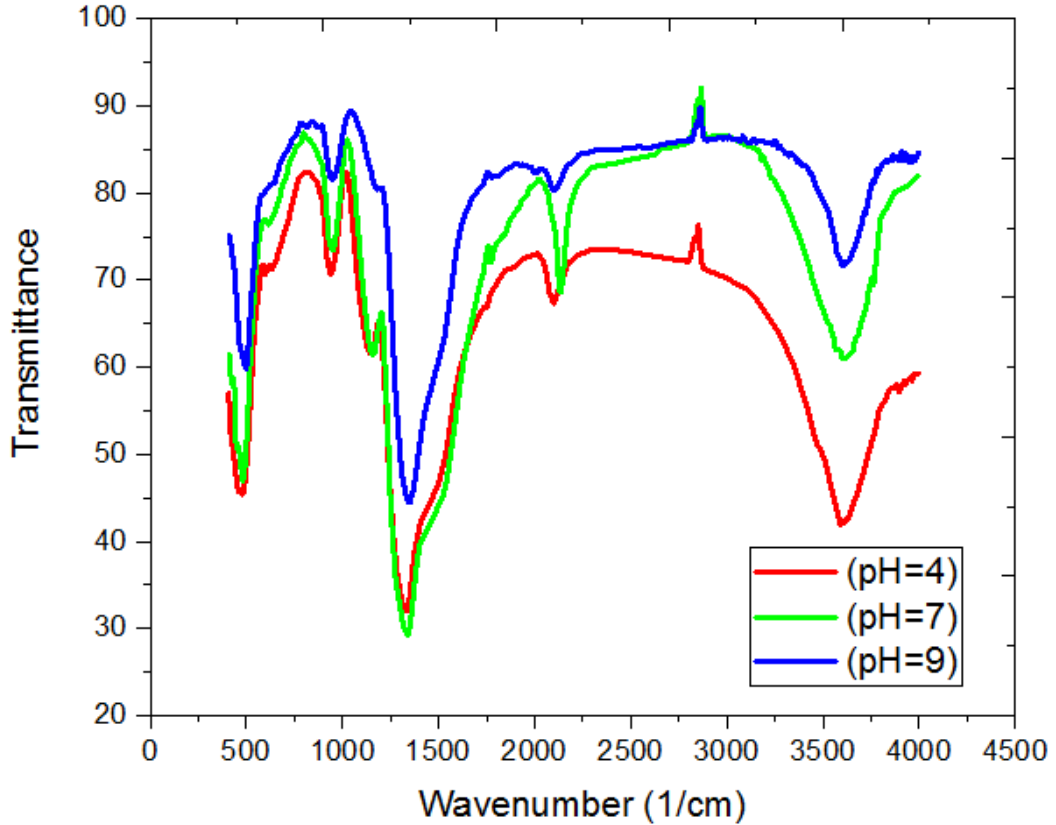


Fig.(3.9): FTIR spectra of SiO₂ samples with different pH values densified by DPSS laser (532 nm) (852.2 mW/cm²).

Figures of FTIR spectra of SiO₂ samples with different pH values (4,7, & 9) densified DPSS laser (532 nm) with different power densities, showed three bands of Si–O–Si bond vibration. The bands of H–O–H bending vibration of H₂O and the O–H vibrations from different species. These results are in a good agreement with [86-88]. It is important to note the Si–OH band vibration which is in a good agreement with [89]. The Si-Si bond due to oxygen vacancies which is in a good agreement with [90, 91].

FTIR bonds and Wavenumbers (1/cm) for SiO₂ samples with different pH values densified by DPSS laser with different power densities are summarized in table (3.3).

Table (3.3): FTIR bonds and Wavenumbers (1/cm) for SiO₂ samples with different pH values densified by DPSS laser (with different power densities).

Bond Type	Wavenumber (1/cm) for 284.09 (mW/cm ²)	Wavenumber (1/cm) for 568.1 (mW/cm ²)	Wavenumber (1/cm) for 852.2 (mW/cm ²)	Wavenumber (1/cm) for 1079.5 (mW/cm ²)	pH
Si-O-Si	478	478	478	478	4
Si-O-Si	823	797	823	823	
Si-O-Si	1142	1207	1170	1170	
Si-O-Si	478	478	487	487	7
Si-O-Si	806	806	806	797	
Si-O-Si	1015	1024	1024	1034	
Si-O-Si	487	487	496	487	9
Si-O-Si	860	870	833	833	
Si-O-Si	1052	1034	1052	1034	
H-O-H	1334	1334	1325	1325	4
H-O-H	1362	1325	1344	1316	7
H-O-H	1362	1362	1353	1362	9
O-H	3595	3604	3595	3604	4
O-H	3604	3600	3609	3609	7
O-H	3604	3604	3604	3604	9
Si-OH	933	933	942	952	4
Si-OH	952	933	942	952	7
Si-OH	961	961	970	970	9
Si-Si	642	605	596	596	4
Si-Si	633	651	614	606	7
Si-Si	596	560	623	620	9

3.4 Morphological Properties of SiO₂ Nanoparticles

3.4.1 Atomic Force Microscope (AFM)

The surface morphology of the prepared SiO₂ samples was investigated using Atomic Force Microscopy (AFM). The AFM images for SiO₂ nanostructure thin films with different pH values densified by oven, DPSS laser, Diode laser, and He-Ne laser are shown in Fig.(3.10) to (3.21). In tables (3.4), (3.5), and (3.6) the roughness and diameter values of SiO₂ samples with different pH values are illustrated.

Table (3.4) AFM parameters of SiO₂ nanostructure thin films with pH=4 for different densification devices.

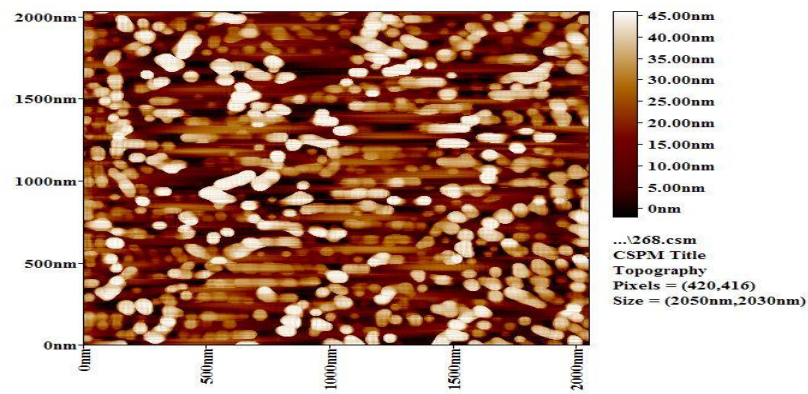
Densification Device	Average Roughness (nm)	Average Diameter (nm)
DPSS Laser	1.78	77.19
Diode Laser	5.59	66.28
He-Ne Laser	0.594	95.88
Oven	11.8	49.06

Table (3.5) AFM parameters of SiO₂ nanostructure thin films with pH=7 for different densification devices.

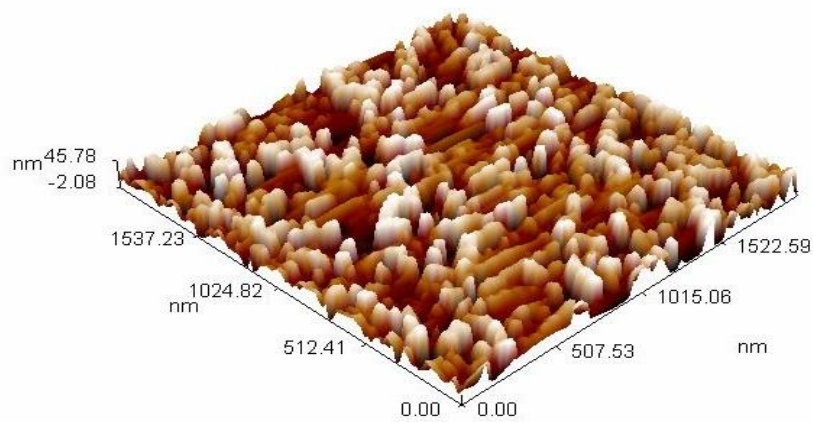
Densification Device	Average Roughness (nm)	Average Diameter (nm)
DPSS Laser	0.728	47.16
Diode Laser	7.16	42.00
He-Ne Laser	2.52	54.48
Oven	0.911	83.30

Table (3.6) AFM parameters of SiO₂ nanostructure thin films with pH=9 for different densification devices.

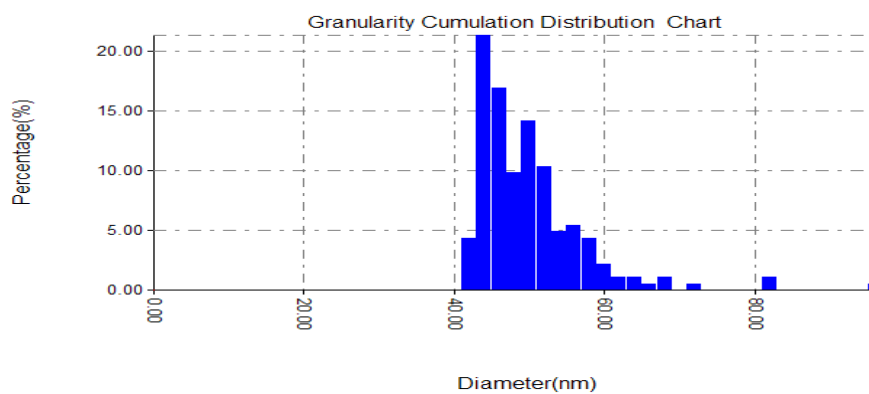
Densification Device	Average Roughness (nm)	Average Diameter (nm)
DPSS Laser	10	58.33
Diode Laser	6.29	79.69
He-Ne Laser	1.51	65.55
Oven	3.56	78.60



(a)

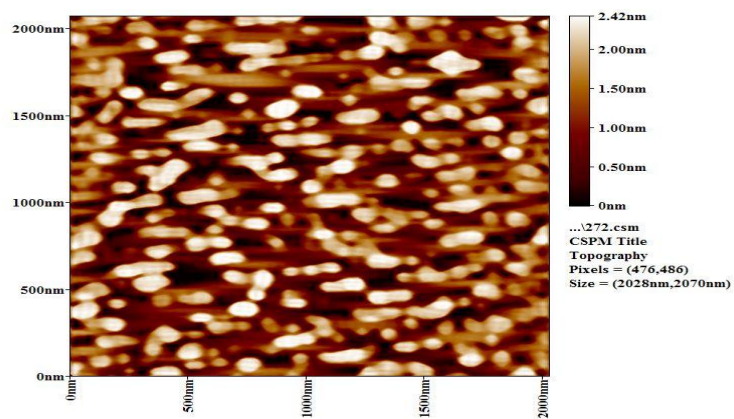


(b)

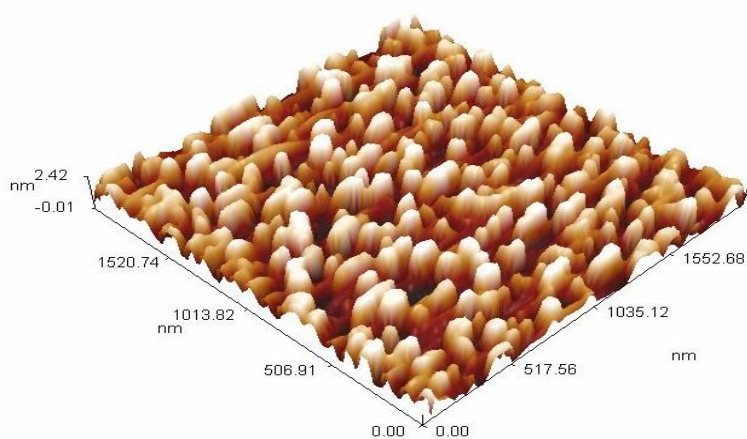


(c)

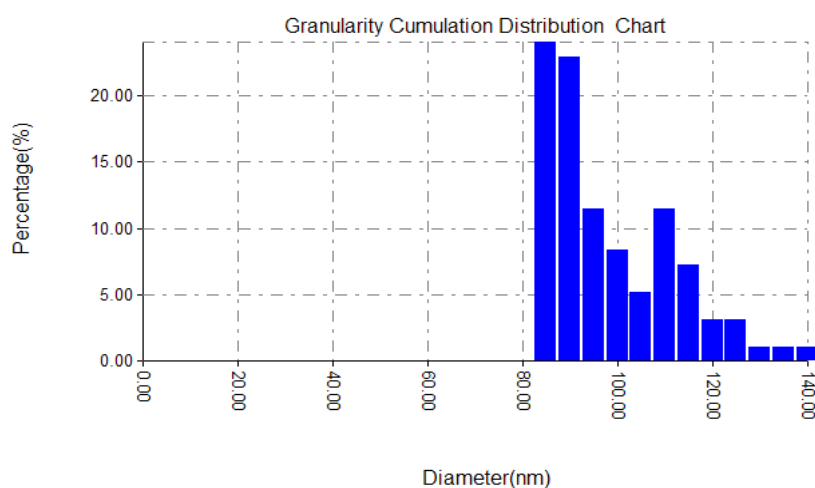
Fig.(3.10): AFM images for SiO₂ nanostructure thin film with pH=4 densified by Oven ; (a) Two-dimensional, (b) three-dimensional and (c) size distribution histogram. The particle size 40-50 nm is dominated.



(a)

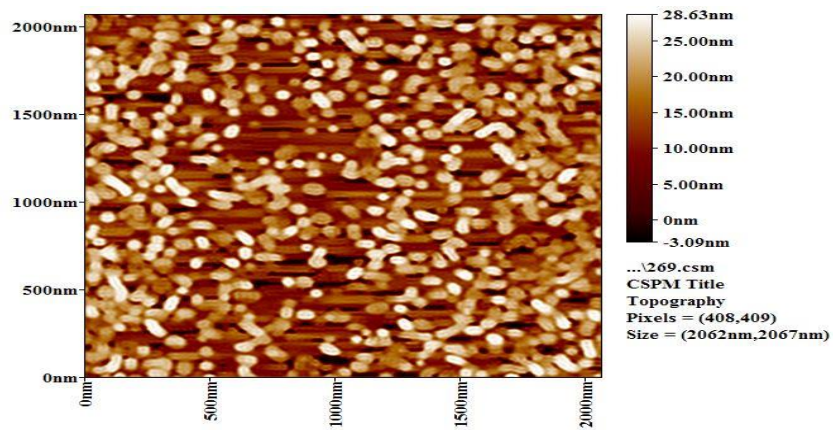


(b)

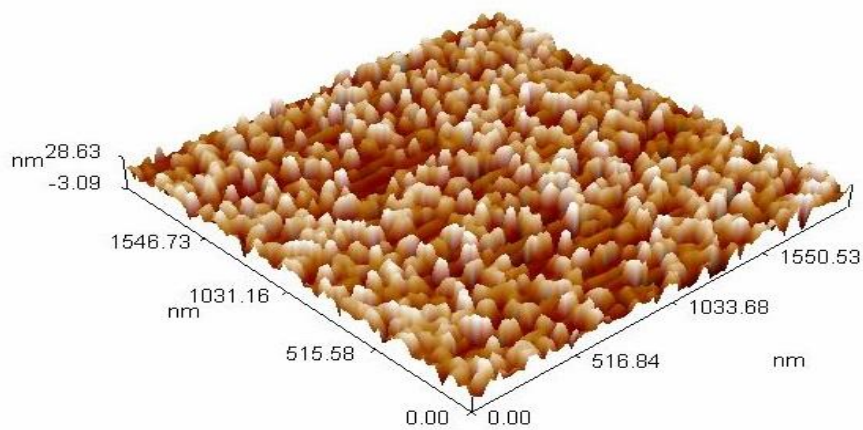


(c)

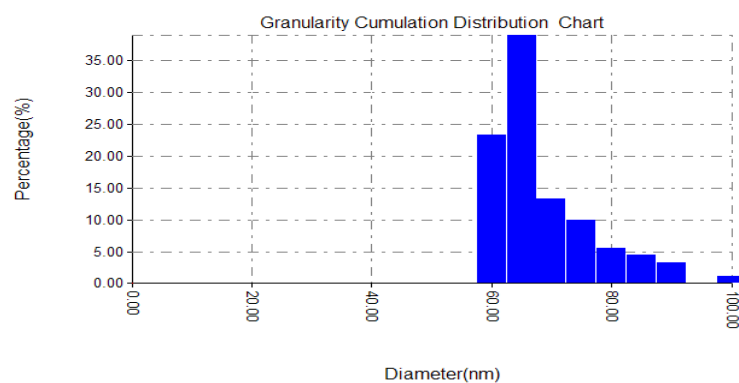
Fig.(3.11): AFM images for SiO_2 nanostructure thin film with pH=4 densified by He-Ne Laser (632 nm) ; (a) Two-dimensional, (b) three-dimensional and (c) size distribution histogram. The particle size 80-115 nm is dominated.



(a)

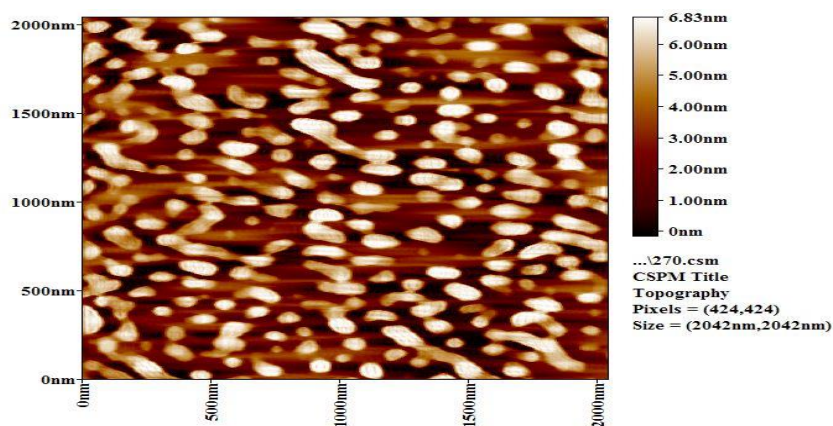


(b)

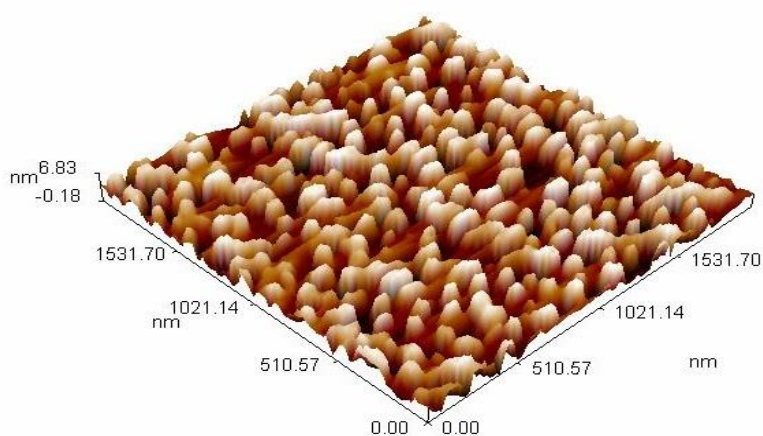


(c)

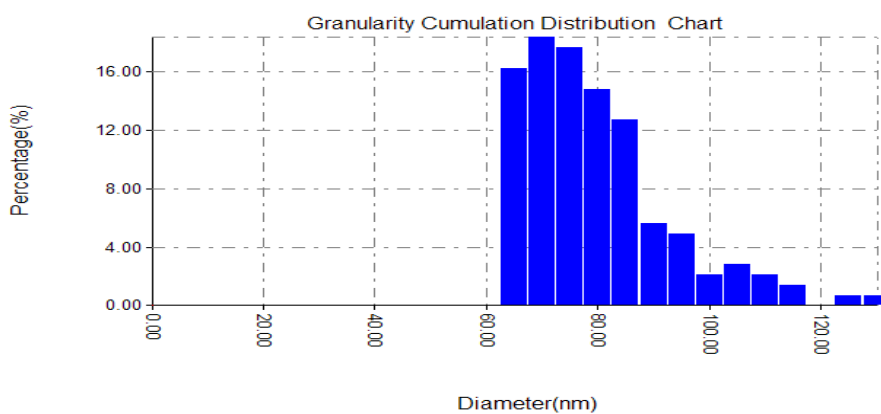
Fig.(3.12): AFM images for SiO₂ nanostructure thin film with pH=4 densified by Diode Laser (410 nm) ; (a) Two-dimensional, (b) three-dimensional and (c) size distribution histogram. The particle size 60-70 nm is dominated.



(a)



(b)



(c)

Fig.(3.13): AFM images for SiO₂ nanostructure thin film with pH=4 densified by DPSS Laser (532 nm) ; (a) Two-dimensional, (b) three-dimensional and (c) size distribution histogram. The particle size 60-85 nm is dominated.

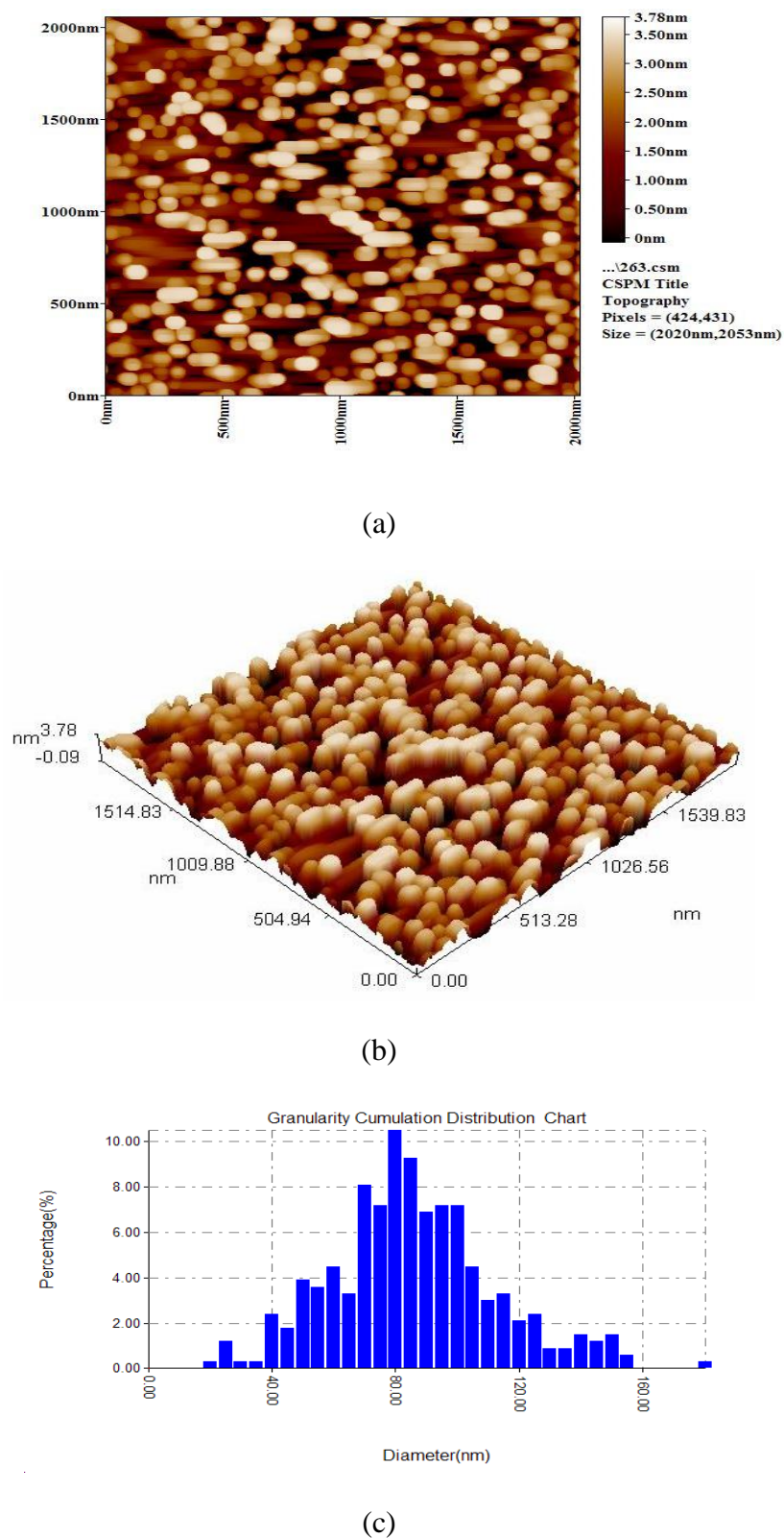
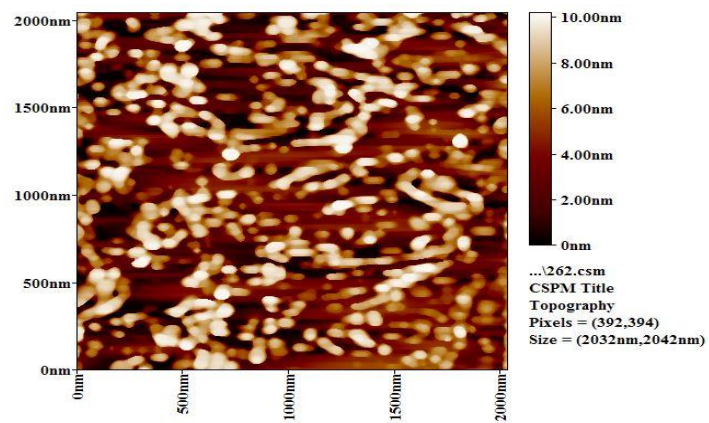
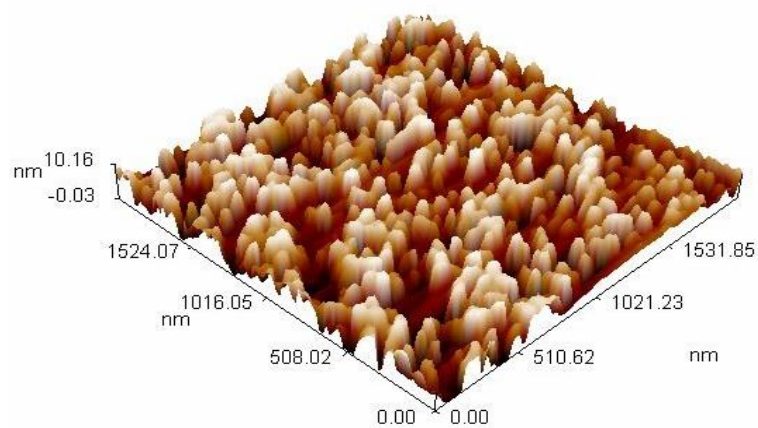


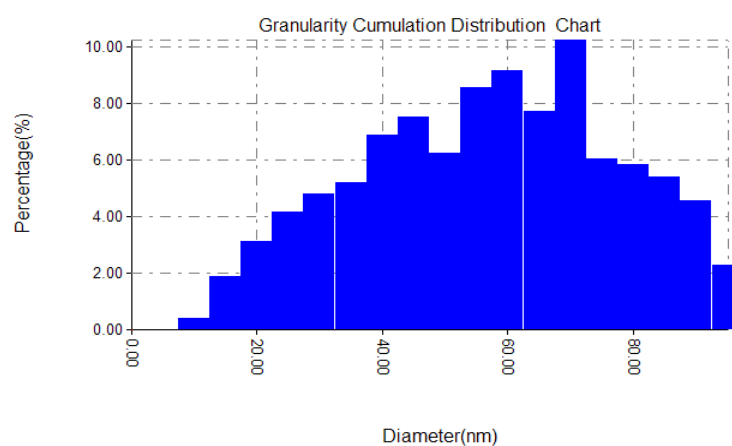
Fig.(3.14): AFM images for SiO₂ nanostructure thin film with pH=7 densified by Oven ; (a) Two-dimensional, (b) three-dimensional and (c) size distribution histogram. The particle size 50-100 nm is dominated.



(a)

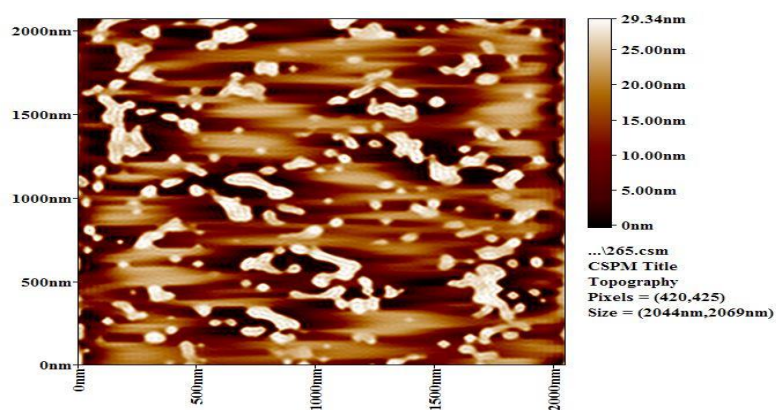


(b)

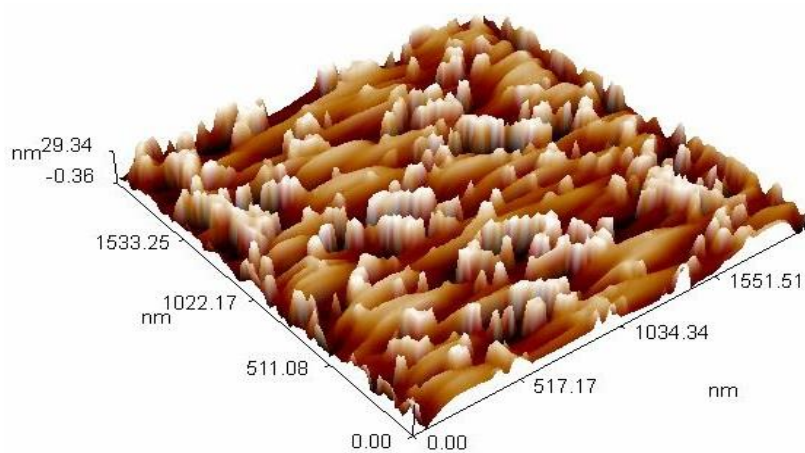


(c)

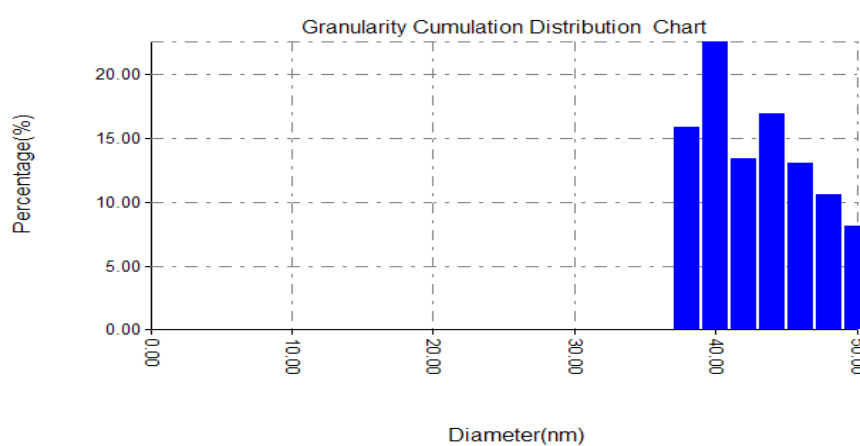
Fig.(3.15): AFM images for SiO₂ nanostructure thin film with pH=7 densified by He-Ne Laser (632 nm) ; (a) Two-dimensional, (b) three-dimensional and (c) size distribution histogram. The particle size 30-85 nm is dominated.



(a)

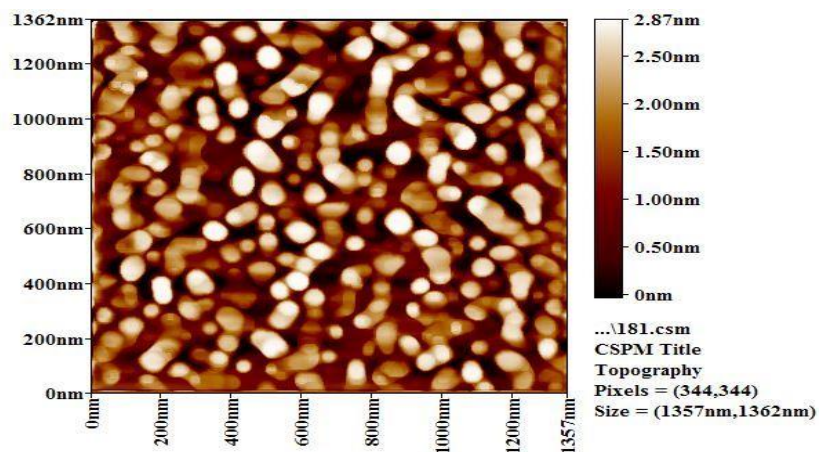


(b)

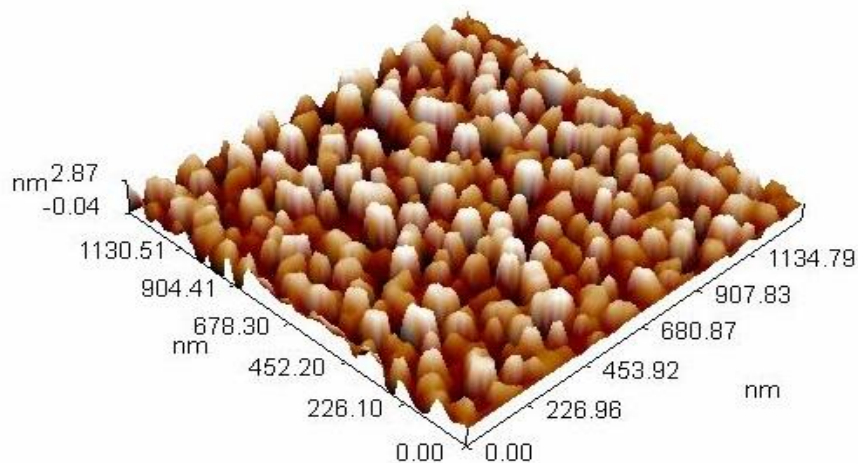


(c)

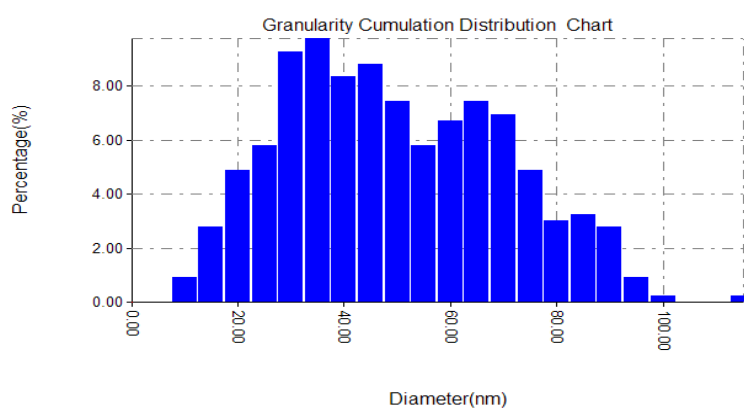
Fig.(3.16): AFM images for SiO₂ nanostructure thin film with pH=7 densified by Diode Laser (410 nm) ; (a) Two-dimensional, (b) three-dimensional and (c) size distribution histogram. The particle size 35-50 nm is dominated.



(a)



(b)



(c)

Fig.(3.17): AFM images for SiO₂ nanostructure thin film with pH=7 densified by DPSS Laser (532 nm) ; (a) Two-dimensional, (b) three-dimensional and (c) size distribution histogram. The particle size 20-85 nm is dominated.

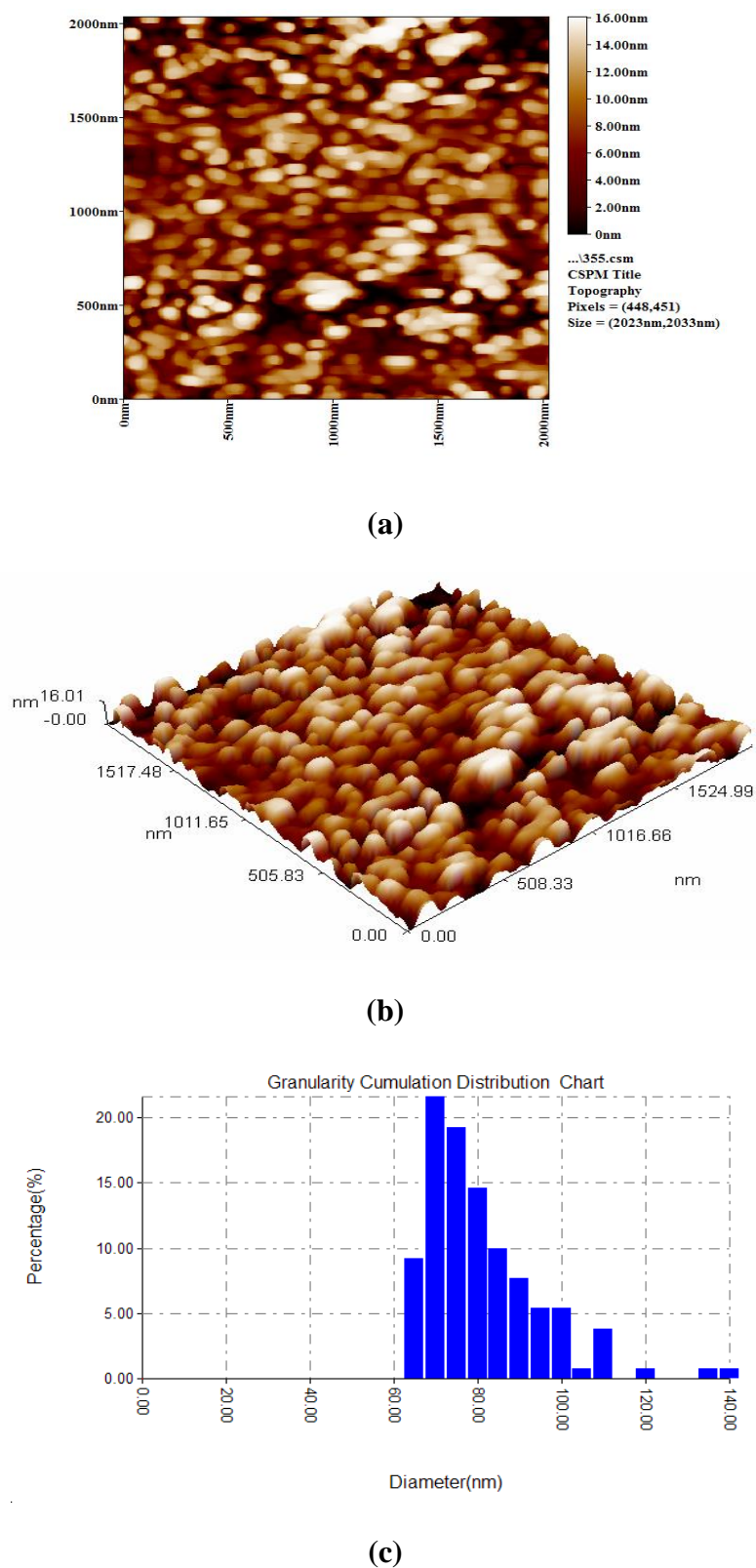
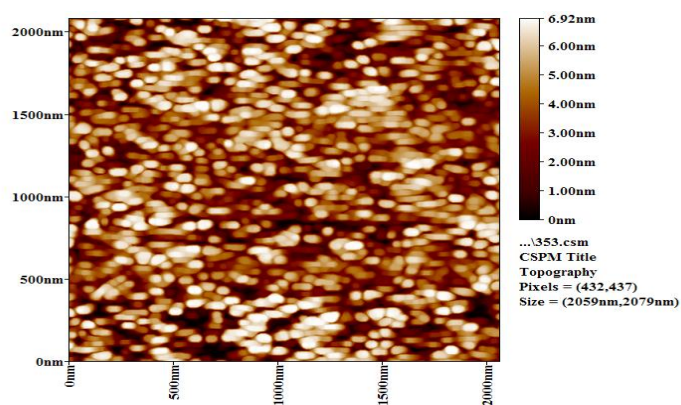
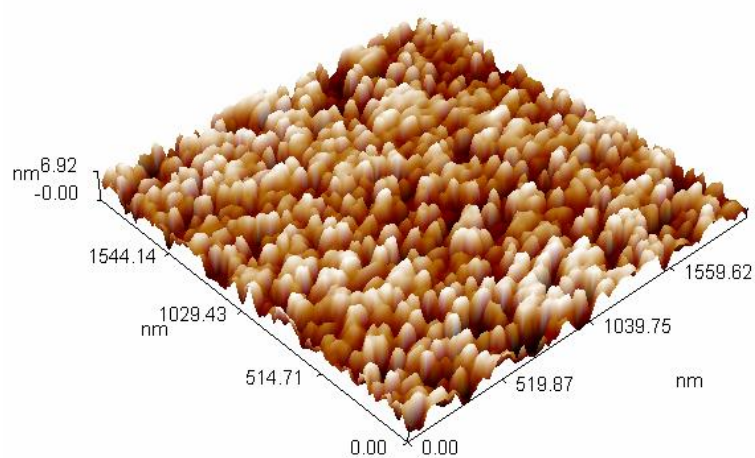


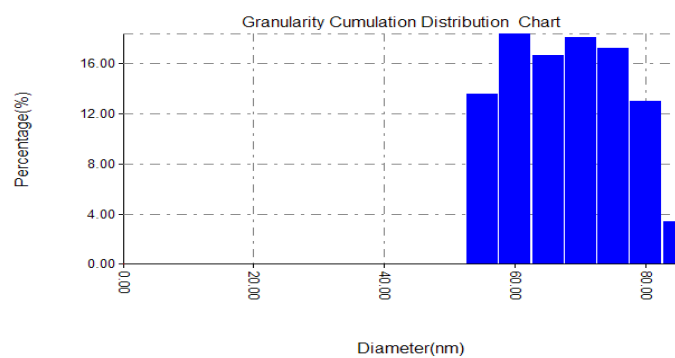
Fig.(3.18): AFM images for SiO₂ nanostructure thin film with pH=9 densified by Oven ; (a) Two-dimensional, (b) three-dimensional and (c) size distribution histogram. The particle size 60-100 nm is dominated.



(a)



(b)



(c)

Fig.(3.19): AFM images for SiO₂ nanostructure thin film with pH=9 densified by He-Ne Laser (632 nm) ; (a) Two-dimensional, (b) three-dimensional and (c) size distribution histogram. The particle size 55-80 nm is dominated.

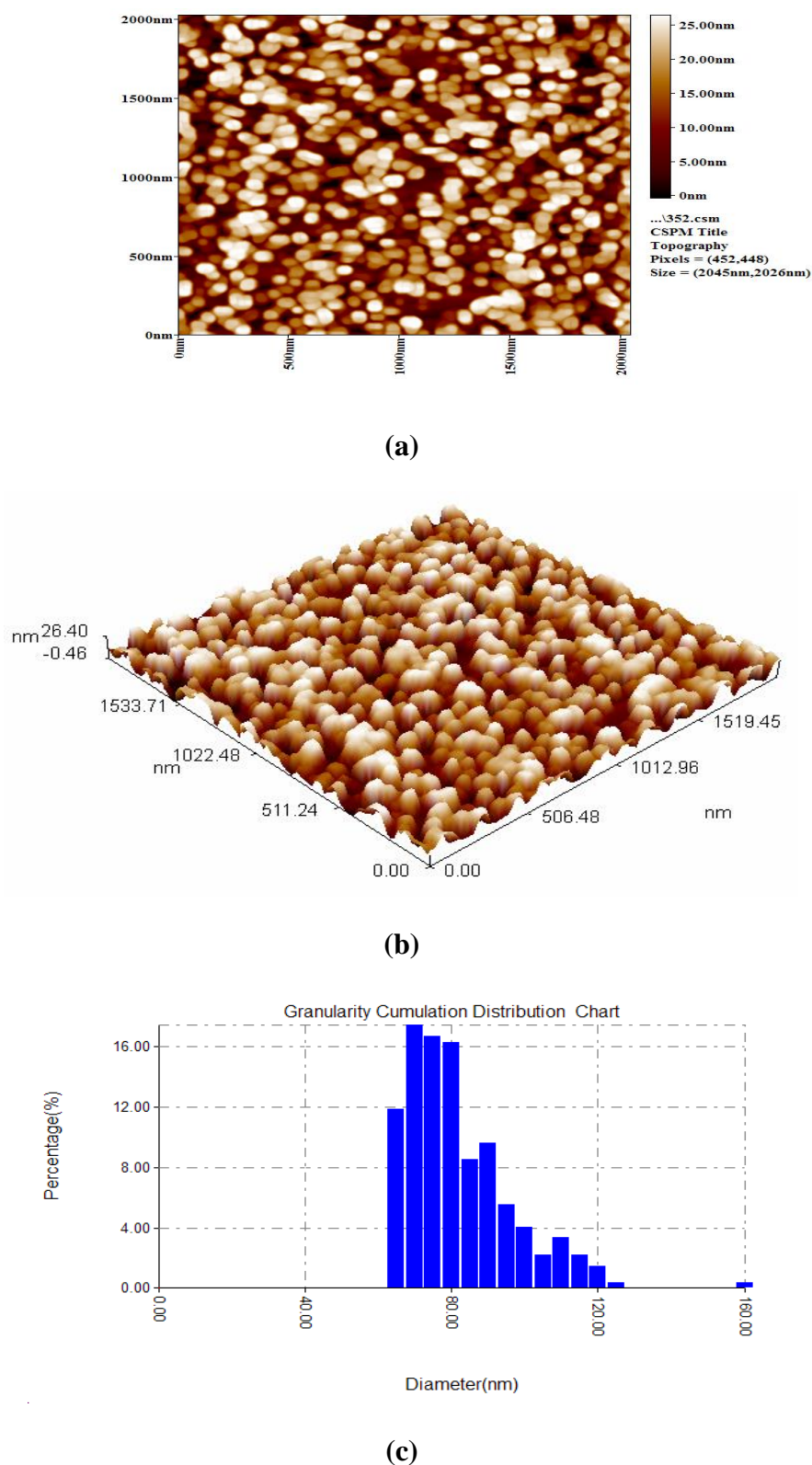


Fig.(3.20): AFM images for SiO₂ nanostructure thin film with pH=9 densified by Diode Laser (410 nm) ; (a) Two-dimensional, (b) three-dimensional and (c) size distribution histogram. The particle size 60-90 nm is dominated.

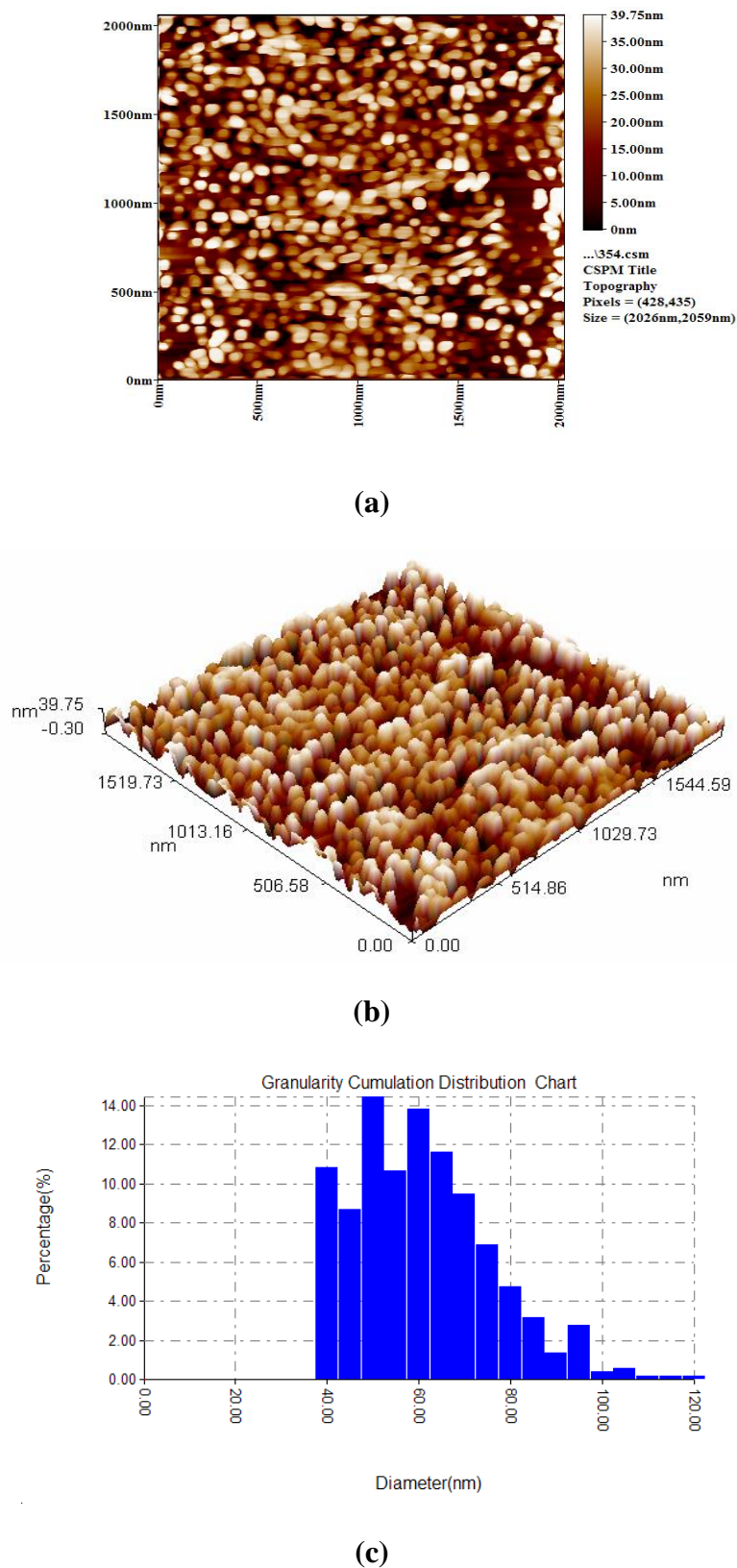


Fig.(3.21): AFM images for SiO₂ nanostructure thin film with pH=9 densified by DPSS Laser (532 nm) ; (a) Two-dimensional, (b) three-dimensional and (c) size distribution histogram. The particle size 40-5780 nm is dominated.

As can be seen from figures which show SiO₂ samples densified by lasers, a granular microstructure and a flat texture, with the lowest surface roughness. At oven densification, the grains get larger and combine to make denser coatings, but the basic structure remains unchanged.

3.4.2 Field Emission Scanning Electron Microscope (FESEM) characteristics

The morphological changes of the prepared SiO₂ nanostructure thin films prepared by Sol-Gel synthesis method at different pH values were analyzed using Field Emission Scanning Electron Microscopy. FESEM can characterize the shape and size of SiO₂ nanostructure thin films. The micrographs FESEM images of SiO₂ samples with pH (4,7, & 9) values, densify by oven , He-Ne laser (632 nm), DPSS laser (532 nm), and Diode laser (410 nm) respectively as shown in Fig.(3.22) to (3.30).

Fig.(3.22), (3.23), and (3.24) show the FESEM images of SiO₂ samples with pH=4 densified by different lasers. SiO₂ nanoparticles have roughly spherical shape with small size nanoparticles around the range of less than 100 nm.

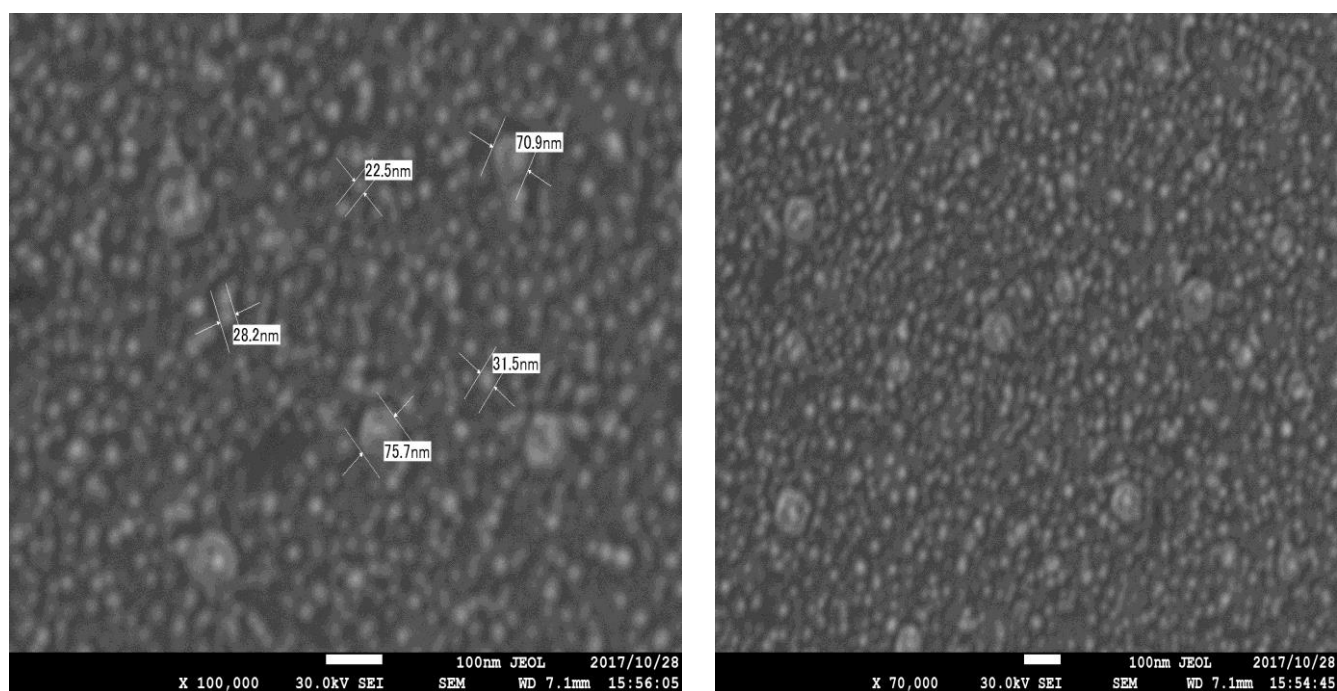


Fig.(3.22) : FESEM images for SiO₂ nanostructure thin film with pH=4 densified by DPSS Laser (532 nm).

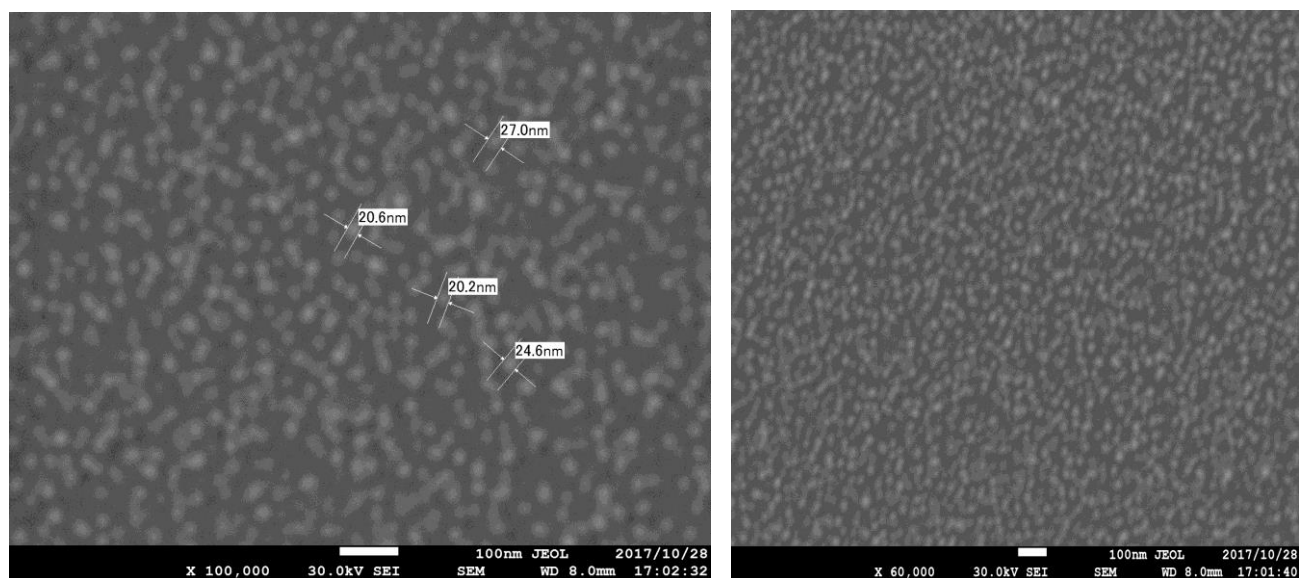


Fig.(3.23) : FESEM images for SiO₂ nanostructure thin film with pH=4 densified by He-Ne Laser (632 nm).

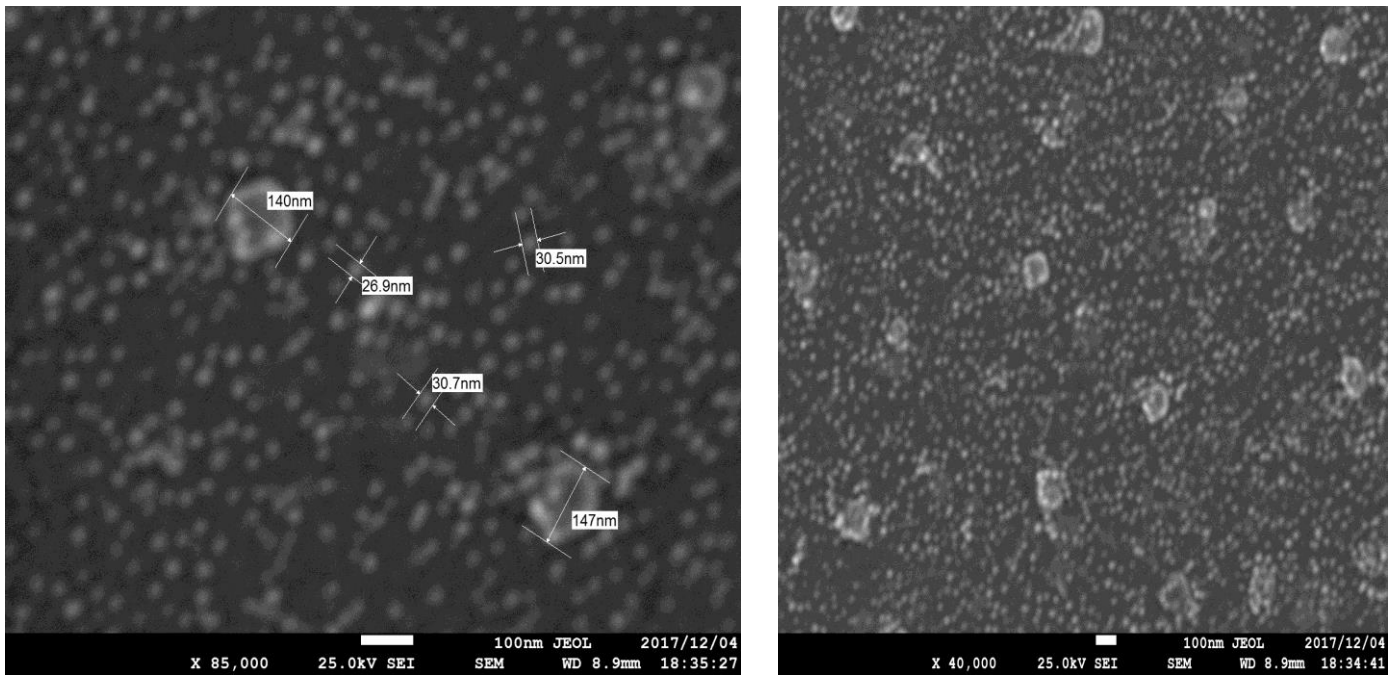


Fig.(3.24) : FESEM images for SiO₂ nanostructure thin film with pH=4 densified by Diode Laser (410 nm).

Fig.(3.25) shows the FESEM images of SiO₂ sample with pH=7 densified by oven. SiO₂ nanoparticles are spherical in shape and their size are ranging between (100-200 nm).

Fig.(3.26), and (3.27) show the FESEM images of SiO₂ samples with pH=7 densified by different lasers. SiO₂ nanoparticles have roughly spherical shape with small size nanoparticles ranging between (20-30 nm).

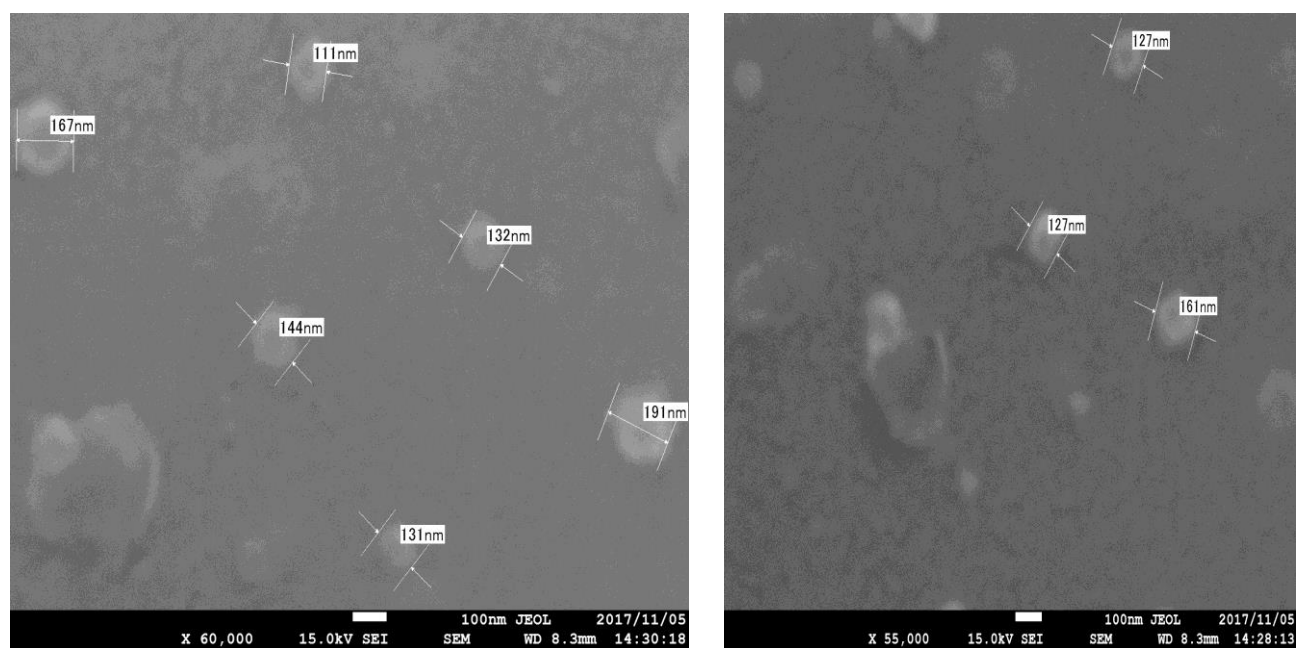


Fig.(3.25) : FESEM images for SiO₂ nanostructure thin film with pH=7 densified by Oven.

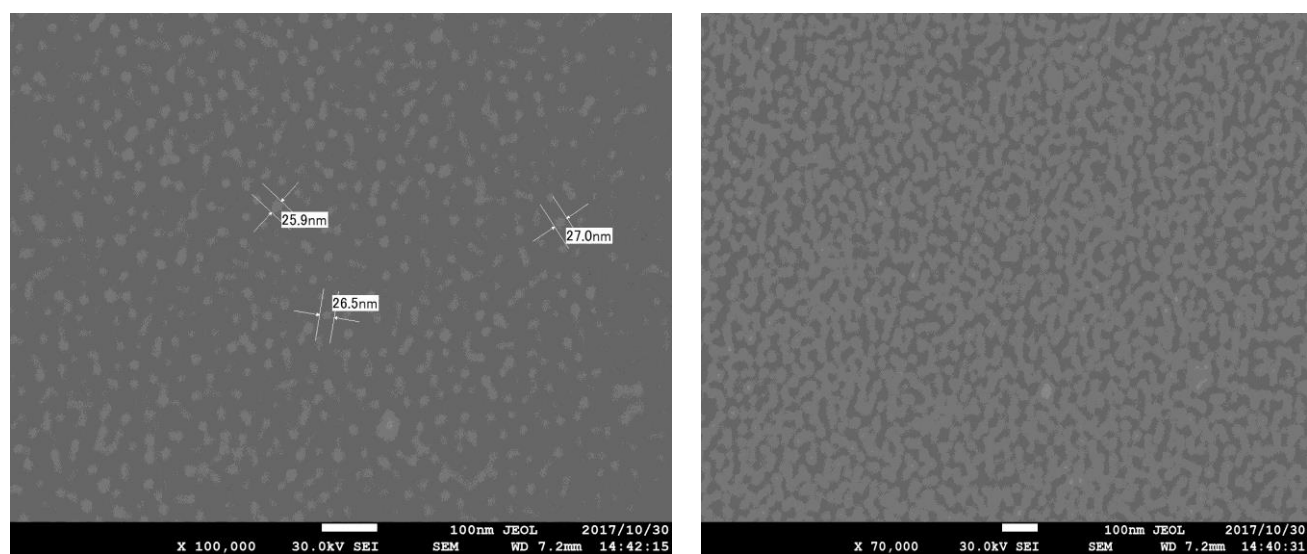


Fig.(3.26) : FESEM images for SiO₂ nanostructure thin film with pH=7 densified by DPSS Laser (532 nm).

(a)

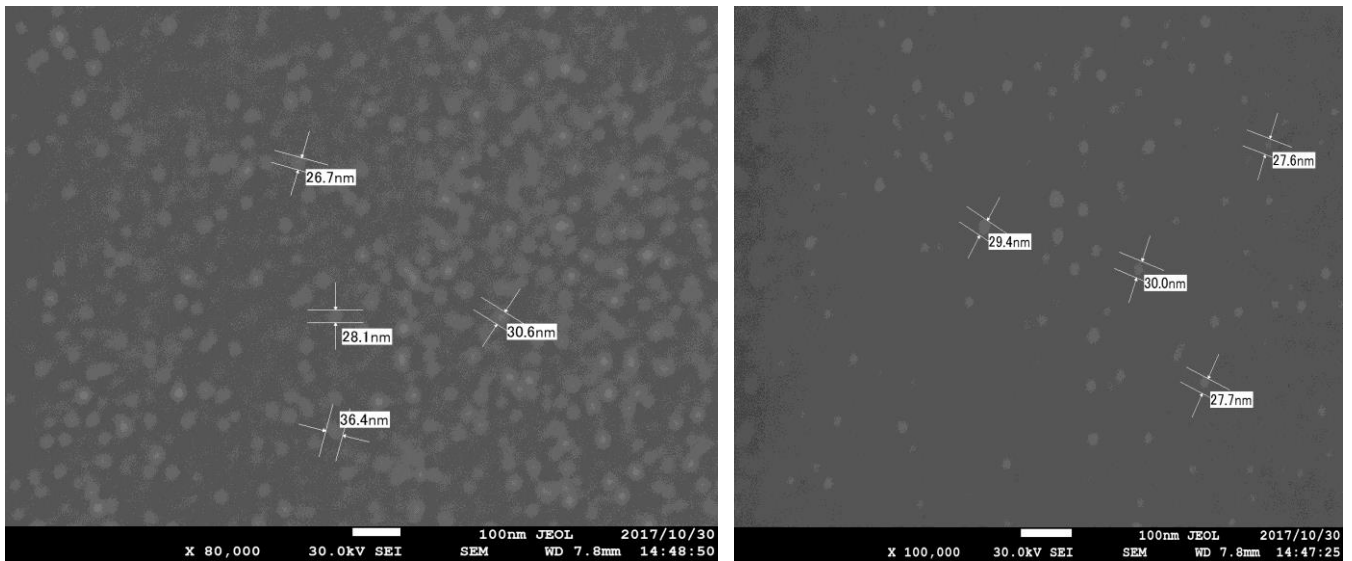


Fig.(3.27) : FESEM images for SiO₂ nanostructure thin film with pH=7 densified by He-Ne Laser (632 nm).

Fig.(3.28) shows the FESEM images for SiO₂ sample with pH=9 densified by oven. SiO₂ nanoparticles are aggregate and agglomerate due to high pH value, but they are still in nanoscale.

Fig.(3.29), (3.30), and (3.31) show the FESEM images for SiO₂ samples with pH=9 densified by different lasers. SiO₂ nanoparticles are also aggregate and agglomerate due to high pH value, but the nanoparticles shape could be recognized which still spherical and their size could be calculated which still in nanoscale ranging between (20-200 nm).

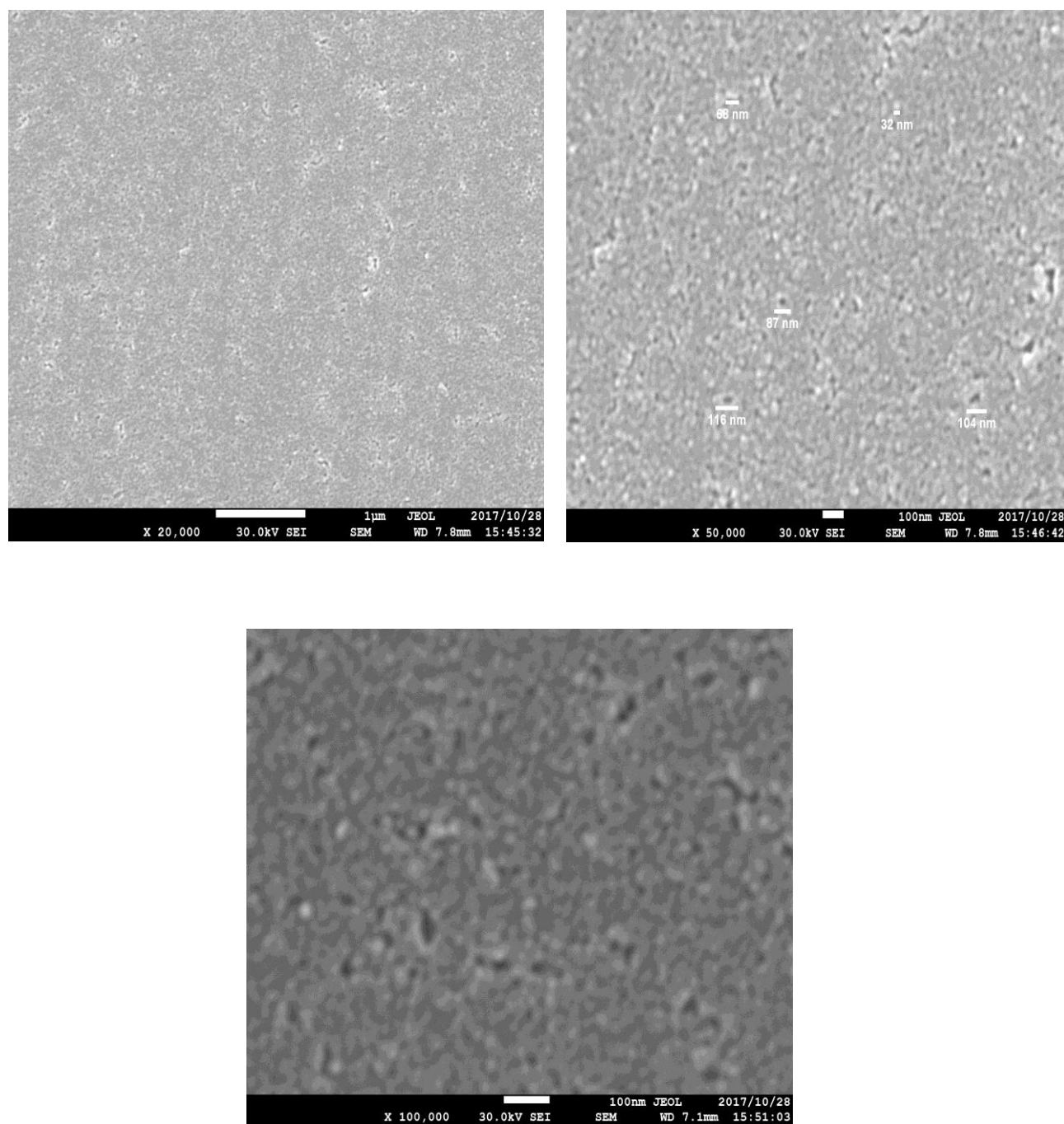


Fig.(3.28) : FESEM images for SiO₂ nanostructure thin film with pH=9 densified by Oven.

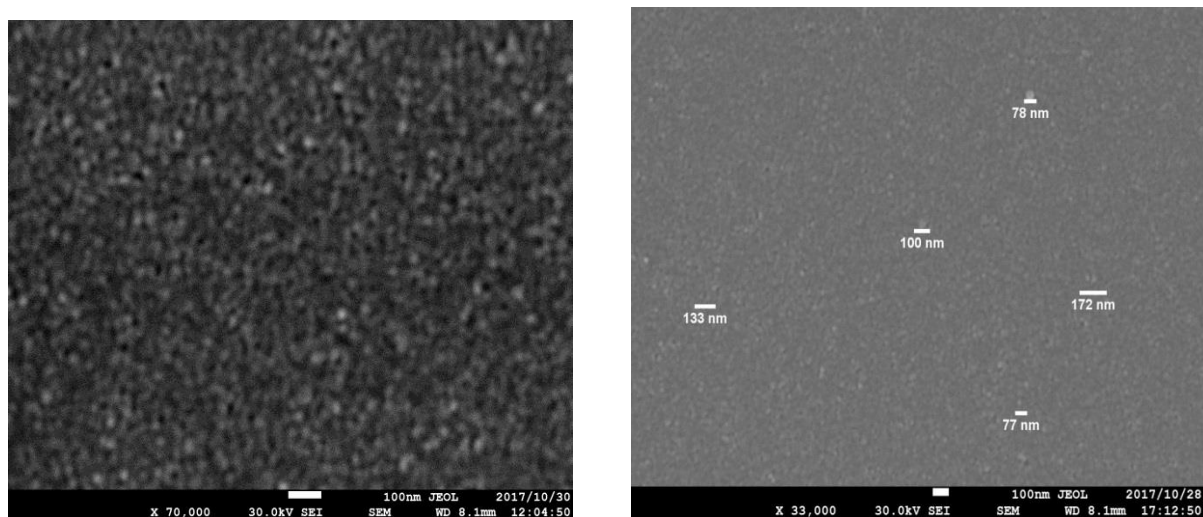


Fig.(3.29) : FESEM images for SiO₂ nanostructure thin film with pH=9 densified by Diode Laser (410 nm).

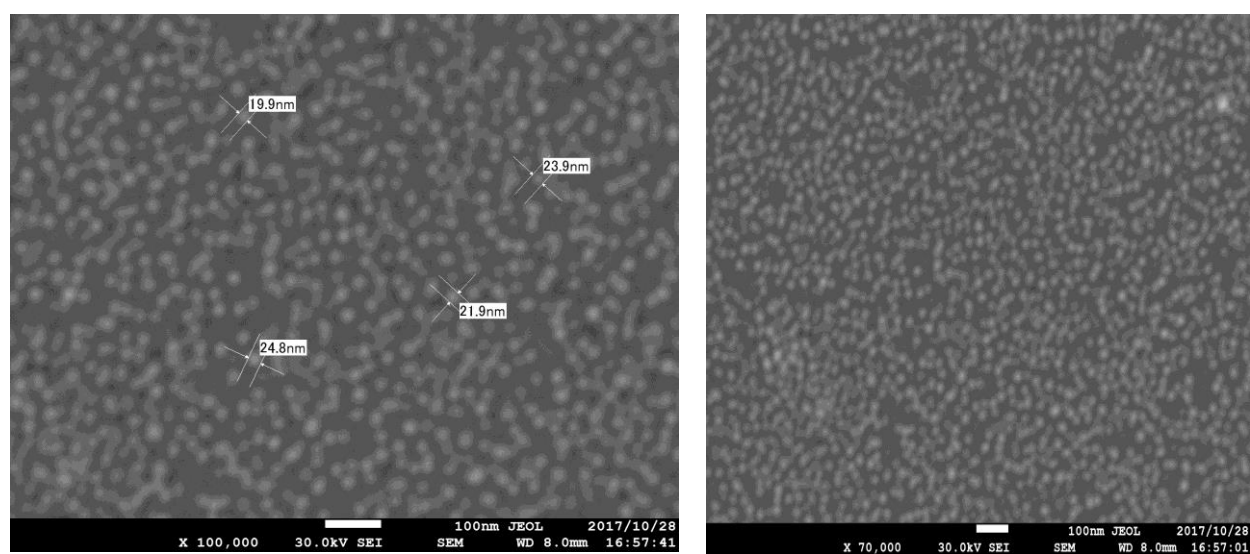


Fig.(3.30) : FESEM images for SiO₂ nanostructure thin film with pH=9 densified by He-Ne Laser (632 nm).

3.4.3 Thickness Measurement

Tables (3.7), (3.8), and (3.9) show the results of measuring the value of thickness of SiO₂ nanostructure thin films prepared by Sol-Gel synthesis method. The values of thickness of SiO₂ nanostructure thin films were measured with different pH values. Tables (3.7) and (3.8) show the thicknesses of SiO₂ nanostructure thin films with pH=4 and pH=7 which are ranging between (200-260 nm), while table (3.9) show the thicknesses of SiO₂ nanostructure thin films with pH=9 which are ranging from (260-270 nm).

Several factors are affecting on specify the thickness of the film such as the pH value of the reaction system. Particle size increases with increasing pH. The particle size of nanostructure thin film of SiO₂ samples depends on the pH value. This result is in a good agreement with [4]. Other factors effect on the thickness value are the number of the dipping process for the film samples and the viscosity of the samples.

Table (3.7): Thickness (nm) of SiO₂ nanostructure thin films with pH=4.

pH= 4	Thickness (nm)
Oven	213.2
DPSS Laser	260.8
He-Ne Laser	260.6
Diode Laser	232.4

Table (3.8): Thickness (nm) of SiO₂ nanostructure thin films with pH=7.

pH= 7	Thickness (nm)
Oven	207.6
DPSS Laser	214.7
He-Ne Laser	268.4
Diode Laser	264.9

Table (3.9): Thickness (nm) of SiO₂ nanostructure thin films with pH=9.

pH= 9	Thickness (nm)
Oven	262.2
DPSS Laser	268.8
He-Ne Laser	265.4
Diode Laser	265.7

3.4.4 Zeta-Potential analysis of SiO₂ nano-solution

The surface charge of the SiO₂ nanoparticles diluted by the solvent solution was measured by zeta-potential. In general, the value is a measure of stability of a surface against agglomeration.

The increase in zeta potential value indicates that the stability of SiO₂ nanoparticles unwillingness of nanoparticles to assemble and get power electric repulsion between them. That means more stability of these nanoparticles. The value of the particle surface charge is important to understand the behavior between the particles in the solvent and indicate the stability of colloidal silica nanoparticles, where the colloids with high zeta potential (negative or positive) are electrically stabilized, while colloids with low zeta potentials tend to aggregate and agglomerate. Nanoparticles with Zeta potential value greater than +30 mV or less than -30 mV are typically stable [92].

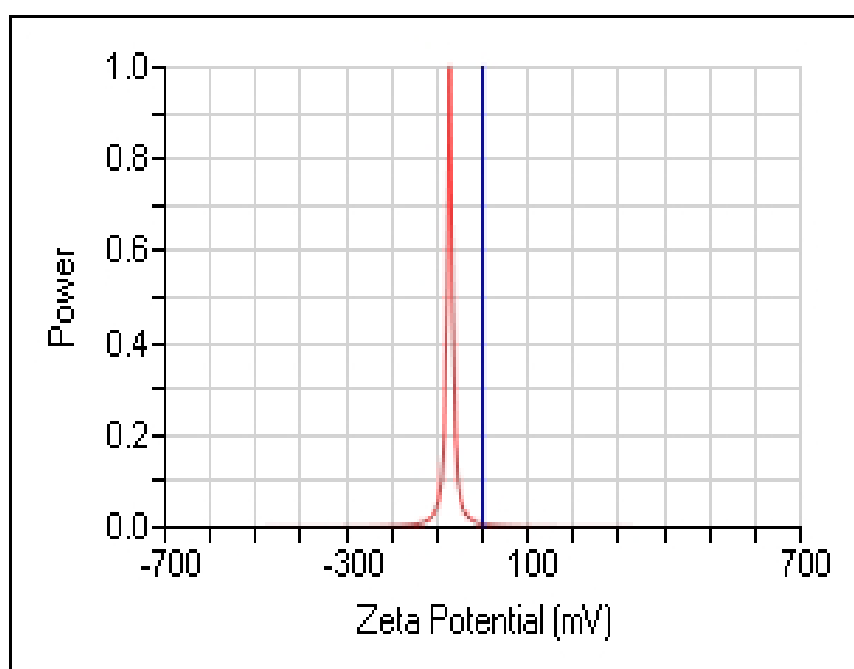
Zeta potential value quotes without a definition of its environment (pH, ionic strength, concentration) is a meaningless number [92]. The most important factor affects Zeta potential is pH value.

Zeta potential surface charge for SiO₂ nanoparticles is illustrated in Fig.(3.31-a), (3.32-a), and (3.33-a). SiO₂ colloidal prepared with different pH values. SiO₂ collide with pH=4 have a good stability, While SiO₂ colloidal with pH=7 have incipient instability. An excellent stability has been found of SiO₂ colloidal with pH=9. The observed zeta potential values and mobility values for the samples are illustrated in the table (3.10) as follows:

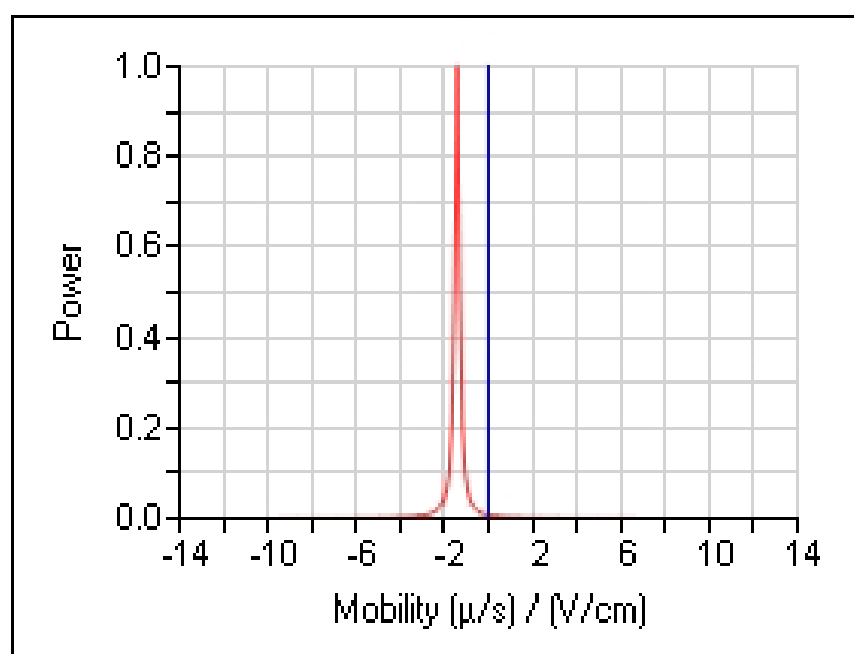
Table (3.10): The values of the zeta potential and the mobility of SiO₂ samples.

pH value	Zeta potential (mV)	The mobility (m ² V ⁻¹ s ⁻¹)
4	-72.11	-1.43
7	-14.70	-0.29
9	-137.59	-2.73

The mobility values which can be explained as the velocity the particle attains per unit electric field, are illustrated in Fig.(3.31-b), (3.32-b), (3.33-b) respectively.

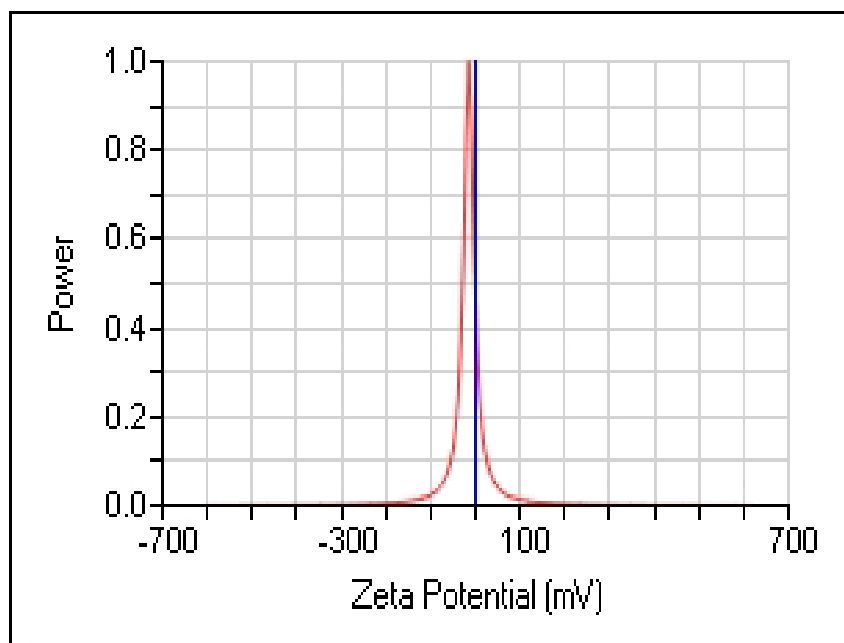


(a)

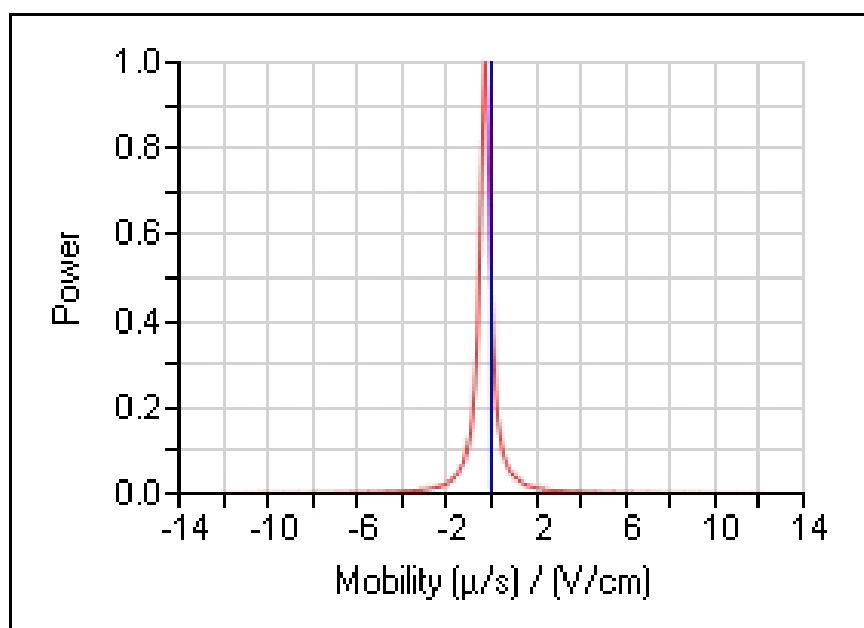


(b)

**Fig. (3.31): The SiO₂ sample with pH=4 ;
a: zeta potential, b: the mobility.**

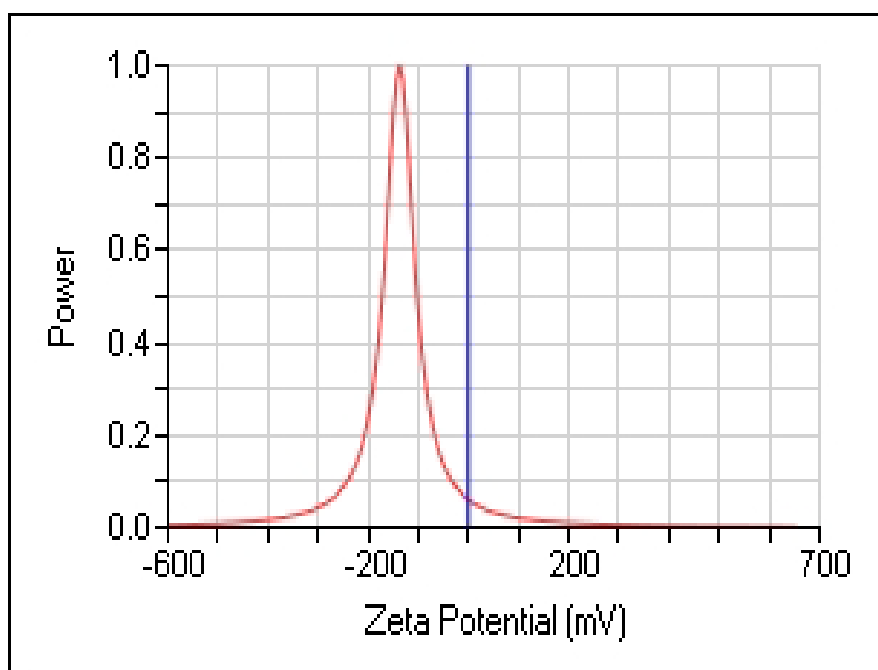


(a)

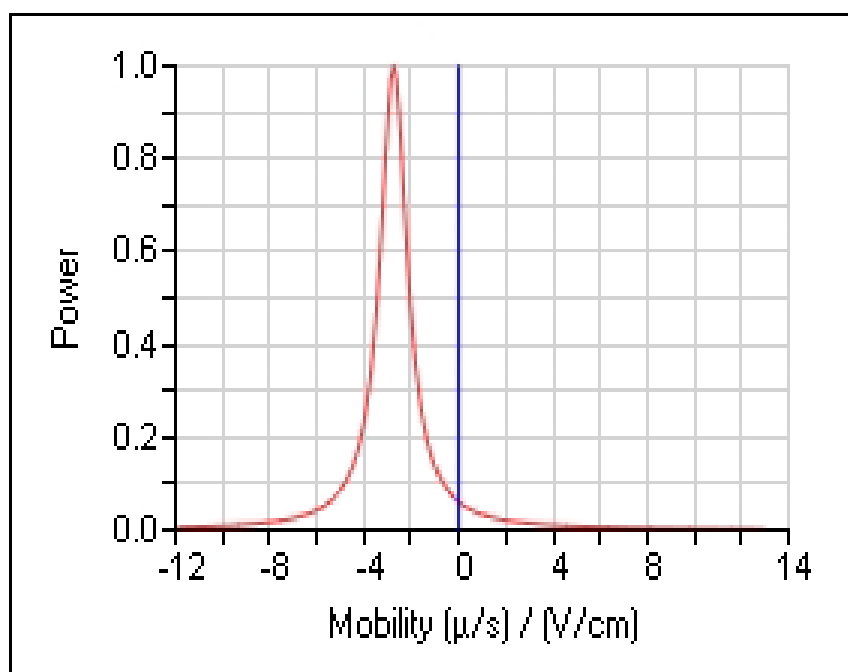


(b)

**Fig.(3.32): The SiO₂ Sol. sample with pH=7;
a: zeta potential, b: the mobility.**



(a)



(b)

**Fig.(3.33): The SiO₂ Sol. sample with pH=9 ;
a: zeta potential, b: the mobility.**

3.4 Conclusions :

From the obtained results, conclusions can be summarized as following:

1. It is possible to obtain modified structure of SiO₂ nanostructure thin film by laser densification.
2. The particle size of nano silica thin film depends on the pH value. Particle size increases with increasing pH of the reaction system.
3. XRD pattern of SiO₂ sample densified by Diode laser (410 nm) results a shift in the Bragg's diffraction angle at ($2\theta=21.7^\circ$) and the structure converted to cristobalite structure.
4. FTIR spectra revealed that the densification process was successful for lasers that have a higher power for different wavelengths, while in similar wavelength it was highest for a higher pH values.
5. FESEM images showed that the smallest particle size of SiO₂ thin film densified by laser was (19.9 nm), while the smallest particle size of SiO₂ thin film densified by oven was (111 nm). This gives an indication that the laser densification produces nanoparticles smaller than oven densification.
6. Diode laser (410 nm) is the best laser used for densification of SiO₂ samples due to its wavelength (closed to UV region) which is in a good matching with SiO₂ absorption range.
7. The power of different lasers did not affect on the structure of the material, while the wavelength was an effective parameter on laser densification.

3.5 Future Work

1. Using Excimer Laser with high powers to get perfect matching with SiO₂ absorption wavelength.
2. Using Sol-Gel synthesis method to prepare SiO₂ as a host to other elements for using in sensing application.

References

- [1] Ghosh, P., "Introduction to Nanomaterials Nanotechnology", 1-19.
- [2] Madras, T. , Chapter - introduction to nanomaterials, (December 2011).
- [3] I. A. Rahman and V. Padavettan, "Synthesis of Silica Nanoparticles by Sol-Gel : Size-Dependent Properties , Surface Modification , and Applications in Silica-Polymer Nanocomposites — A Review," , Journal of Nanomaterials, vol. 2012, pp. 1-15, 2012.
- [4] K. Karlsruhe, "Nanostructured materials : state of the art and perspectives," Nanostructured Materials. , vol. 6, pp. 3–14, 1995.
- [5] R. Nandanwar, P. Singh, and F. Z. Haque, "Synthesis and Characterization of SiO₂ Nanoparticles by Sol-Gel Process and Its Degradation of Methylene Blue," , American Chemical Science Journal, vol. 5, no. 1, pp. 1–10, 2015.
- [6] C.J Brinker and G.W. Sherer, "Sol-Gel Science", Academic press, San Diego, 1990.
- [7] N. Francis, P. Balakrishnan, and S. Mathew, "Sensor Applications Using Sol-Gel Technique," , international journal of innovative research in electrical, electronics, instrumentation and control engineering, vol. 3, no. 12, pp. 28–32, 2015.
- [8] H. L. Tuller and L. C . Klein "sol-gel optics processing and applications" Springer Science Business Media, New York, 1994.
- [9] J. E. Lee and S. S. Saavedra, "Evanescent sensing in doped sol-gel glass films," , Analytica Chimica Acta, vol. 285, pp. 265–269, 1994.
- [10] B. D. Macraith, "Enhanced evanescent wave sensors based on sol-gel-derived porous glass coatings *," , Sensors and Actuators B, vol. 1, pp. 29–34, 1993.

- [11] G. Cao, nanostructures & nanomaterials Synthesis, Properties & Applications, Imperial College Press, USA, 2004.
- [12] S. U. Abideen, “Chemiluminescent Reactions Catalyzed by Nanoparticles of Gold , Silver , and Gold / Silver Alloys,” 2012.
- [13] Y. D. Glinka, S. Lin, and Y. Chen, “Two-photon-excited luminescence and defect formation in SiO₂ nanoparticles induced by 6 . 4-eV ArF laser light,”, PHYSICAL REVIEW B, Vol. 62, no. 7, pp. 4733–4743, 2000.
- [14] Y. D. Glinka, S. Lin, and Y. Chen, “The photoluminescence from hydrogen-related species in composites of SiO₂ nanoparticles of SiO₂ nanoparticles,”, applied physics letters, Vol. 75, No. 6, pp.778-780, 1999.
- [15] Y. D. Glinka, S. Lin, and Y. Chen, “Time-resolved photoluminescence study of silica nanoparticles as compared to bulk type-III fused silica,” physical review B, vol.66, no. 035404, pp.1–10, 2002.
- [16] A. Colder, F. Huisken, E. Trave, G. Ledoux, and O. Guillois, “Strong visible photoluminescence from hollow silica nanoparticles,” vol.15, pp. 1–4, 2004.
- [17] J. Zou and X. Chen, “Using silica nanoparticles as a catalyst carrier to the highly sensitive determination of thiamine,”, Microchemical Journal, vol. 86, pp. 42–47, 2007.
- [18] S. H. A. Hussin, A. H. Alhamdani, and A. N. Abdalgaffar “Optical and Morphological Characteristics for Sili-con Dioxide NPs Prepared by Sol-Gel Method,” International Journal of Scientific & Engineering Research, Vol.7, no.8, pp. 234- 237, 2016.
- [19] E. Reverchon and R. Adami, “Nanomaterials and supercritical fluids,” J. of Supercritical Fluids, vol. 37, pp. 1–22, 2006.

- [20] S. Nicoleta et al., "Silica Nanoparticles Induce Oxidative Stress and Autophagy but Not Apoptosis in the MRC-5 Cell Line," *Int. J. Mol. Sci.*, pp. 29398–29416, 2015.
- [21] Nandnawar R., et al. " Synthesis and Properties of Silica Nanoparticles by sol-gel method for the application in green chemistry", *Material Science Research India*, vol.10, no.1, pp.85-92, 2013.
- [22] H. Giesche, "Synthesis of Monodispersed Silica Powders I . Particle Properties and Reaction Kinetics," *Journal of the European Ceramic Society*, vol. 14, pp. 189–204, 1994.
- [23] R. Paper, L. P. Singh, S. K. Agarwal, S. K. Bhattacharyya, U. Sharma, and S. Ahalawat, "Preparation of Silica Nanoparticles and Its Beneficial Role in Cementitious Materials," *Nanomater. nanotechnol.*, vol. 1, no. 1, pp. 44–51, 2011.
- [24] P. Jinxing, G. Yun, X. Yan, and Z. Chaocan, "Preparation of SiO₂ Nanoparticles by Silicon and Their Dispersion Stability," *Journal of Wuhan University of Technology - Mater. Sci. Ed.*, vol. 20, no. 2, pp. 74–76, 2005.
- [25] C. Huan and S. Shu-qing, "Silicon nanoparticles : Preparation , properties, and applications *," *Chin. Phys. B*, vol. 23, no. 8, pp. 1–14, 2014.
- [26] C. Dhand et al., "Methods and strategies for the synthesis of diverse nanoparticles and their applications: a comprehensive overview," *RSC Adv.*, vol. 5, pp. 105003–105037, 2015.
- [27] M. J. Kao, F. C. Hsu, and D. X. Peng, "Synthesis and Characterization of SiO₂ Nanoparticles and Their Efficacy in Chemical Mechanical Polishing Steel Substrate," *Advances in Materials Science and Engineering*, vol. 2014, pp. 1-8, 2014.

- [28] R. K. Iler, "The Chemistry of Silica Solubility, Polymerization, Colloid and Surface Properties, and Biochemistry", A Wiley-Interscience Publication, New York, 1979.
- [29] C.J.Brinker, A.J.Hurd and N.K.J.Ward [in]:"Ultrastructure processing of Advanced Ceramics" Eds., J.D.Mackenzie and D.R.Ulrich, "Fundamentals of Sol-Gel Thin-Film Formation", John Wiley and Sons, New York, Chapter 15, pp.223-240, 1984.
- [30] J.Chrusciel and L.Slusarki "Synthesis of Nanosilica by the sol-Gel Method and its activity Toward Polymers", Mater.Sci. , vol .21, No. 4, pp. 461-469, 2003.
- [31] Z. Jiwei, Z. Liangying, Y. Xi, and S. N. B. Hodgson, "Characteristics of laser-densified and conventionally heat treated sol - gel derived silica - titania films," Surface and Coatings Technology, vol.138, pp. 135–140, 2001.
- [32] Giovanni Schiavon, "Sol-Gel Derived Nanocomposites synthesis Spectroscopy, Atomic Force Microscopy", Ph.D. Theses, Technische München University, Czech, 2000.
- [33] Kirk Othmer, "Encyclopedia of chemical technology", Wiley Interscience ,vol. 22, p.503, 1994.
- [34] L.L.Hench and J.K.West, "The Sol-Gel Process", Chem. Rev., vol.90, No.1, pp.33-72, 1990.
- [35] S.H.Garofalini and G.Martin, "Molecular Simulation of the Polymerization of Silica Acid Molecules and Network Forming", J.phys.chem, vol.98, pp.1311-1316, 1994.
- [36] B.D.Marc Craith, et al. "Sol-Gel Coating for Optical Chemical Sensors and Biosensors", Sensors and Actuators B, vol. 29, pp. 51-57, 1995.

- [37] D.Levy, C.J.Serna, A.Serrano,J.Vidal and J.M.Oton, "Gel glass-Dispersed Liquid- Crystal Optical Shutters", *PIE Sol-Gel Optics II*, Vol. 1758, pp. 476-484, 1992.
- [38] G.W.Scherer, in : "Ultrastructure processing of Advanced Ceramics" Eds. J.D.Mackenzie and D.R.Ulrich, "Theory of Drying Gels", John Wiley and Sons, New York, chapter 20, pp.295- 302, 1984.
- [39] Scherer G.W., "Drying Gels", *J.Non-Cryst.Solids*,Vol.99, pp.324-358, 1988.
- [40] A. Kołodziejczak-radzimska and T. Jesionowski, "Zinc Oxide—From Synthesis to Application: A Review," *Materials*, vol. 7, pp. 2833–2881, 2014.
- [41] C. A. Milea and C. Bogatu, "the influence of parameters in silica sol-gel process," *Bulletin of the Transilvania University of Braşov • Series I*, vol. 4, no. 1, pp. 59-66, 2011.
- [42] H. K. Schmidt, E. Geiter, M. Mennig, H. Krug, C. Becker, and R. Winkler, "The Sol-Gel Process for Nano-Technologies : New Nanocomposites with Interesting Optical and Mechanical Properties," *Journal of Sol-Gel Science and Technology*, vol. 404, pp. 397–404, 1998.
- [43] M. Laguna and J. Estella, "Effects of aging and drying conditions on the structural and textural properties of silica gels," *Microporous and Mesoporous Materials*, vol. 102, pp. 274–282, 2007.
- [44] B. Topuz and C. Muhsin, "Preparation of particulate / polymeric sol – gel derived microporous silica membranes and determination of their gas permeation properties," *Journal of Membrane Science*, vol. 350, pp. 42–52, 2010.
- [45] S. D. Section and K. A. Publishers, "Catalysts and the structure of SiO₂ sol-gel films," *journal of materials science*, vol. 35, pp. 1835–1841, 2000.

- [46] B. C. Marzolin, S. P. Smith, M. Prentiss, and G. M. Whitesides, "Fabrication of Glass Microstructures by Micro-Molding of Sol-Gel Precursors**," *Adv. Mater.*, vol. 10, no. 8, pp. 571–574, 1998.
- [47] M. Morpurgo, D. Teoli, M. Pignatto, M. Attrezzi, F. Spadaro, and N. Realdon, "Acta Biomaterialia The effect of Na_2CO_3 , NaF and NH_4OH on the stability and release behavior of sol – gel derived silica xerogels embedded with bioactive compounds," *Acta Biomater.*, vol. 6, no. 6, pp. 2246–2253, 2010.
- [48] S.A. Attia, et al. , " Review on Sol-Gel Derived Coatings : Process, Techniques, and Optical Applications", *Journal of Material Science and Technology*, vol.18, no.3, pp. 211-218, 2002.
- [49] C. J. Brincker, A. J. Hurd, P. R. Schunk, G. C. Frye, and C. S. Ashley: " Review of sol-gel thin film formation", *Journal of Non-Crystalline Solids*, vol. 147/148, pp. 424-436, 1992.
- [50] X. Jiang, and H. Gao, "Neurotoxicity of Nanomaterials and Nanomedicine", Academic Press is an imprint of Elsevier, United Kingdom, 2017.
- [51] M. R. Hamblin and P. Avci , " Applications of Nanoscience in Photomedicine", Woodhead Publishing is an imprint of Elsevier, 2015.
- [52] K. Cheng, R. Anthony, U. R. Kortshagen, and R. J. Holmes, "High-Efficiency Silicon Nanocrystal Light-Emitting Devices," *Nano Lett.*, vol. 11, pp. 1952–1956, 2011.
- [53] D. P. Puzzo, E. J. Henderson, M. G. Helander, Z. Wang, A. Ozin, and Z. Lu, "Visible Colloidal Nanocrystal Silicon Light-Emitting Diode," *Nano Lett.*, vol. 11, pp. 1585–1590, 2011.
- [54] G. Conibeer et al., "Silicon quantum dot nanostructures for tandem photovoltaic cells," *Thin Solid Films*, vol. 516, pp. 6748–6756, 2008.

- [55] G. Conibeer et al., "Silicon nanostructures for third generation photovoltaic solar cells," *Thin Solid Films*, vol. 512, pp. 654–662, 2006.
- [56] E. Cho et al., "Silicon quantum dot / crystalline silicon solar cells," *Nanotechnology*, vol. 19, pp. 1-5, 2008.
- [57] Y. Qu, X. Zhong, Y. Li, L. Liao, and X. Duan, "Photocatalytic properties of porous silicon nanowires †," *J. Mater. Chem.*, vol. 20, pp. 3590–3594, 2010.
- [58] M. Shao, L. Cheng, X. Zhang, D. Duo, D. Ma, and S. Lee, "Excellent Photocatalysis of HF-Treated Silicon Nanowires," *J. AM. CHEM. SOC.*, pp. 1–2, 2009.
- [59] Z. Kang, C. H. A. Tsang, N. Wong, Z. Zhang, and S. Lee, "Silicon Quantum Dots : A General Photocatalyst for Reduction , Decomposition , and Selective Oxidation Reactions," *J. AM. CHEM. SOC.*, vol. 129, pp. 12090–12091, 2007.
- [60] D.J. Taylor, B.D. Fabes and M.G. Steinthal, "Laser Densification of Sol-Gel coating ", *Mat. Res. Soc. Symp. Proc.*, vol. 180, pp. 1047–1052, 1990.
- [61] D.J. Taylor and B.D. Fabes, "Laser processing of sol-gel coatings", *Journal of Non-Crystalline Solids*, Vol.147&148, pp. 457-462, 1992.
- [62] T. Chia, L.L. Hench, C. Qin, and C.K. Hsieh, in: *Better Ceramics Through Chemistry IV*, *Mater. Res. Soc. Symp. Series*, Vol. 180 (Materials Research Society, Pittsburgh, PA), p. 819, 1990.
- [63] T.C. Zaugg and B.D. Fabes, 'Thermal modeling of laser fired sol-gel films', presented in Symposium A, *Better Ceramics Through Chemistry*, MRS Spring Meeting, San Francisco, CA, 1990.
- [64] Mordike B. L., " Recent developments in the surface treatment of materials", *CO₂ Lasers and Applications*, Vol. 1276, pp. 332- 342, 1990.

- [65] Mandal S, Planells AD, Hunt HK. "Impact of deposition and laser densification of Silicalite-1 films on their optical characteristics", *Microporous Mesoporous Mater.*, 223:68–78, 2016.
- [66] Mariño M, Rieu M, Viricelle JP, Garrelie F. "Laser induced densification of cerium gadolinium oxide: Application to single-chamber solid oxide fuel cells", *Appl Surf Sci.*, 374:370–4, 2016.
- [67] Zocca A, Colombo P, Günster J, Mühler T, Heinrich JG. "Selective laser densification of lithium aluminosilicate glass ceramic tapes", *Appl Surf Sci.*, 265:610–4, 2013.
- [68] D. A. Ward and E. I. Ko, "Preparing Catalytic Materials by the Sol-Gel Method," *Ind. Eng. Chem. Res.*, vol. 34, pp. 421–433, 1995.
- [69] L. A. Rocha et al., "Sol – gel entrapped cobalt complex," *Materials Characterization*, vol.50, pp. 101–108, 2003.
- [70] V. Lafond, P. H. Mutin, and A. Vioux, "Non-hydrolytic sol – gel routes based on alkyl halide elimination: toward better mixed oxide catalysts and new supports Application to the preparation of a SiO₂ – TiO₂ epoxidation catalyst," *Journal of Molecular Catalysis A: Chemical*, vol. 183, pp. 81–88, 2002.
- [71] R.R. Krchnavek, H.H. Gilgen, and R.M. Osgood, "Maskless Laser Writing of Silicon Dioxide," *J. Vac. Sci. Technol.*, B2, Vol. 4, pp. 641-644, 1984.
- [72] D. J. Shaw and T. A. King, "Densification of sol—gel silica glass by laser irradiation," *Sol-Gel Optics*, vol. 1328, pp. 474-481, 1990.
- [73] T.C. Zaugg et al. "Waveguide Formation by Laser Irradiation of Sol-Gel Coatings", in *Submolecular Glass Chemistry and Physics*, Boston: SPIE., pp. 26-35, 1991.
- [74] B.D. Fabes et al., *Laser Densification of Optical Films*. Proc. SPIE 1758, ed. J.D. Mackenzie., pp. 227-234, 1992.

- [75] Birnie P.D., "Laser processing of chemically derived dichroic Filters", *Optical Engineering*, Vol. 32, pp. 2960-2965, 1993.
- [76] K. S. Rao, K. El-Hami, T. Kodaki, K. Matsushige, and K. Makino, "A novel method for synthesis of silica nanoparticles," *J. Colloid Interface Sci.*, vol. 289, pp. 125–131, 2005.
- [77] Ö. Kesmez, H. Erdem Çamurlu, E. Burunkaya, and E. Arpaç, "Preparation of antireflective SiO₂ nanometric films," *Ceram. Int.*, vol. 36, pp. 391–394, 2010.
- [78] E. Krumov, J. Dikova, N. Starbov, and K. Starbova, "Laser modification and chemical metalization of sol-gel zirconia thin films as potential material for catalytic applications," *Bulg. Chem. Commun.*, vol. 45, no. SPEC. ISSUE B, pp. 90–93, 2013.
- [79] D. Hawelka, J. Stollenwerk, N. Pirch, K. Wissenbach, and P. Loosen, "Improving surface properties by laser-based drying, gelation, and densification of printed sol-gel coatings," *J. Coatings Technol. Res.*, vol. 11, no. 1, pp. 3–10, 2014.
- [80] H. A. Khayoon, "Characterization Study of Nanostructured SiO₂ Thin Films Prepared By Sol Gel Technique," 2016.
- [81] G. H. Awan and S. Aziz, "synthesis and applications of TiO₂ nanoparticles," *Pakistan Eng. Congr. 70th Annu. Sess. Proc.*, pp. 403–412, 2007.
- [82] J. R. Martinez, S. Palomares-Sanchez, G. Ortega-Zarzosa, F. Ruiz, and Y. Chumakov, "Rietveld refinement of amorphous SiO₂ prepared via sol-gel method," *Mater. Lett.*, vol. 60, pp. 3526–3529, 2006.
- [83] R. Sumathi, R. Thenmozhi, "Preparation of Spherical Silica Nanoparticles by Sol-Gel Method," *International Conference on Systems, Science, Control, Communication, Engineering and Technology*, pp. 401–405, 2016.

- [84] G. Zhang, Y. Xu, D. Xu, and D. Wang, "High Pressure Research : An Pressure-induced crystallization of amorphous SiO₂ with silicon – hydroxy group and the quick synthesis of coesite under lower temperature," , High Pressure Research, Vol. 28, No. 4, 641–650, 2008.
- [85] D. Sun, "Effect of Zeta Potential and Particle Size on the Stability of SiO₂ Nanospheres as Carrier for Ultrasound Imaging Contrast Agents," Int. J. Electrochem. Sci., vol. 11, pp. 8520–8529, 2016.
- [86] P. Innocenzi, "Infrared spectroscopy of sol – gel derived silica-based films: a spectra-microstructure overview," Journal of Non-Crystalline Solids, vol. 316, pp. 309–319, 2003.
- [87] D. Balköse, U. Köktürk, and H. Yilmaz, "Study of cobaltous chloride dispersion on the surface of the silica gel," Appl. Surf. Sci., vol. 147, pp. 77–84, 1999.
- [88] X. Li, Z. Cao, Z. Zhang, and H. Dang, "Surface-modification in situ of nano-SiO₂ and its structure and tribological properties," Appl. Surf. Sci., vol. 252, pp. 7856–7861, 2006.
- [89] I. A. Rahman, P. Vejayakumaran, C. S. Sipaut, J. Ismail, and C. K. Chee, "Size-dependent physicochemical and optical properties of silica nanoparticles," Mater. Chem. Phys., vol. 114, pp. 328–332, 2009.
- [90] P. Vitanov, A. Harizanova, T. Ivanova, and H. Dikov, "Low-temperature deposition of ultrathin SiO₂ films on Si substrates," J. Phys. Conf. Ser., vol. 514, pp. 1–5, 2014.
- [91] R. F. S. Lenza and W. L. Vasconcelos, "Preparation of silica by sol-gel method using formamide," Mater. Res., vol. 4, no. 3, pp. 189–194, 2001.
- [92] K. Khoshnevisan, and M. Barkhi , "Zeta potential," May 2015.

الخلاصة

هدف العمل الحالي هو تصنيع ثنائي اوكسيد السيليكون ذو التركيب النانوي بطريقة Sol-Gel متضمنة التكتيف الإعتيادي والتكتيف بإستخدام الليزر. تم تحضير الاغشية الرقيقة من ثنائي اوكسيد السيليكون بمزج أورثوسيليكات رباعي المثل، كحول الاثيل و ماء منزوع الايونات وحامض الهيدروكلوريك او اوكسيد الصوديوم كمحفز وبقيم مختلفة من الأس الهيدروجيني (9, 7, 4). حُضرت جميع الأغشية بنفس الظروف والتي تتضمن (النسبة المولية، وقت الخلط ، وقت التخميم ، ودرجة حرارة التجفيف).

تمت معاملة الاغشية حرارياً بإستخدام الفرن عند 200 درجة سيليزية لمدة ساعتين او بإستخدام الليزر لمدة 15 دقيقة. تم استخدام ثلاثة انواع من الليزر لعملية التكتيف :- ليزر الهيليوم- نيون بطول موجي 632 نانومتر و كثافة الطاقة (0.056 ملي واط/سم²) ، ليزر الدايدود بطول موجي 410 نانومتر وبكثافة الطاقة (56.8 ملي واط/سم²) ، و ليزر الدايدود بطول موجي 532 نانومتر وبقيم كثافة الطاقة تتراوح بين (284.09 الى 1079.5 ملي واط/سم²). فحصت الأغشية بإستخدام تقنية حيود الاشعة السينية ، طيف الامتصاص للاشعة فوق البنفسجية والمرئية ، AFM, FTIR, FESEM و Zeta Potential.

بين فحص حيود الاشعة السينية ان تركيب ثنائي اوكسيد السيليكون هو غير متبلور عند استخدام الفرن و ليزر الدايدود (532 نانومتر). من ناحية أخرى ظهرت ازاحة في قيمة زاوية الحيود و تحول تركيب ثنائي اوكسيد السيليكون الى تركيب (cristobalite) عند استخدام ليزر الدايدود (410 نانومتر) في عملية التكتيف.

اظهرت فحوصات اطياف الامتصاص للاشعة فوق البنفسجية والمرئية أن أقصى امتصاص عند 196.8 نانومتر والذي يؤكد تكون جسيمات السيليكا النانوية. بالإضافة إلى ذلك، فإن نتائج FTIR أثبتت ان تحضير جسيمات السيليكا النانوية كان ناجحاً.

بينت تحاليل AFM و صور FESEM ان تركيب الاغشية النانوية يتألف من جسيمات ثنائي اوكسيد السيليكون الكروية النانومترية. تم الكشف عن استقرارية جيدة بالجهد لثنائي اوكسيد السيليكون الغروي مع الأس الهيدروجيني 9 .

من النتائج المُستحصلة يمكن الاستنتاج بأن التركيب المعدل للأغشية الرقيقة من ثنائي اوكسيد السيليكون يمكن تحضيرها بإستخدام التكتيف بالليزر. التكتيف بالليزر لجسيمات ثنائي اوكسيد السيليكون المصنعة بطريقة Sol-Gel يفوق التكتيف بإستخدام الفرن عند 200 درجة سيليزية.



وزارة التعليم العالي والبحث العلمي

جامعة بغداد

معهد الليزر للدراسات العليا

تأثير التكتيف بالليزر على ثنائي اوكسيد السيليكون

ذو البنية النانوية المُحضَّر بتقنية Sol - Gel

رسالة مقدمة الى

معهد الليزر للدراسات العليا / جامعة بغداد / لاستكمال متطلبات نيل شهادة

ماجستير علوم في الليزر / الفيزياء

من قبل

نور محمد عبدالملك

بكالوريوس علوم الفيزياء - 2014

بإشراف

الأستاذ المساعد الدكتور محمد كريم ظاهر

2018 م

1439 هـ